DISEASE IN A CHANGING OCEAN: ECOIMMUNOLOGICAL APPROACHES TO CORAL REEF ECOLOGY

by
LAUREN ELIZABETH FUESS

DISSERTATION

Submitted in partial fulfillment of the requirements for the degree of Doctor of Philosophy at
The University of Texas at Arlington
May, 2018

Arlington, Texas

Supervising Committee:

Laura D. Mydlarz, Supervising Professor
Andrew Baker
Todd Castoe
Jeffery Demuth
Matthew Fujita

ABSTRACT

DISEASE IN A CHANGING OCEAN: ECOIMMUNOLOGICAL APPROACHES TO CORAL REEF ECOLOGY

Lauren E. Fuess, Ph.D.

The University of Texas at Arlington, 2018

Supervising Professor: Laura D. Mydlarz

Increasing prevalence of anthropogenic stressors and climate change have resulted in rapid increases in the incidence and severity marine disease affecting a number of vulnerable taxa. Cnidarians, including both reef-building (scelaractinian) and other species of corals, have been among those taxa most affected by these increases. The rise of wildlife epizootic outbreaks, both in the oceans and in terrestrial ecosystems, has resulted in equal increases of studies of ecoimmunology. Research in these areas aims to understand how variation in disease susceptibility and immune response affect the ecology of vulnerable communities. Here I employ a variety of ecoimmunological approaches to study questions of cnidarian ecoimmunology. In the first half of my dissertation I describe cellular level pathways and patterns of expression that result in variation in disease susceptibility and immune dysfunction in a number of Caribbean corals. The second half of my dissertation shifts to studies of potential trade-offs associated with immunity. Here, I highlight key tradeoffs between growth and immunity that have significant implications for future community dynamics. Finally, the last chapter examines trade-offs between symbiosis and immune response and discussed the potential implications of this relationship under rapid change and increasing disease. Together the research presented here

provides novel insight into cnidarian ecoimmunology and addresses several key knowledge gaps in current understanding of cnidarian immunity and disease ecology. The results presented here will improve our ability to predict coral reef communities under future climate change and disease scenarios.

ACKNOWLEDGEMENTS

This dissertation would not have come to fruition without the hard work and support of my advisor, Dr. Laura Mydlarz who has been an incredible mentor and supporter of my scientific journey. Additionally my committee members, Andrew Baker, Todd Castoe, Jeffery Demuth, and Matthew Fujita provided both research support and guidance during my graduate career. Thanks to Mydlarz Lab members who have helped me along the way: Jorge Pinzon, Whitney Mann, Matthew Steffenson, Joshua Beach-Letendre, Contessa Ricci, Bradford Dimos and Nicholas Macknight. Thanks are also due to my undergraduate research assistant, Caleb Butler, for his work on the later portions of this research. Thank you to the biology department at the University of Texas at Arlington, faculty, staff, and graduate students for their support over the years. In particular thank you to fellow graduate students Dylan Parks, Collin Funkehouser, Matthew Mosely, and Shannon Beston for their intellectual support at various stages of this work. Furthermore, this project was supported by various groups at UTA including the Castoe (Audra Andrew) and Clark Labs (Robert Grinshpon), as well as the staff of the Genomics Core Facility (Kimberly Bowles and Melissa Muenzler). Finally, I am grateful to all the outside groups who assisted with fieldwork as part of this project. This includes: Ernesto Weil and his laboratory (University of Puerto Rico Mayaguez), Vanessa Brinkhuis (Florida Fish and Wildlife Conservation Commission), Andrew Baker and his laboratory, especially Ana Palacio, (University of Miami), and Marilyn Brandt and her laboratory (University of the Virgin Islands). Thank you to you all, as this project would not have happened without your support. Funding was provided by UTA Phi Sigma Society, and the National Science Foundation's Biological Oceanography and Integrative and Organismal Systems departments. Additional support came from an NSF Graduate Research Fellowship.

DEDICATION

For my grandmother, Marilyn Fuess, who spent 13 years tirelessly supporting and fostering my love of both the oceans and science. And for the family and friends who supported her in those efforts: Terry, Cindy, Rick and Leslie Fuess, Willa and Alan Fabian. I would not be where I am today if it wasn't for their love and support.

TABLE OF CONTENTS

ACKNOWLEDGEMENTS iv

DEDICATION v

CHAPTER ONE - INTRODUCTION 1

CHAPTER TWO - ASSOCIATIONS BETWEEN TRANSCRIPTIONAL CHANGES AND PROTEIN PHENOTYPES PROVIDE INSIGHTS INTO IMMUNE REGULATION IN CORALS 4

CHAPTER THREE - LIFE OR DEATH- DISEASE TOLERANT CORAL SPECIES ACTIVATE AUTOPHAGY FOLLOWING IMMUNE CHALLENGE 49

CHAPTER FOUR - TRANSCRIPTIONAL ANALYSES PROVIDE NEW INSIGHT INTO THE LATE STAGE IMMUNE RESPONSE OF A DISEASED CARIBBEAN CORAL 90

CHAPTER FIVE - MODULATION OF THE TGFβ PATHWAY AFFECTS IMMUNE RESPONSE IN A SCELARACTINIAN CORAL: POTENTIAL ECOLOGICAL IMPLICATIONS OF SYMBIOSIS 131

CHAPTER SIX- CONCLUSION 160

REFERENCES 162

CHAPTER ONE

INTRODUCTION

Throughout recent decades increasing anthropogenic stressors and environmental change have resulted in unprecedented increases in the number, type, and severity of epizootic outbreaks affecting a diversity of plant and animal taxa (Burge *et al.* 2014;Daszak *et al.* 2001;Mydlarz *et al.* 2006). The rapid rise of epizootic outbreaks has not only decimated numerous vulnerable marine and terrestrial taxa (Harvell *et al.* 2004;Kilpatrick *et al.* 2010;Smith *et al.* 2006), but has also revealed large gaps in existing scientific knowledge regarding the role of disease and immunity in shaping ecosystems. Identification of these knowledge gaps has resulted produced a new subfield of ecology, known collectively as the field of ecoimmunology. This field operates on the basis of two basic assumptions: immunity confers some cost to an individual and not all individuals are equally resistant to all pathogens (Hawley&Altizer 2011). Based on these assumptions, ecoimmunology seeks to understand a number of questions related to the causes and consequences of immune variation within and between species, including understanding the fitness costs of immunity (Graham *et al.* 2011) and the effects of population genetic variability (Lazzaro *et al.* 2006;Lazzaro *et al.* 2004), natural selection and evolution on immune variation (Jiggins&Kim 2006, 2007;Seppala 2015).

Marine ecosystems provide countless ecosystem services, including the production of food, filtration of water, protection of shorelines, and generation of revenue from ecotourism (Adger *et al.* 2005;Danielsen *et al.* 2005;Holmlund&Hammer 1999;Ruckelshaus *et al.* 2013). Despite their importance, marine ecosystems have experienced considerable degradation caused by over-exploitation and other anthropogenic stressors (Halpern *et al.* 2007;Halpern *et al.* 2008;Jackson *et al.* 2001;Lotze *et al.* 2006;Pauly *et al.* 2005;Syvitski *et al.* 2005). This includes severe declines

due to increasing marine disease outbreaks (Burge *et al.* 2014;Harvell *et al.* 1999;Harvell *et al.* 2004;Ward&Lafferty 2004). In recent decades, there has been a dramatic rise in the prevalence of marine disease among a number of taxa including: turtles, corals, marine mammals, mollusks, and urchins (Ward&Lafferty 2004). Among these species, arguably none have been more impacted than coral reefs, which have faced unprecedented global declines due to rapidly increasing marine disease (Croquer&Weil 2009;Daszak *et al.* 2001;Harvell *et al.* 1999;Sutherland *et al.* 2004;Weil *et al.* 2009a;Weil&Rogers 2011). Corals are ecologically essential organisms, forming the structural and trophic basis of diverse coral reef ecosystems (Sebens 1994) and providing many important ecosystem services, such as serving as coastal protection and supporting fishing industries (Spurgeon 1992). However, despite these severe disease-related declines, and the importance of affected species, many gaps still exist in our knowledge of marine diseases. These include lack of information regarding the origins and spread of marine diseases, infectious stages and host ranges, and immune responses of host organisms (Harvell *et al.* 2004).

This dissertation seeks to increase understanding of coral host immune response and to examine factors contributing to variation in immunity within and between species. The first two chapters specifically focus on describing immune responses in cnidarians (**Chapter 2**) and their variation between species (**Chapter 3**). In contrast the second portion of my dissertation examines various immune trade-offs. **Chapter 4** examines the fitness costs of mounting an immune response while **Chapter 5** examines the role of the transforming growth factor beta (TGFβ) and the potential implications of this relationship in the context of trade-offs between immunity and symbiosis. Together the five chapters of my dissertation greatly enhance understanding of the causes and consequences of variation in immune response in cnidarians.

The findings presented here provide an excellent starting point for future avenues of coral ecoimmunological research and add to a growing body of literature in this field.

CHAPTER TWO

ASSOCIATIONS BETWEEN TRANSCRIPTIONAL CHANGES AND PROTEIN PHENOTYPES PROVIDE INSIGHTS INTO IMMUNE REGULATION IN CORALS[1]

Lauren E. Fuess[a], Jorge H. Pinzón C[a,*], Ernesto Weil[b], Laura D. Mydlarz[a]

Fuess L. E., Pinzon C. J., Weil E., Mydlarz L. D. (2016) Associations between transcriptional changes and protein phenotypes provide insights into immune regulation in corals. Developmental & Comparative Immunology 62, 17-28.

[a] Department of Biology, University of Texas Arlington, Arlington, Texas, United States of America
[b] Department of Marine Sciences University of Puerto Rico, Mayagüez, Puerto Rico, United States of America
[*] **Present Address:** University of Texas Southwestern Medical Center, Dallas, Texas, United States of America

ABSTRACT

Disease outbreaks in marine ecosystems have driven worldwide declines of numerous taxa, including corals. Some corals, such as *Orbicella faveolata*, are particularly susceptible to disease. To explore the mechanisms contributing to susceptibility, colonies of *O. faveolata* were exposed to immune challenge with lipopolysaccharides. RNA sequencing and protein activity assays were used to characterize the response of corals to immune challenge. Differential expression analyses identified 17 immune-related transcripts that varied in expression post-immune challenge. Network analyses revealed several groups of transcripts correlated to immune protein activity. Several transcripts, which were annotated as positive regulators of immunity were included in these groups, some were downregulated following immune challenge. Correlations between expression of these transcripts and protein activity results further supported the role of these transcripts in positive regulation of immunity. The observed pattern of gene expression and protein activity may elucidate the processes contributing to the disease susceptibility of species like *O. faveolata*.

INTRODUCTION

Marine disease outbreaks have become one of the most serious threats to marine ecosystems (Burge *et al.* 2014;Harvell *et al.* 1999;Harvell *et al.* 2004;Ward&Lafferty 2004). Increases in marine disease have affected a diversity of taxa including: turtles, corals, marine mammals, mollusks, and urchins (Ward&Lafferty 2004). Scleractinian corals form the basis of coral reefs (Bozec *et al.* 2013;Graham&Nash 2013), which are some of the most diverse ecosystems on the planet (Bellwood&Hughes 2001;Bellwood *et al.* 2006;Odum&Odum 1955;Renema *et al.* 2008;Roberts 1995;Sebens 1994). However, coral reefs are currently in decline due to losses in coral coverage as a result of increasing disease prevalence (Daszak *et al.* 2001;Harvell *et al.* 1999;Sutherland *et al.* 2004).

Some corals, such as the major reef building Caribbean coral *Orbicella faveolata*, are particularly susceptible to disease (Sutherland *et al.* 2004;Weil 2004;Weil&Rogers 2011). *O. faveolata* is affected by as many as eight different diseases, including single pathogen bacterial diseases such as white plague type II, as well as microbial consortium diseases such as yellow band, black band, red band and darks spot syndrome, and diseases of unknown cause such as tumor growth syndrome (Weil 2004;Weil&Rogers 2011). Outbreaks of these diseases, coupled with other stressors, have driven massive declines in populations of this species across the Caribbean (Bruckner&Hill 2009;Nugues 2002;Weil *et al.* 2009a). Our understanding of *O. faveolata* susceptibility is limited due to a lack of knowledge in coral immunity.

Components of each of the three main processes of invertebrate immunity (i.e. pathogen recognition, signaling pathways, and effector responses) have been documented in corals and are essential to the host's defense against disease (Palmer&Traylor-Knowles 2012). Pattern recognition receptors (PRRs) are essential for pathogen recognition in invertebrate systems.

These molecules recognize and bind to potential microbial pathogens, triggering molecular pathways and inducing immune responses through signaling pathways (Akira&Takeda 2004;Akira *et al.* 2006;Janeway&Medzhitov 2002;Kawai&Akira 2011;Kumar *et al.* 2011;Takeuchi&Akira 2010). Signaling pathways consist of a number of intermediate molecules which promote the necessary changes in gene expression and protein activity to generate an effective defense response against potential pathogen(s) (Aderem&Ulevitch 2000;Akira&Takeda 2004;Akira *et al.* 2006;Arthur&Ley 2013;Newton&Dixit 2012;O'Shea&Plenge 2012). This chain of immune events is recognized as the "effector responses". Effector responses include, but are not limited to, the production of antimicrobial compounds and the activation of phagocytic cells (Aderem&Ulevitch 2000;Medzhitov 2007;Underhill&Ozinsky 2002).

Representative segments of all three immune processes have been described in corals and other cnidarians. A number of different immune receptors have been identified, including Toll-like receptors (TLRs) (Burge *et al.* 2014;Franzenburg *et al.* 2012;Miller *et al.* 2007;Poole&Weis 2014;Shinzato *et al.* 2011;Wolenski *et al.* 2011), and various types of lectins (Hayes *et al.* 2010;Kvennefors *et al.* 2010;Schwarz *et al.* 2007;Wood-Charlson&Weis 2009). Unfortunately, there is a paucity of data supporting their functional role in the recognition of pathogens in coral systems (Burge *et al.* 2013;Libro *et al.* 2013). In addition to signaling pathways, such as the melanin synthesis (Mydlarz *et al.* 2008;Palmer *et al.* 2008) and complement pathways (Brown *et al.* 2013;Miller *et al.* 2007), corals and other cnidarians, have been found to produce a number of immune effector responses such as the antioxidants catalase (Dash&Phillips 2012;Merle *et al.* 2007;Palmer *et al.* 2011), peroxidase (Mydlarz *et al.* 2009;Mydlarz&Harvell 2007;Palmer *et al.* 2011), and superoxide dismutase (Couch *et al.* 2008;Dash *et al.* 2007;Richier *et al.* 2003), as

well as antimicrobial compounds (Jensen *et al.* 1996;Vidal-Dupiol *et al.* 2011a;Vidal-Dupiol *et al.* 2011b).

Advancements of next generation technology have led to rapid increases in our understanding of coral genomics and transcriptomics (Barshis *et al.* 2014;Barshis *et al.* 2013;Miller *et al.* 2011;Palumbi *et al.* 2014;Pinzon *et al.* 2015;Shinzato *et al.* 2011). Many studies have examined modulation of coral immunity in response to a variety of stressors, including immune challenge (Anderson *et al.* 2016;Burge *et al.* 2013;Libro *et al.* 2013;Libro&Vollmer 2016;Pinzon *et al.* 2015;Weiss *et al.* 2013;Wright *et al.* 2015). Additionally, many studies have described and documented changes in immune proteins associated with the coral response to disease (Couch *et al.* 2008;Mann *et al.* 2014;Mydlarz&Harvell 2007;Mydlarz&Palmer 2011;Vidal-Dupiol *et al.* 2011a;Vidal-Dupiol *et al.* 2011b). However, no studies to our knowledge have used both a genomic and protein-based approach to study coral immune response, resulting in limited understanding of the connections between changes in gene expression and phenotypic response.

In order to better understand the genomic mechanisms underlying the coral immune response, and observed phenotypic differences in this non-model system, this study experimentally exposed colonies of *Orbicella faveolata* to bacterial pathogen-associated molecular patterns (PAMPs) and determine changes in both protein activity and gene expression on each. By leveraging existing knowledge and well-developed protein activity assays, gene expression and protein activity data were correlated to one another using novel analytical techniques in order to better understand the connections between gene expression and proteins. Using these novel techniques we show that complementing gene expression with protein activity

data can provide new insight regarding the response of corals to immune challenge and provide a more holistic image of coral response to immune challenge.

METHODS

Sample Collection

Coral fragments were collected in July of 2012 from five randomly selected *Orbicella faveolata* colonies from on Media Luna reef (17˚ 56.096 N; 67˚ 02.911 W) near La Parguera, Puerto Rico. Six small fragments (5 x 5 cm) were chipped off randomly from each colony with a hammer and chisel for a total of 30 fragments. Upon collection, the fragments were placed in labeled zip-lock bags and transported in ambient seawater to an indoor running saltwater facility at the Dept. of Marine Sciences (University of Puerto Rico – Mayagüez in Isla Magueyes). At the facility, three fragments from each colony were randomly assigned to one of the two treatment groups (control and PAMP exposure).

Five fragments from the same treatment were placed in one of six large plastic containers. Each container was aerated using an electric air pump and supplied with continuous flow of seawater. To control for temperature, the water was initially contained in a 500 gallon barrel where the temperature was maintained at 26°C using electric heaters and chillers when needed. Overhead lamps were used to maintain a 12 hour light/dark cycle. Fragments were maintained in these conditions for seven days prior to experimentation to allow for acclimatization and healing from fragmentation.

Experimental Design

Following the acclimatization period, continuous water flow and aeration were ceased and water levels in each of the large containers reduced to 3L. A piece of PVC pipe (6.35 cm high and 5.08 cm wide) was placed around each coral fragment, making a temporary

microenvironment. Using a micropipette, 1 mL of 7.57 mg/mL lippopolysaccharides (LPS), a pathogen-associated molecular pattern (PAMP), from *Escherichia coli* 0127:B8 (Sigma-Aldrich L3129-100MG) was added just above the surface of each treatment fragment. Final concentration of LPS in the container was 10 μg/mL spread over the five fragments on each PAMP exposure container. Control fragments received 1 mL of sterile seawater used in preparation of the LPS solution.

Exposure conditions were maintained for 30 minutes to ensure the LPS was taken into the coral, after which the aeration was resumed. Then the fragments were allowed in continuous flow for an additional 4 hours before being removed and frozen in liquid nitrogen. All samples were shipped on dry ice to the University of Texas at Arlington, where they were divided in two, leaving a small (~1 cm^2) piece for RNA extraction and the rest for protein extraction. Samples were then stored at -80°C until tissues were collected.

Protein extraction

Proteins were extracted over ice using a Paansche airbrush (Chicago, IL, USA) with coral extraction buffer (50 mmol tris buffer, pH 7.8, with 0.05 mmol dithiothreitol). Tissues were then homogenized using a Power Gen 125 tissue homogenizer with a medium saw tooth generator (Fisher Scientific, Pittsburgh, PA, USA) for 60 seconds on ice. Samples were then left on ice for 10 minutes. From the resulting extract, 1 mL was reserved for melanin analysis. The remaining volume was centrifuged for 5 minutes at 4°C and 3500 RPM in an Eppendorf centrifuge 5810R. The resulting supernatant, or coral extract, was split into two ~2 mL aliquots mL which were frozen in liquid nitrogen and stored at -80°C (Mydlarz & Palmer 2011).

Total protein in each sample was determined using the Red660 protein assay (G Biosciences, St. Louis, MO) standardized to BSA. These concentrations were used to standardize all biochemical assays conducted on the samples. All colorimetric assays were run in duplicate on 96 well plates using a Synergy two multi-detection microplate reader and Gen5 software (Biotek Instruments, Winooski, VT, USA).

Prophenoloxidase Assays (PPO)

Phenoloxidase was measured by diluting 20 µL of coral extracts in 20 µL of 50 mM phosphate buffer, pH 7.0. Samples were incubated with 25 µL trypsin (0.1 mg/mL) for 30 minutes at room temperature. After incubation, 30 µL of 10 mM Dopamine was added to each well. Absorbance of the product was then read every minute for 20 minutes at 490 nm. PPO activities were calculated as the change of absorbance (final-initial) per mg protein per minute at the steepest point of the 20 minute curve (Mydlarz&Palmer 2011).

Antioxidant Assays

Activity of three antioxidants was assessed: catalase (CAT), peroxidase (POX), and superoxide dismutase (SOD). Catalase activity was measured by adding 5 µL sample and 45 µL 50 mM phosphate buffer, pH 7.0 to a UV transparent microliter plate (Costar, Corning Life Sciences, Lowell, MA, USA). Subsequently, 75 µL of 25 mM hydrogen peroxide was added to each well to initiate the reaction. Absorbance at 240 nm was determined every 30 seconds for 15 minutes. Scavenged H_2O_2 was calculated by subtracting the final absorbance from the initial and a standard curve of hydrogen peroxide to determine the concentration (mM). Results were standardized by mg of protein (Mydlarz&Palmer 2011)**.**

To measure peroxidase, 20 µL of sample were diluted in 10 mM phosphate buffer, pH 6.0. Then 50 µL of 25 mM guiacol (Sigma-Aldrich) in 10 mM phosphate buffer, pH 6.0 were

added to each well. The reaction was initiated with 20 µL of 20 mM hydrogen peroxide and optical density was measured every minute for 15 minutes at 470 nm. Results were calculated as change in absorbance per minute, normalized according to mg of protein (Mydlarz&Harvell 2007).

The SOD Assay Determination Kit-WST (Fluka, Switzerland) was used to measure superoxide dismutase activity (Mydlarz & Palmer 2011). The procedure followed the manufacture's protocol, briefly, 10 µL of coral extract was incubated with 10 µL deionized water, 200 µL WST-1 and 20 µL xanthine oxidase for 20 minutes at 37°C. Percent inhibition of absorbance was then measured at 450 nm by comparing the absorbance of the samples to that of the control wells. Activity is reported as superoxide dismutase activity standardized by mg protein (Mydlarz&Palmer 2011).

Antibacterial Activity

Antibacterial activity of each sample was assessed against *Vibrio alginolyticus* using a strain isolated from *O. faveolata* (Strain provided by K. Ritchie, Mote Marine Laboratory, GenBank # X744690). This bacterial species has been proposed as the putative causative agent of Yellow Band Disease (Cervino *et al.* 2004;Cervino *et al.* 2008). Bacteria were grown overnight in salt amended (2.5 % NaCl) Luria Broth (EMD Chemicals, Gibbson, NJ) and diluted to a final optical density of 0.2 at 600nm prior to use in the assay. Sample wells consisted of 140 µL of each sample and 60 µL of diluted bacteria. Plates were then incubated in the spectrophotometer for 6 hours at 29°C, with reads at 600 nm recorded every 10 minutes. Growth rate of the bacteria was determined as the change in absorbance during the logarithmic phase of growth (Pinzon *et al.* 2014a).

2.7 Melanin Analysis

The portion of extract reserved for melanin analysis was lyophilized in a tarred two mL microcentrifuge tube overnight. Following removal of the water contact, the total dry tissue weight in the 1 mL aliquot was determined. Then, a spatula full of glass beads (~200 uL in volume) was added to each tube and vortexed for 10 seconds. Lastly, 400 µL of 10 M NaOH was added and the tubes were vortexed for 20 seconds. Tubes were incubated for 48 hours at room temperature in the dark. After incubation, the tubes were centrifuged for 10 minutes at room temperature at 1000 RPM. The supernatant (40 uL) was transferred a ½ well UV plate (Costar, Corning Life Sciences, Lowell, MA, USA). Absorbance was recorded at 410 and 490 nm and a standard curve of melanin dissolved in 10 M NaOH was used to convert absorbance to mg melanin (Mydlarz&Palmer 2011). The results are presented as mg of melanin per mg of tissue.

RNA Extractions and Sequencing

Total RNA was extracted from a small fragment (~3-5 µg) of tissue and skeleton using the RNAqueous Kit with DNAse step kit (Life Technologies AM1914). Fragments were initially ground with 800 µL of Lysis Buffer in a 2 mL microcentrifuge tube for 2 minutes. The tube was then centrifuged on an AccuSpin Micro (Fisher Scientific) and 700 µL of the supernatant were removed and placed in a new tube with 700 µl of 64% Ethanol solution from the kit. The resulting solution was passed through the kit's column and washed once with the wash one solution and twice with the wash two solution. The column was spun dry for 2 minutes and the resulting RNA was eluted with 50 µL elution solution. Possible DNA contamination was removed from samples by mixing 25 µL of the final extract with 1.5 µL DNase solution and 2.95 µL of Master Mix and incubating at 37°C for 1 hour. This solution

was then incubated at room temperature for 2 minutes with 2.95 μL inactivation reagent. The final extract (~30 μL) was transferred to a new tube and stored at -80°C.

cDNA Library Prep and Sequencing

Following extraction the three replicates from each colony within a treatment were pooled for RNA library sequencing, due to budgetary constraints (n = 5 per treatment). The quality of the combined extract was assessed using an Agilent BioAnalyzer 2100 at the University of Texas at Arlington Genomics Core facility. Samples with quality values (RIN number) greater than 8 were processed for cDNA library creation using an Illumina TruSeq RNA with Poly-A selection libraries kit (Illumina). Combined samples were sent to the University of Texas Southwestern Medical Center Genomics Core facility for library construction and sequencing. All 10 libraries were sequenced on a single lane.

Transcriptome Assembly and RNA-seq analysis

RNA-seq libraries were sorted and assessed for quality of reads. Adaptors and low quality reads were removed using Trimmomatic v. 3 (Lohse et al. 2012). Non-host sequences were filtered out using methods described in Pinzon et al 2015. All alignments were performed using BLAT (parameters: 90% identity and e-value < 0.000001). Duplicate hits were removed and coral-only sequences were retrieved for further analysis using cdbfasta/cdbyank (http://sourceforge.net/projects/cdbfasta/).

Differential expression analyses were conducted using Cufflinks software package (v. 2.2.1;(Trapnell *et al.* 2013). Read counts for each transcript were obtained by aligning coral only reads from each sample to the *O. faveolata* reference transcriptome (Pinzon *et al.* 2015) using default parameters in the Cufflinks package (Trapnell *et al.* 2013). Normalized expression values were then generated in the Cuffdiff package with the default parameters

(Trapnell *et al.* 2013). These normalized expression values were then compared between treatment groups using default parameters of the Cuffdiff package to estimate average $\log_2$fold change of each transcript. These $\log_2$fold change values were used to identify significantly differentially expressed transcripts (adjusted $p < 0.05$) across treatments.

Transcriptome Annotation and Gene Ontology (GO) Analyses

Following transcriptome assembly, transcriptomic sequences were annotated against the UniProtKB/Swiss-Prot and TrEMBL databases (blastx algorithm, 1.0E-5 e-value threshold). Enriched GO terms associated with the differentially expressed transcripts were identified using the Database for Annotation, Visualization and Integrated Discovery (DAVID) v. 6.7. Analyses were performed using the Biological Processes domain of annotations. A list of UniProt accession numbers for all annotated transcripts in the transcriptome was used as a background. GO terms with a Benjamini-Hochberg adjusted p-value lower than 0.05 were considered significantly enriched.

Weighted Co-Expression Network Analysis

Gene expression data was analyzed using the Weighted Co-Expression Network Analysis (WGCNA) R package (Langfelder&Horvath 2008) to identify modules of co-expression between transcripts and proteins for all samples combined. Normalized read counts for all differentially expressed transcripts were $\log_2$ transformed. These values were used to create a signed, consensus network using automatic network construction methods (parameters: soft power=20, minimum module size = 8, deep split = 2, merged cut height = 0.4, minimum KE for module assignment = 0.2, verbose = 3, cutHeight = 0.999). Eigengene values (average expression of all transcripts in a module) of each module were correlated to results from the five biochemical assays using a Pierson correlation. Correlations were conducted on two sets

of samples: all of the samples (n = 10) and samples from the PAMP exposure only (n = 5). Modules with significant correlations (p-value ≤ 0.05) were selected for further analyses. Gene ontology (GO) enrichment for each significant module was conducted in DAVID using SwissProt IDs (spIDs) for all annotated transcripts in a given module, with spIDs of all significantly differentially expressed transcripts used as a background.

Statistical Analysis: Gene expression to Phenotype Correlations

To account for potential intracolonial variation this experiment was run with three replicates per colony. Proteins were extracted and assayed for each replicate. However, as mentioned above, RNA extracts from each of the three replicates from each colony within a treatment were pooled for RNA library sequencing (resulting in n = 5). In order to compare gene expression with protein data, protein data was averaged for each colony and treatment group, resulting in a sample size of 5 for this analysis.

All transcripts belonging to modules with significant correlations to one or more measures of immunity were assessed for correlations to protein activity from one of the assays performed in this study, herein referred to as 'immune phenotypes'. While there were no statistical differences between the controls and corals exposed to PAMPs within the biochemical assays, we used this data to examine the possible correlation between gene expression and the activity of immune proteins. Log_2 transformed normalized (FPKM) read counts from cufflinks for each transcript of interest were correlated to values for each of the immune assays using a Pierson correlation. Correlations were calculated using the same two sets of samples used for module to trait correlations (all samples i.e. controls and PAMP exposure, n = 10, or the PAMP exposed subset of samples, n = 5). Two separate sample sets were used in order to identify transcripts, such as effector molecules, which are correlated to

immune protein activity under all conditions, as well as transcripts, such as receptors, which would only be correlated to immune protein activity when in the presence of an elicitor such as bacterial PAMPs.

RESULTS

Transcriptome Assembly

Sequencing of all ten samples (5 control, 5 PAMP treated) resulted in a total of 120,020,664 paired end reads. Sequencing reads are available for download on NCBI (SRA Accession # SRP044398). Final alignment of quality assessed and trimmed reads to the O. faveolata reference transcriptome resulted in consensus 31,958 contigs with an N50 value of 1928 base pairs. Comparison of these consensus sequences to the UniProtKB/Swiss-Prot database yielded annotations for 10,638 (~33%) transcripts.

Differential Expression and Gene Ontology Analysis

Of the 31,947 expressed transcripts, 371 were differentially expressed, 111 downregulated and 260 upregulated in the PAMP-exposed compared to control samples. Only 40% (149) of these genes could be annotated against UniProt and TrEMBL protein databases (**Supplementary Table 1**). Gene ontology analyses of these 149 annotated differentially expressed transcripts found no enriched biological processes. However, from this set of genes, we identified 17 involved in immune processes (**Figure 1, Table 1)**. These immune-related transcripts could be categorized as one of three processes of immunity: recognition, signaling, and effector response.

Immune Recognition

Seven putative immune recognition transcripts were differentially expressed upon exposure to immune challenge: galaxin, an apolipophorin, a transcript containing a

leucine-rich repeat (LRR) domain, and four mucin-like proteins, Galaxin, which may have a dual function as a recognition molecule (Heath-Heckman *et al.* 2014), decreased in expression 1.5 log_2fold in samples exposed to PAMPs. The homologue of the insect pattern recognition molecule apolipophorin (Whitten *et al.* 2004;Zdybicka-Barabas&Cytryńska 2013) increased in expression by 1.4 log_2fold. Additionally, a protein containing a LRR-domain, which is characteristic of immune receptors such as TLRs (Buchanan&Gay 1996), decreased in expression by 1.5 log_2fold in samples exposed to bacterial PAMPs. Finally, we documented four mucin-like proteins that were significantly differentially in our treated samples. Mucin domains are common to immune receptors in the TIM family (T cell, immunoglobulin, mucin) (Anderson *et al.* 2007;Kuchroo *et al.* 2003;Zhang *et al.* 2012). Expression of three of these mucin-domain containing proteins was increased (1.8, 3.3, 5.0 log_2fold increases); however expression of the fourth was decreased 1.9 log_2fold in immune challenged samples.

Signaling Processes

Four transcripts involved in either downstream TLR signaling or regulation of NF-κB were differentially expressed. Two transcripts associated with TLR signaling, ATP-binding cassette sub-family A member one (Yvan-Charvet *et al.* 2010) and deleted in malignant brain tumor one (DMBT1; (Rosenstiel *et al.* 2007), were upregulated with one and 1.3 log_2fold change respectively. In contrast, expression of γ-taxilin, a negative regulator of TLR signaling (Yu *et al.* 2006), decreased in expression (γ-taxilin had no detectable expression in treatment samples). Finally, a transcript involved in activity of NF-κB, γ-secretase subunit PEN-2 (Poellinger&Lendahl 2008), increased 1.7 log_2fold in samples exposed to bacterial PAMPs.

Effector Processes

Six transcripts identified as immune effectors were differentially expressed. Two heat shock transcripts (Hsps), *Hsp70* and *Hsp90*, which play roles in immune effector responses (Asea *et al.* 2002;Kaufman 1990;Mayor *et al.* 2007), increased in expression (*Hsp70* increased 1 log_2fold; *Hsp90* expression was not measurable in control samples). A transcript involved in phagocytosis, Ras-like GTP-binding protein Rho (Caron&Hall 1998), increased 1.8 log_2fold in corals following exposure to bacterial PAMPs. Additionally, 3 transcripts which may function in antioxidant responses were differentially expressed following exposure to bacterial PAMPs: a GFP-like fluorescent chromoprotein (Palmer *et al.* 2009), Peroxisomal biogeneisis factor 11C (PEX11C; (Aruoma 1998;Schrader *et al.* 1998), and peroxidasin (Nelson *et al.* 1994). Expression of the GFP-like transcript decreased 1.6 log_2fold, while PEX11C and peroxidasin increased 1.7 and 2.1 log_2fold respectively.

WGCNA network construction

WGCNA network construction of 371 transcripts resulted in eight modules ranging in size from 10 to 57 transcripts. Additionally, a ninth module contained 1 gene which could not be grouped in any other module. This module was excluded from further analyses. Seven of these modules were significantly correlated with an immune phenotype in the control or PAMP exposed subsets of samples. In the control subset, bacterial doubling time was positively correlated with Module 7 ($r = 0.94$, $p = 0.01$). Also in the control subset, melanin was positively correlated with Module 4 ($r = 0.93$, $p = 0.02$) (**Supplementary Figure 1**). In the PAMP exposed subset, Modules 4 ($r = -0.92$, $p = 0.03$) and 8 ($r = -0.99$, $p = 1e^{-04}$) were and negatively correlated with melanin. Prophenoloxidase activity was positively correlated

to both Module 5 (r = 0.93, $p = 0.02$) and 6 (r = 0.89, $p = 0.04$). Peroxidase was positively correlated to Module 5 (r = 0.95, $p = 0.008$) and negatively correlated to Module 2 (r = -0.91, $p = 0.03$) (**Supplementary Figure 2**).

While none of the seven modules significantly correlated to any immune phenotype showed significant gene ontology enrichment, a number of immune-related transcripts were found in these modules (**Supplementary Table 2**). For example: Module 4 included putative immune recognition molecule: galaxin. Module 7 included the receptor, apolipophorin, signaling molecules DMBT1 and γ-secretase subunit PEN-2, and the effector *Hsp70*.

Expression to Protein Correlations

Analysis of protein data alone revealed no significant differences between control and PAMP-treated samples (**Table 2**). However, of the 247 transcripts included in the seven significant modules, 91 (36.8%) were significantly correlated to one or more immune phenotypes in the entire set (35 transcripts; $n = 10$) or in the PAMP treatment (76 transcripts; $n = 5$). Of these 91 transcripts, 45 were assigned annotations with sufficient confidence (e-value < $1.0E^{-5}$; transcripts annotated as uncharacterized/hypothetical/predicted proteins excluded; **Table 2**). Correlations of relevant immune and stress transcripts with immune phenotypes are summarized in **Figures 2** and **3**.

DISCUSSION

Climate change and other anthropogenic stressors have been affecting natural communities at what appears an unprecedented scale. One of the most prominent impacts of climate change on natural communities has been drastic increases in the prevalence of disease or disease-like symptoms, causing unprecedented declines in many taxa including corals (Aronson&Precht 2001;Bellwood *et al.* 2004;Daszak *et al.* 2001;Harvell *et al.* 1999;Hughes *et al.* 2003;Schutte *et*

al. 2010). Despite this continuing and growing issue, our knowledge of the cellular and molecular mechanisms used by corals to resist and battle infections is still limited. Progress has been made in identifying elements of immunity on both phenotypic and genetic scales (Brown *et al.* 2013;Miller *et al.* 2007;Mydlarz&Harvell 2007;Mydlarz *et al.* 2008;Mydlarz *et al.* 2010;Mydlarz&Palmer 2011;Palmer *et al.* 2009;Poole&Weis 2014). Still, current knowledge is fragmented and few studies have investigated pathways of immunity or the relationship between changes in gene expression and immune protein activity (Vidal-Dupiol *et al.* 2014). Here we provide a comprehensive description of the response of the Caribbean coral *Orbicella faveloata* to an immune challenge with PAMPs. Our analyses include both transcriptional and biochemical data that document changes in gene expression and protein activity associated with the corals' immune response (**Figure 4**).

Transcriptional Expression Patterns

In this study we documented significant changes in 17 potential immune transcripts. This group of seventeen transcripts was representative of all three major processes of invertebrate immunity: recognition, signaling, and effector responses. Seven transcripts from this group were potential immune recognition transcripts, four of which increased post-PAMP exposure and three of which decreased. Interestingly, three transcripts identified as potential immune recognition molecules all decreased following exposure to bacterial PAMPs: galaxin, a mucin-like protein, and a LRR-domain containing protein. Galaxin has previously been described as a protein component of the coral exoskeleton (Watanabe *et al.* 2003), however other studies have also suggested this molecule may function in the recognition of symbionts in squid-*Vibrio* associations (Heath-Heckman *et al.* 2014). In this study, expression of

galaxin decreased significantly following exposure to PAMPs, suggesting a more complex or novel role for this protein in coral immunity.

A gene known as TIM-3 (T cell, immunoglobulin, mucin-3) with a mucin domain, both positively and negatively regulates expression of immune cytokines (Zhang *et al.* 2012). While three of the four documented mucin-like transcripts increased in expression following exposure to PAMPs, a fourth transcript decreased significantly. It is possible that the function of mucin domain-containing proteins in corals is divided between splice variants or gene duplicates as observed in our results, thus explaining the conflicting patterns of expression of mucin-like protein transcripts seen here. A transcript containing a LRR domain was downregulated in immune-challenged corals. LRR domains are key components of many immune recognition molecules (Bell *et al.* 2003;Inohara *et al.* 2005;Martinon&Tschopp 2005). In many Cnidarians, such as *Psudeodiploria strigosa*, TLR-like receptors are believed to be constructed of two separate transcripts, one containing the LRR domain, and the second containing a TIR domain (Ocampo *et al.* 2015). In the Cnidarian, *Hydra*, the gene HyLRR-2 encodes a protein that binds flagellin and elicits an immune response in the presence of other immune receptor genes (Bosch *et al.* 2009). Finally, other immune recognition molecules which contain LRR, such as NOD-like receptors, have been described in *Orbicella faveolata* (Anderson *et al.* 2016). The downregulation of the galaxin and LRR recognition transcripts is counter-intuitive based on the function inferred from their annotations.

In addition to documenting changes in several potential immune recognition transcripts, we also identified four putative signaling molecules which were differentially expressed following exposure to bacterial PAMPs. One of these, γ-taxilin, which negatively regulates TLR4 signaling by inhibiting activating transcription factor four activity (Yu *et al.* 2006),

was downregulated following immune challenge likely promoting immune response. Upregulated immune signaling transcripts included ATP-binding cassette sub-family A member 1 (ABCA1), which negatively regulates cytokine production by macrophages and resultant TLR4 signaling (Yvan-Charvet *et al.* 2010). This pattern of expression is contrary to expected patterns following immune stimulation by bacterial PAMPs as it likely results in immune suppression.

Finally, six transcripts involved in effector responses were differentially expressed. These included two heat shock proteins (70 and 90). Both of these proteins, which act as molecular chaperones (Feder&Hofmann 1999), assist in coral response to stress (Barshis *et al.* 2013;Black *et al.* 1995;Császár *et al.* 2009;DeSalvo *et al.* 2008). Expression of both *Hsp70* and *Hsp90*, increased following exposure to bacterial PAMPs. Expression of several other effector transcripts including two transcripts potentially involved in antioxidant response, PEX11C (Aruoma 1998;Schrader *et al.* 1998) and peroxidasin (Nelson *et al.* 1994), and the phagocytosis associated transcript Rho (Caron&Hall 1998), also increased following exposure to bacterial PAMPs. However, expression of a third transcript, green fluorescent protein (GFP), decreased following exposure to bacterial PAMPs. Even though GFP's have been shown to decrease during heat stress (DeSalvo *et al.* 2008;Dove *et al.* 2006;Roth&Deheyn 2013;Smith-Keune&Dove 2008), their possible function as antioxidant suggest that they should increase as part of an appropriate immune response (Mydlarz&Palmer 2011;Palmer *et al.* 2009).

WGCNA Analysis

Analysis of all differentially expressed transcripts with WGCNA software yielded eight modules of co-expressed transcripts. Each module should consist of transcripts with similar

biological function and be relatable to specific downstream responses, i.e. protein activity. While lack of annotations limited characterization of many of these modules, several patterns could be ascertained. Module 3, containing 35 annotated transcripts, included six transcripts associated with actin activity. Module 7, with 22 annotated transcripts, contained transcripts associated with lipid processing (four in total). Finally, Module 6 contained 12 annotated transcripts, four of which were associated with apoptotic processes. Seven of these modules were significantly correlated at least one immunity phenotype (i.e. protein activity). Module 5 correlated to both prophenoloxidase and peroxidase activity, indicating that they contain transcripts that either regulate or are regulated by these immune proteins. This link provides further support to previous findings that the production of peroxidase (Cerenius&Soderhall 2004) and other antioxidants (Mydlarz&Palmer 2011) is associated with the melanin synthesis cascade.

Correlations between transcript expression and immune phenotypes

To further explore the roles of specific transcripts in the immune response of corals, we correlated the expression of individual transcripts to immune-related protein activity to add new depth to studies of gene expression. While correlation does not necessary equal causation, our approach attempts to isolate, or filter, the transcripts associated with a general stress response from those more directly related to the biochemical immune response. Using this approach, we identified six immune receptor transcripts, galaxin, LRR and IQ domain-containing transcript, and three mucin-like transcripts, as well as one signaling transcript (DMBT1) that were correlated to an immune phenotype. Galaxin was positively correlated to prophenoloxidase and peroxidase activity, even though it was downregulated after PAMP treatment. This suggests that the transcript may in fact be serving as a recognition molecule

and activator of immunity. LRR and IQ-domain-containing protein expression was negatively correlated to antibacterial activity. Based on these correlation results, this protein may in fact be involved in negative regulation of antibacterial activity, thus explaining its downregulation following immune challenge. Furthermore, two mucin-like transcripts were both upregulated and significant correlated to one or more immune phenotypes (comp263105 to prophenoloxidase and peroxidase and comp347198 to catalase) in samples exposed to PAMP. Each transcript was correlated to a different measure of immunity, suggesting that either duplication or alternative splicing of a mucin, or similar immune receptor genes, may have led to division of labor which each unique transcript activating a separate arm of immunity. Finally, the DMBT1 signaling transcript was positively correlated to antibacterial activity when all samples were analyzed. This is indicative of its proposed role in agglutination and inactivation of bacterial pathogens (Bikker *et al.* 2002).

Our results indicated a number of transcripts related to effector responses were correlated to at least one measure of immune-related protein activities. This is consistent with the nature of the biochemical assays, which measure activity of effector responses. In total we found three immune effector transcripts which were correlated to one or more measures of immunity: *Hsp70,* GFP, and PEX11C. Expression of *Hsp70* was positively correlated to prophenoloxidase activity, supporting previous findings that *Hsp70* expression increases following immune challenge in corals (Brown *et al.* 2013). While there is no known direct link between prophenoloxidase activity and expression of *Hsp70,* it is possible similar upstream pathways regulates these processes.

PEX11C and GFP, two effector transcripts associated with antioxidant activity, were positively correlated to both prophenoloxidase and peroxidase activity in the PAMP

treatment. PEX11 proteins control the proliferation of peroxisomes, which are major sites of hydrogen peroxide degradation. Peroxidases also contribute to the degradation of hydrogen peroxide in other parts of the cell (Aruoma 1998). Co-regulation of peroxidase proteins, PEX11, and other antioxidant transcripts would explain this correlation. Coral fluorescent proteins, such as GFP, have antioxidant properties and contribute to immune functions in corals (Palmer *et al.* 2009). The results of correlation analyses provide strong evidence that both of these transcripts contribute to peroxidase activity in samples. Furthermore, production of multiple antioxidants is correlated to prophenoloxidase activity in corals (Mydlarz&Palmer 2011), thus explaining the correlation between expression of PEX11 and GFP to prophenoloxidase in addition to peroxidase activity during exposure to PAMPs. Importantly, while the results of our correlation analyses suggest that GFP expression is positively correlated to immune activity, this transcript was downregulated during immune challenge.

Global patterns of immune regulation and conclusions

While many transcripts, such as *Hsp70* and DMBT1, were regulated in the expected pattern to confer resistance and immunity to a pathogen, there were other transcripts that displayed counter-intuitive patterns of regulation. Several of these transcripts were not only annotated as potential immune genes, but also were significantly correlated to immune phenotypes. While it is possible that observed downregulation of these transcripts is an artifact of the time point selected for sampling, it is also possible that these genes are undergoing dysfunctional regulation (referred to as "dysregulation"). "Dysregulation" of transcripts may significantly affect the response of *O. faveolata* to disease and may partially explain previously documented susceptibility of the species to disease (Bruckner&Hill

2009;Sutherland *et al.* 2004;Weil 2004;Weil&Rogers 2011). . Similar phenomena have been noted in other systems, where "dysregulation" of immune transcripts and consequential immune compromise result from transcriptomic mutations (Hodge *et al.* 1996;Kobasa *et al.* 2007;Welker *et al.* 2007). Our findings here suggest that similar patterns may exist in corals, thus potentially explaining disease susceptibility in certain coral species (Raymundo *et al.* 2005;Sutherland *et al.* 2004;Ward *et al.* 2006;Weil *et al.* 2009a). Further studies examining immune response at multiple time points in corals will be necessary to fully understand the extent and importance of potential immune transcript "dysregulation" in *O. faveolata*.

In conclusion, by using novel approaches to compare changes in immune-related proteins activity to those in transcript expression, we were able to identify transcripts involved in the three major aspects of coral immune response: recognition, signaling, and effector responses. Our findings extend beyond transcriptional description by correlating expression of individual transcripts to biochemical measures of immune proteins activity. Further use of similar methods will serve to expand our knowledge of invertebrate immunity in general, and specifically regarding the mechanisms controlling host responses to infection in corals. These data provide a foundational resource that will lead to even greater understanding of important questions of invertebrate immunity.

ACKNOWLEDGEMENTS

The authors would like to acknowledge the Department of Marine Sciences, University of Puerto Rico Mayagüez (UPRM) for partial funding for boat and diving, logistical support and laboratory space. Additionally, the authors would like to thank Duane Sanabria, Luis Rodriguez, and Derek Soto for support in the field and the staff of the Genetics Core Facility (UTA) for assistance with laboratory work and anonymous reviewers for edits to improve the manuscript. The analyses

were run on a server provided by the UTA Office of Information Technology. Samples were collected under the specification of research collection permits to the Department of Marine Science UPRM.

FIGURES AND TABLES

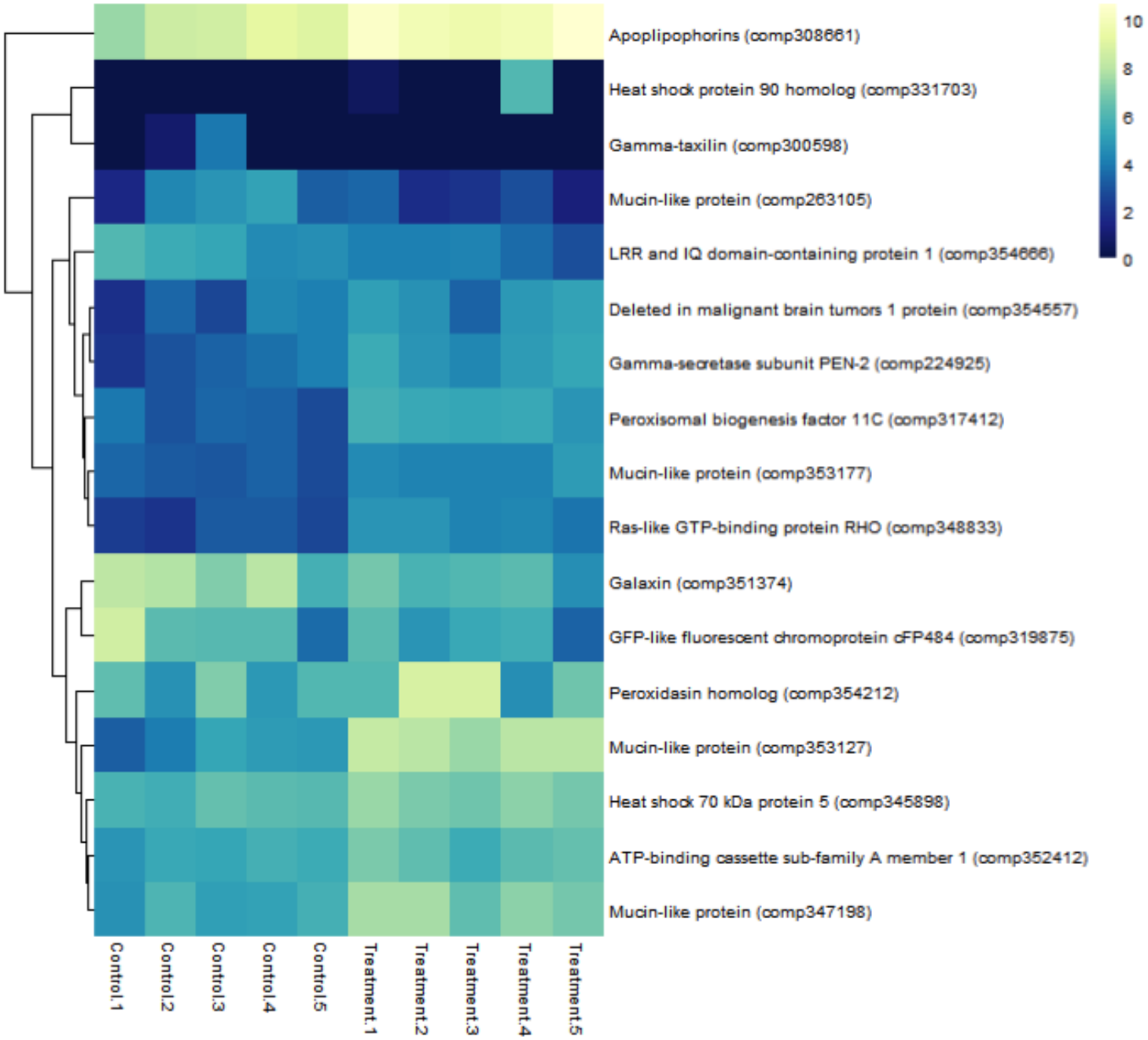

Figure 1: Heatmap of expression of the 17 differentially expressed transcripts involved in immunity, clustered based on expression values.

Table 1: Immune Gene Blast Annotation Results

List of blast results for annotated, differentially expressed immune genes. Transcripts were annotated against the Uniprot/SwissProt and TrEMBL databases using default parameters with a minimum e-value cutoff of 1E-5. Listed in alphabetical order by protein name.

Locus	spID	Protein Name	Percent match	eValue	Bit Score
comp308661	Q9U943	Apolipophorins	29.06	7.00E-37	155
comp352412	P41233	ATP-binding cassette sub-family A member 1	48.06	0	1702
comp354557	Q9UGM3	Deleted in malignant brain tumors 1 protein	39.96	7.00E-95	348
comp351374	D9IQ16	Galaxin	36.58	4.00E-35	142
comp224925	Q8JHF0	Gamma-secretase subunit PEN-2	63.41	1.00E-31	119
comp300598	Q9NUQ3	Gamma-taxilin	30.95	4.00E-22	100
comp319875	Q9U6Y3	GFP-like fluorescent chromoprotein cFP484	62.86	3.00E-76	237
comp345898	Q90593	Heat shock 70 kDa protein 5	84.73	0	961
comp331703	P41887	Heat Shock Protein 90 Homolog	73.72	6.00E-64	213
comp354666	Q96JM4	LRR and IQ domain-containing protein 1	29.39	4.00E-80	300
comp263105	B3EWY9	Mucin-like Protein	49.71	1.00E-41	167
comp347198	B3EWY9	Mucin-like Protein	37.48	9.00E-128	432
comp353127	B3EWY9	Mucin-like Protein	34.02	1.00E-51	203
comp353177	B3EWZ6	Mucin-like Protein	38.89	5.00E-34	147
comp354212	Q3UQ28	Peroxidasin homolog	35.81	4.00E-91	321
comp317412	Q96HA9	Peroxisomal membrane protein 11C	39.24	2.00E-46	169
comp348833	P01122	Ras-like GTP-binding protein RHO	73.77	2.00E-19	92.8

Table 2: **Protein Assay Results**

Results of the protein activity assays for all five phenotypic measures of immunity. No assays showed significant differences ($p < 0.05$) between control and treatment groups.

	Control	Treatment
Prophenoloxidase		
Average	1.88	2.20
Standard Error	0.34	.35
Melanin		
Average	3.04	3.56
Standard Error	.60	0.12
Catalase		
Average	1130.39	1230.49
Standard Error	123.76	207.52
Peroxidase		
Average	7.36	8.34
Standard Error	0.80	1.08
Superoxide Dismutase		
Average	15278.17	16589.71
Standard Error	1450.81	1580.367
Anibacterial Activity		
Average	3.58	3.65
Standard Error	0.12	0.12

Table 3: Correlations between putative immune transcripts and immune protein activity
Summary of transcripts with significant ($p < .05$) Pearson correlations to one or more measures of immune protein activity. Annotations were determined via blastx against the UniProtKB/Swiss-Prot database (1.0E-5 e-value threshold). Listed in alphabetical order by protein name.

Transcript ID	Protein name	Protein activity assay	Treatment	r	*p*
comp343799	2-acylglycerol O-acyltransferase 1	Prophenoloxidase	PAMP	-0.988	0.002
		Peroxidase	PAMP	-0.913	0.030
comp333208	2-acylglycerol O-acyltransferase 2-A	Melanin	PAMP	0.925	0.024
comp351374	39S ribosomal protein L41-A, mitochondrial	Catalase	PAMP	0.881	0.048
comp346081	3-hydroxypropionyl-coenzyme A dehydratase	Antibacterial Activity	PAMP	0.931	0.021
comp345898	78 kDa glucose-regulated protein (*Hsp70*)	Prophenoloxidase	All	0.643	0.045
		Melanin	PAMP	-0.985	0.002
comp226382	Arrestin-domain containing protein 4	Antibacterial Activity	All	0.672	0.033
comp341607	Bifunctional ATP-dependent dihydroxyacetone kinase/FAD-AMP lyase (cyclizing)	Prophenoloxidase	PAMP	0.931	0.021
		Peroxidase	PAMP	0.971	0.006
comp317101	Calumenin	Superoxide Dismutase	All	0.638	0.047
		Prophenoxidase	PAMP	0.956	0.011
comp339880	Carbonic anhydrase 2	Antibacterial Activity	PAMP	0.980	.003
comp347148	Carbonic anhydrase 2	Antibacterial Activity	PAMP	0.970	.006
comp340734	CTD small phosphatase-like protein	Antibacterial Activity	All	0.655	0.040
comp349474	Cyclic AMP-dependent transcription factor ATF-5	Catalase	PAMP	0.910	0.032
comp340439	Cysteine string protein	Antibacterial Activity	PAMP	0.958	0.010
comp349461	Cytochrome C oxidase subunit NDUFA4	Antibacterial Activity	All	0.641	0.048
comp345160	Cytochrome P450 3A24	Prophenoloxidase	PAMP	-0.959	0.010

		Peroxidase	PAMP	-0.989	0.001
comp354557	Deleted in malignant brain tumors one protein	Antibacterial Activity	All	-.700	0.024
comp347593	EGF-like repeat and discoidin I-like domain-containing protein 3	Peroxidase	PAMP	-0.969	0.006
comp343301	Estradiol 17-beta-dehydrogenase 8	Prophenoloxidase	All	-0.656	0.039
comp351548	Ferric-chelate reductase 1	Superoxide dismutase	PAMP	0.907	0.034
comp332277	Flavin Reductase	Prophenoloxidase	All	0.702	0.024
comp353272	Formate acetyltransferase 2	Doubling Time	All	0.652	0.041
comp351374	Galaxin	Prophenoloxidase	PAMP	0.956	0.011
		Peroxidase	PAMP	0.948	0.014
comp319875	GFP-like fluorescent chromoprotein cFP484	Prophenoloxidase	PAMP	0.922	0.026
		Peroxidase	PAMP	0.921	0.027
comp315290	High mobility group protein B3	Antibacterial Activity	All	0.640	0.046
comp354666	Leucine-rich repeat and IQ domain-containing protein 1	Antibacterial Activity	All	0.662	0.037
comp353127	MAM and LDL-receptor class A domain-containing protein 2	Melanin	PAMP	-0.882	0.048
comp263105	Mucin-like protein	Prophenoloxidase	PAMP	0.960	0.010
		Peroxidase	PAMP	0.907	0.034
comp347198	Mucin-like protein	Catalase	PAMP	0.948	0.014
comp345211	Multidrug resistance-associated protein 1	Melanin	PAMP	-0.880	0.049
comp354720	NADH-ubiquinone oxidoreductase chain 4	Prophenoloxidase	PAMP	0.910	0.032
		Peroxidase	PAMP	0.931	0.021
comp317412	Peroxisomal biogenesis factor 11C	Prophenoloxidase	PAMP	0.968	0.007
		Peroxidase	PAMP	0.937	0.019
comp343191	Probable UMP/CMP kinase 1	Prophenoloxidase	All	0.733	0.016
		Superoxide	All	0.671	0.034

		Dismutase			
comp331913	Protein zinc induced facilitator-like 1	Prophenoloxidase	PAMP	-0.923	0.025
		Peroxidase	PAMP	-0.943	0.016
comp337513	RNA-binding protein Musashi homolog 1	Antibacterial Activity	PAMP	0.914	0.030
comp337740	Sodium-coupled monocarboxylate transporter 1	Melanin	PAMP	-0.952	0.013
comp333933	Succinate dehydrogenase [ubiquinone] cytochrome b small subunit B, mitochondrial	Antibacterial Activity	PAMP	0.943	0.016
comp352754	Tetratricopeptide repeat protein 28	Peroxidase	PAMP	-0.934	0.020
comp354523	Tetratricopeptide repeat protein 28	Prophenoloxidase	PAMP	-0.934	0.020
		Peroxidase	PAMP	-0.918	0.028
comp328348	Tetratricopeptide repeat protein 28	Peroxidase	PAMP	-.955	.011
comp353371	Tubulin beta chain	Superoxide Dismutase	PAMP	.881	.049
comp343899	Tyrosine-protein kinase STK	Antibacterial Activity	All	0.641	0.046
comp327632	Ubiquinone/menaquinone biosynthesis C-methyltransferase UbiE	Prophenoloxidase	All	.637	.047
		Melanin	PAMP	-0.928	0.023
comp350393	Uncharacterized skeletal organic matrix protein 2	Peroxidase	PAMP	-0.895	0.040
comp325048	Unconventional myosin-IXb	Melanin	PAMP	-0.949	0.014
comp345834	Valine-tRNA ligase	Prophenoloxidase	PAMP	0.934	0.020

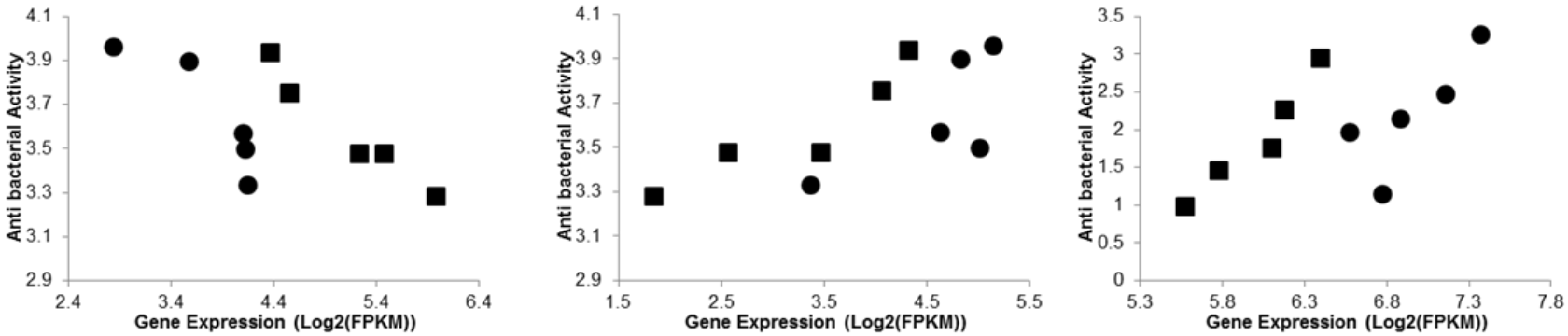

Figure 2: Summary of significant gene to immune-related protein activity pearson correlations for all samples (*n*=10). a) correlations between antibacterial activity (doubling time) and expression of LRR and IQ domain-containing protein 1 (r= -0.688, *p* = 0.028); b) correlations between antibacterial activity and expression of DMBT1 (r= 0.711, *p*=0.021); c) correlations between PPO activity and expression of heat shock 70 kDa protein 5 (r=0.643, *p*=0.045).

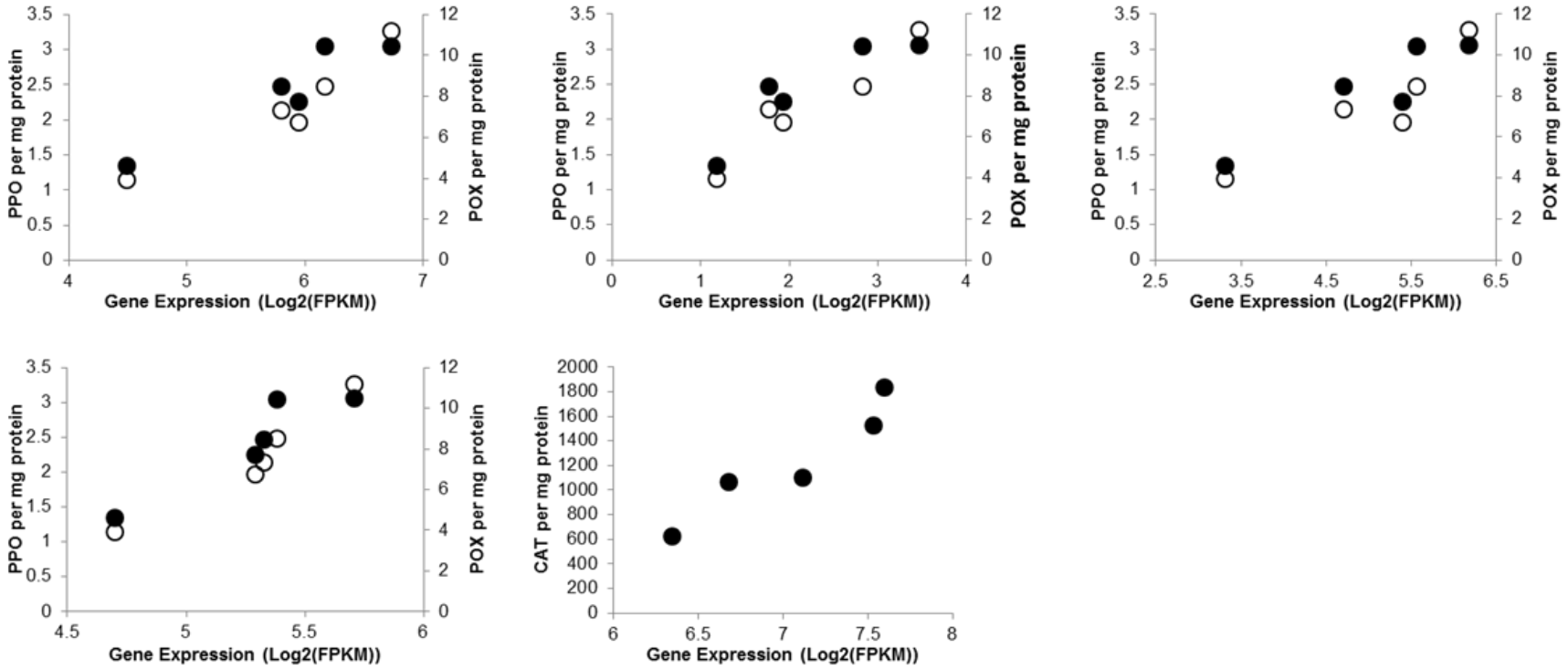

Figure 3: Summary of significant transcript to phenotype correlations for the LPS subset of samples (*n*=5). a) correlations between galaxin expression and activity of prophenoloxidase (PPO; r=0.956, *p=0.011*) and peroxidase (POX; r=0.948, *p*=0.014); b) correlations between mucin-like protein (comp263105) expression and activity of PPO (r=0.960, *p*=0.010) and POX (r=0.907, *p*=0.034); c) correlations between GFP-like fluorescent chromoprotein cFP484 expression and activity of PPO (r=0.922, *p*=0.026) and POX (r=0.921, *p*=0.027); d) correlations between peroxisomal biogenesis factor 11C expression and activity of PPO (r=0.98, *p*<0.01) and POX (r=0.937, *p*=0.019); f) correlations between mucin-like protein (comp347198) expression and activity of catalase (CAT; r=0.948; *p*=0.014)

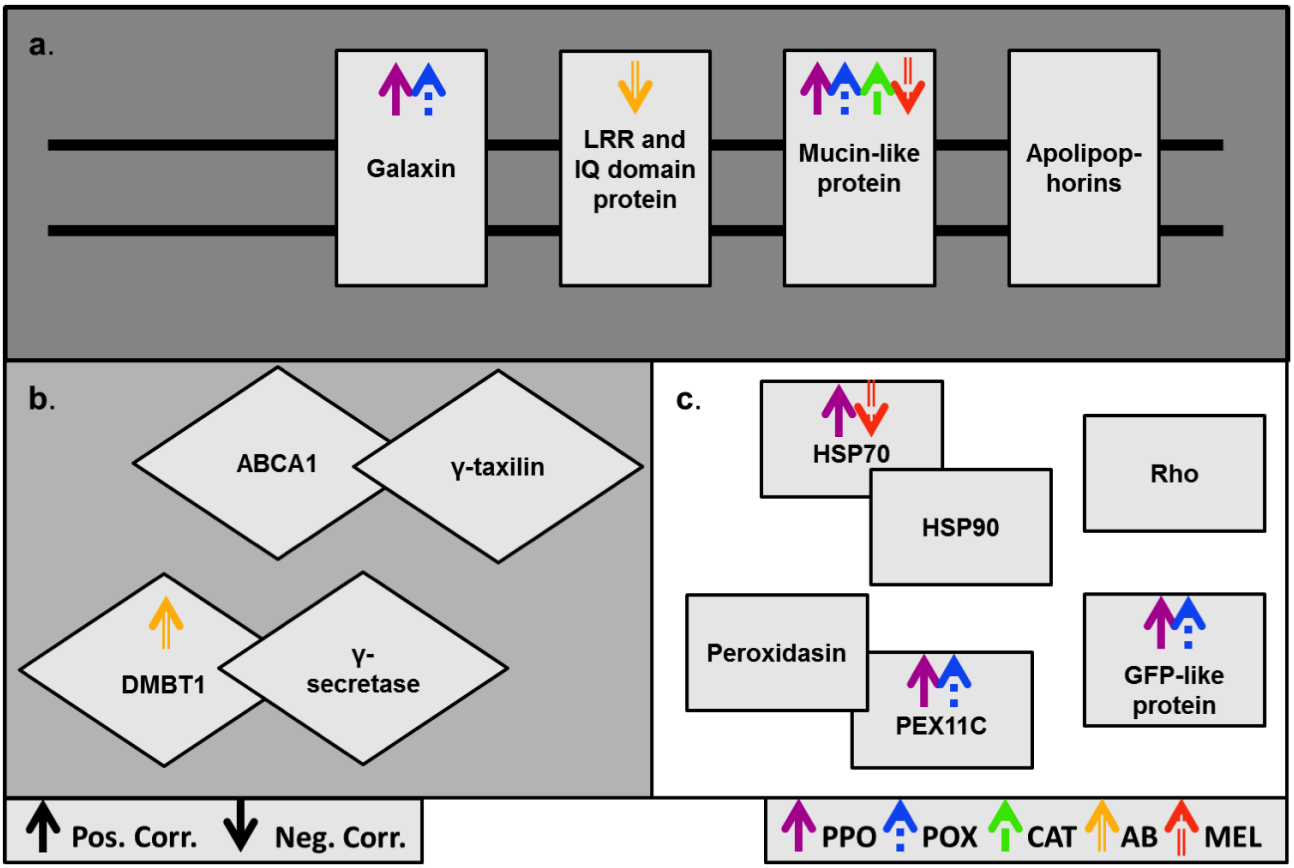

Figure 4: Summary of the significantly differentially expressed transcripts involved in immunity divided by immune component (**a.** receptors, **b.** signaling molecules, **c.** effector molecules). Arrows indicate correlation between transcript expression and immune protein activity. Directionality of arrows corresponds to the direction of correlation (up = positive correlation, down = negative correlation)

SUPPLEMENTARY FIGURES AND TABLES

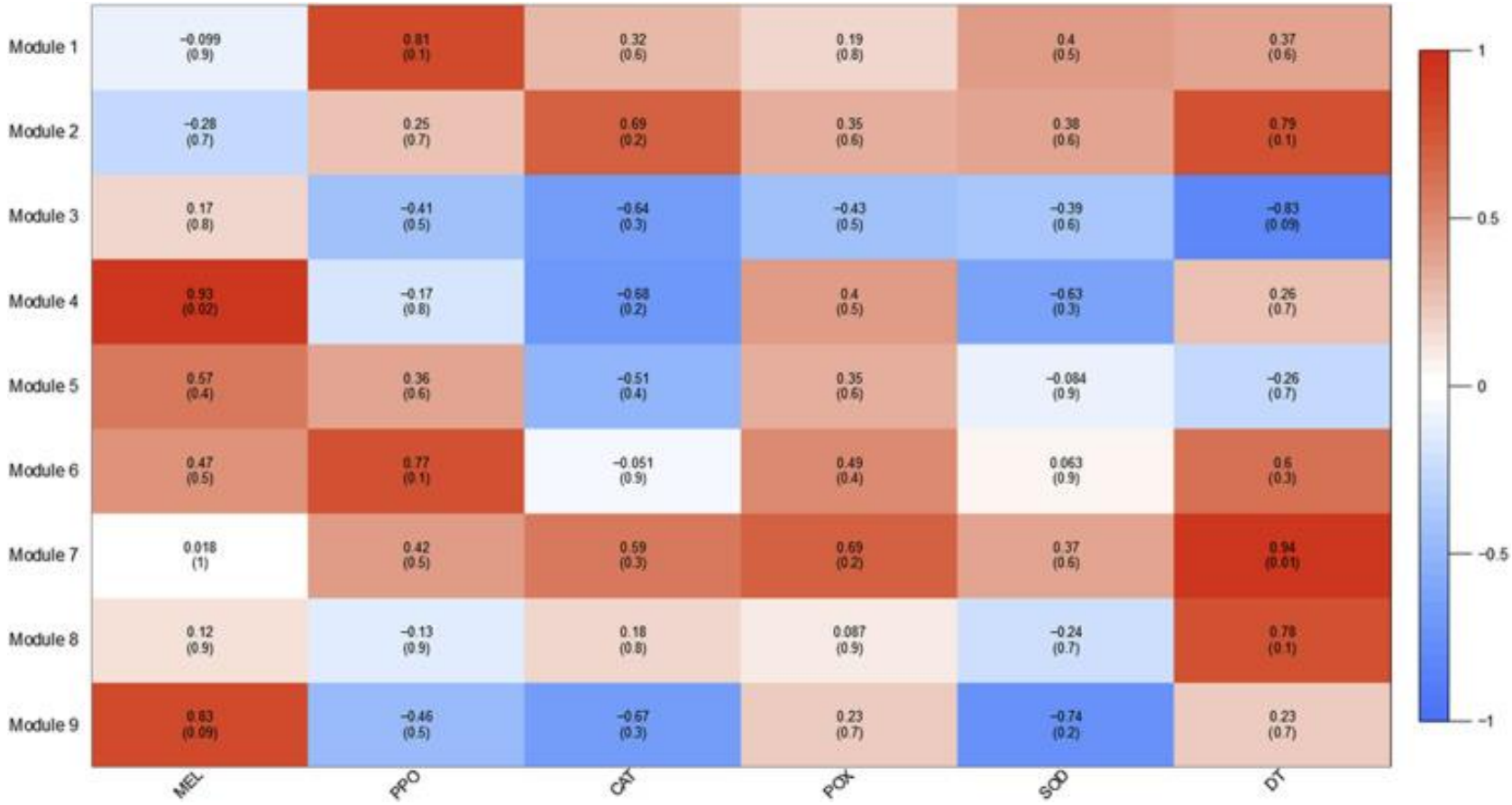

Supplementary Figure 1: Summary of module to immune phenotype correlations for the control subset of samples generated in the WGCNA R package.

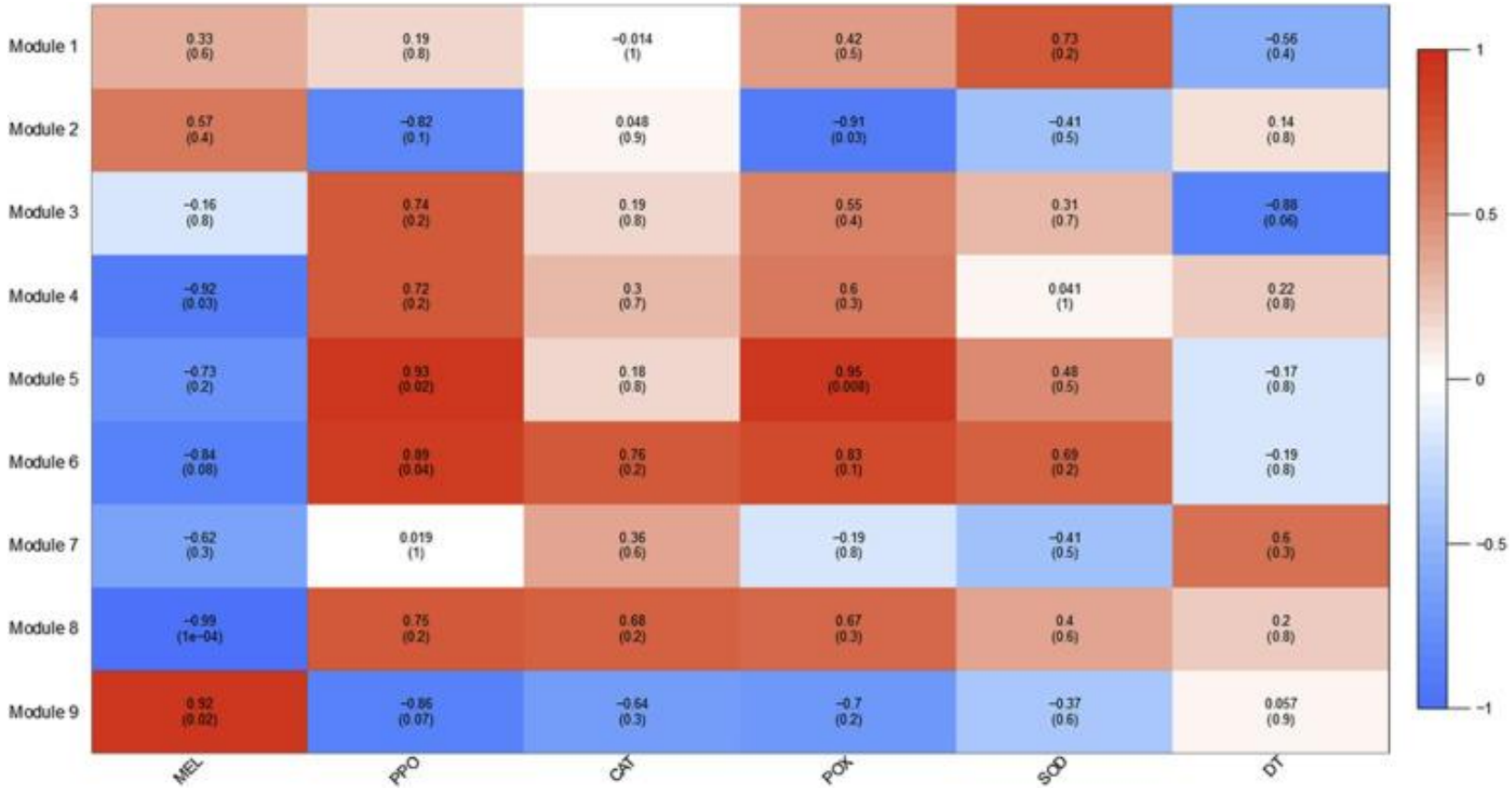

Supplementary Figure 2: Summary of module to immune phenotype correlations for the PAMP subset of samples generated in the WGCNA R package.

Supplementary Table 1: List of blast results for all annotated differentially expressed transcripts. Transcripts were annotated against the Uniprot/SwissProt and TrEMBL databases using default parameters with a minimum e-value cutoff of 1E-5.

Locus	spID	Protein names	Percent Match	Evalue	Bit Score
comp343799_c0_seq4	Q70VZ7	2-acylglycerol O-acyltransferase 1	55.72	9.00E-119	373
comp333208_c0_seq1	Q2KHS5	2-acylglycerol O-acyltransferase 2-A	50.61	3.00E-99	313
comp351374_c3_seq3	Q6DJI4	39S ribosomal protein L41-A, mitochondrial	71.84	2.00E-41	153
comp346081_c0_seq1	A4YI89	3-hydroxypropionyl-coenzyme A dehydratase	41.21	7.00E-38	144
comp194590_c0_seq1	Q945U1	40S ribosomal protein S15	82.68	1.00E-66	207
comp197889_c0_seq1	P55833	40S ribosomal protein S27	87.5	3.00E-47	154
comp265124_c0_seq1	P04646	60S ribosomal protein L35a	58.18	1.00E-29	75.1
comp345898_c2_seq1	Q90593	78 kDa glucose-regulated protein	84.73	0	961
comp352569_c0_seq1	P62484	Abl interactor 2	56.32	6.00E-50	184
comp149645_c0_seq1	Q39596	Actin	97.01	4.00E-41	135
comp329145_c0_seq7	P18603	Actin, clone 403	99.32	0	615
comp406307_c0_seq1	P53458	Actin-5	96.15	1.00E-09	59.7
comp297771_c0_seq1	Q96293	Actin-8	81.15	5.00E-68	215
comp343594_c0_seq1	Q8JZN5	Acyl-CoA dehydrogenase family member 9, mitochondrial	58.95	0	660
comp348081_c0_seq1	Q6GLK2	Acyl-coenzyme A thioesterase THEM4	34.97	3.00E-22	100
comp320404_c0_seq1	P11617	Adenosine receptor A2a	37.02	6.00E-41	164
comp353972_c3_seq1	Q8NKE2	Alternative oxidase, mitochondrial	48.82	2.00E-77	263
comp308661_c0_seq1	Q9U943	Apolipophorins	29.06	7.00E-37	155
comp226382_c0_seq1	Q8NCT1	Arrestin domain-containing protein 4	29.19	4.00E-29	124
comp352412_c0_seq1	P41233	ATP-binding cassette sub-family A member 1	48.06	0	1702
comp346166_c0_seq2	Q99758	ATP-binding cassette sub-family A member 3	47.38	0	1444
comp67778_c0_seq1	P58428	ATP-binding cassette sub-family G member 8	52.88	4.00E-29	115
comp341607_c0_seq1	Q8VC30	Bifunctional ATP-dependent dihydroxyacetone kinase/FAD-AMP lyase	50.08	4.00E-167	525
comp317101_c0_seq1	Q28BT4	Calumenin	38.66	3.00E-51	185
comp347148_c1_seq1	P00919	Carbonic anhydrase 2	49.81	2.00E-73	242
comp339880_c0_seq2	P00920	Carbonic anhydrase 2	38.58	3.00E-45	166

comp339880_c0_seq3	P00920	Carbonic anhydrase 2	38.58	1.00E-44	165
comp345652_c0_seq1	P52826	Carnitine O-acetyltransferase	46.79	0	561
comp347368_c7_seq1	Q60HG9	Carnitine O-palmitoyltransferase 2, mitochondrial	58.68	0	661
comp353029_c1_seq1	P35224	Catenin beta	65.41	1.00E-107	339
comp348632_c0_seq1	Q26636	Cathepsin L	58.82	2.00E-125	401
comp325136_c0_seq4	Q9LDI3	CBL-interacting serine/threonine-protein kinase 24	36.76	4.00E-23	102
comp326659_c0_seq4	Q05062	Cell division control protein 42 homolog	58.41	1.00E-39	137
comp304916_c0_seq1	A7RFT2	Cell division cycle protein 123 homolog	59.64	1.00E-131	393
comp337569_c0_seq1	Q6DFB7	Centrosomal protein POC5	31.98	1.00E-52	189
comp340734_c1_seq1	P58465	CTD small phosphatase-like protein	64.81	2.00E-104	331
comp349474_c2_seq1	Q9Y2D1	Cyclic AMP-dependent transcription factor ATF-5	72.29	2.00E-25	115
comp340439_c2_seq2	P56101	Cysteine string protein	69.09	7.00E-47	168
comp353622_c1_seq1	Q9WTR6	Cystine/glutamate transporter	41.03	7.00E-109	360
comp349461_c2_seq1	Q0MQ97	Cytochrome c oxidase subunit NDUFA4	65.33	1.00E-26	111
comp345160_c1_seq2	Q29496	Cytochrome P450 3A24	40.69	1.00E-88	292
comp345160_c1_seq4	Q29496	Cytochrome P450 3A24	45.69	6.00E-66	228
comp354557_c0_seq1	Q9UGM3	Deleted in malignant brain tumors 1 protein	39.96	7.00E-95	348
comp345208_c0_seq13	P25784	Digestive cysteine proteinase 3	74.55	9.00E-21	91.7
comp305061_c0_seq1	O60884	DnaJ homolog subfamily A member 2	33.5	1.00E-28	117
comp348369_c0_seq234	O94451	E3 SUMO-protein ligase pli1	31.22	1.00E-16	93.2
comp345134_c0_seq1	Q9UJA9	Ectonucleotide pyrophosphatase/phosphodiesterase family member 5	32.86	2.00E-68	241
comp347593_c1_seq2	O43854	EGF-like repeat and discoidin I-like domain-containing protein 3	41.44	3.00E-59	217
comp333547_c0_seq1	Q2KIG0	Electron transfer flavoprotein-ubiquinone oxidoreductase, mitochondrial	78.17	0	986
comp411229_c0_seq1	P08712	Endoplasmin	49.02	2.00E-12	73.2
comp345684_c0_seq1	Q7TQA3	Epidermal retinol dehydrogenase 2	49.83	2.00E-97	306
comp343301_c0_seq1	Q92506	Estradiol 17-beta-dehydrogenase 8	55.6	2.00E-81	275
comp291344_c0_seq1	Q5R5F5	Eukaryotic initiation factor 4A-I	88.58	5.00E-129	380
comp243360_c0_seq1	P48598	Eukaryotic translation initiation factor 4E	39.39	8.00E-38	138
comp139993_c1_seq1	P39730	Eukaryotic translation initiation factor 5B	54.29	2.00E-79	271
comp329150_c0_seq1	D3ZAT9	Failed axon connections homolog	35.59	4.00E-48	174

comp337451_c1_seq1	O18728	Fascin-2	39.5	1.00E-108	341
comp320510_c0_seq1	Q9GKT2	Fatty acid hydroxylase domain-containing protein 2	50.79	9.00E-118	361
comp351548_c0_seq5	Q8K385	Ferric-chelate reductase 1	34.24	4.00E-43	166
comp249169_c0_seq1	Q14315	Filamin-C	92.59	3.00E-23	108
comp332277_c2_seq1	P30043	Flavin reductase	52.26	9.00E-55	201
comp353272_c0_seq1	P32674	Formate acetyltransferase 2	27.08	3.00E-37	155
comp293392_c1_seq1	P32604	Fructose-2,6-bisphosphatase	60.51	1.00E-134	400
comp351374_c0_seq1	D9IQ16	Galaxin	36.58	4.00E-35	142
comp224925_c0_seq1	Q8JHF0	Gamma-secretase subunit PEN-2	63.41	1.00E-31	119
comp300598_c1_seq1	Q9NUQ3	Gamma-taxilin	30.95	4.00E-22	100
comp342432_c0_seq1	Q7Z6J2	General receptor for phosphoinositides 1-associated scaffold protein	47.06	6.00E-88	323
comp208687_c0_seq1	A5LGW7	Genome polyprotein	26.7	3.00E-07	60.5
comp319875_c0_seq1	Q9U6Y3	GFP-like fluorescent chromoprotein cFP484	62.86	3.00E-76	237
comp336017_c0_seq1	Q13480	GRB2-associated-binding protein 1	31.76	1.00E-34	153
comp346920_c0_seq5	P30676	Guanine nucleotide-binding protein G(i) subunit alpha	86.72	0	657
comp214516_c0_seq1	O42249	Guanine nucleotide-binding protein subunit beta-2-like 1	83.18	5.00E-60	193
comp337279_c0_seq1	Q5ZJH9	H/ACA ribonucleoprotein complex subunit 4	72.62	0	648
comp333471_c0_seq1	P02516	Heat shock protein 23	38.21	1.00E-16	87
comp331703_c0_seq9	P41887	Heat shock protein 90 homolog	73.72	6.00E-64	213
comp315290_c1_seq1	O54879	High mobility group protein B3	60.82	4.00E-51	184
comp222097_c0_seq1	P07746	High mobility group-T protein	44.59	6.00E-08	60.1
comp341857_c4_seq1	Q6PBI4	Histone deacetylase 9-B	42.16	2.00E-07	63.9
comp236374_c0_seq1	Q5RCC9	Histone H3.3	100	2.00E-31	112
comp349241_c4_seq1	P06756	Integrin alpha-V	28.43	3.00E-99	348
comp352569_c2_seq1	Q5S1U6	Interferon-related developmental regulator 1	44.26	9.00E-95	315
comp352047_c3_seq1	Q9K9H0	Isocitrate lyase	67.31	0	580
comp39848_c0_seq1	Q6S004	Kinesin-related protein 6	38.74	2.00E-11	70.1
comp354666_c0_seq1	Q96JM4	Leucine-rich repeat and IQ domain-containing protein 1	29.39	4.00E-80	300
comp337689_c0_seq1	O60488	Long-chain-fatty-acid--CoA ligase 4	54.48	0	757
comp347496_c0_seq1	P27615	Lysosome membrane protein 2	35.24	2.00E-87	298
comp346945_c0_seq1	Q6NUT3	Major facilitator superfamily domain-containing protein 12	33.77	8.00E-81	277

comp352047_c2_seq1	P95329	Malate synthase	52.47	3.00E-173	515
comp332278_c0_seq1	Q9NPA2	Matrix metalloproteinase-25	36.33	1.00E-89	298
comp353741_c0_seq1	Q9Z2Z6	Mitochondrial carnitine/acylcarnitine carrier protein	63.42	7.00E-124	399
comp347198_c0_seq1	B3EWY9	Mucin-like protein	37.48	9.00E-128	432
comp353127_c5_seq1	B3EWY9	Mucin-like protein	34.02	1.00E-51	203
comp263105_c1_seq1	B3EWY9	Mucin-like protein	49.71	1.00E-41	167
comp353177_c0_seq1	B3EWZ6	Mucin-like protein	38.89	5.00E-34	147
comp345211_c1_seq1	Q864R9	Multidrug resistance-associated protein 1	71.43	4.00E-27	116
comp341853_c3_seq1	A8PWF6	Myosin-1	49.06	6.00E-09	70.5
comp354720_c2_seq1	O47497	NADH-ubiquinone oxidoreductase chain 4	63.4	1.00E-135	440
comp351722_c4_seq1	Q6UXZ4	Netrin receptor UNC5D	35.52	3.00E-43	176
comp317592_c0_seq2	P14017	Orotidine 5'-phosphate decarboxylase	61.23	2.00E-155	462
comp347668_c1_seq1	P24610	Paired box protein Pax-3	44.79	1.00E-64	233
comp354212_c0_seq1	Q3UQ28	Peroxidasin homolog	35.81	4.00E-91	321
comp317412_c0_seq1	Q96HA9	Peroxisomal membrane protein 11C	39.24	2.00E-46	169
comp346397_c0_seq2	O14111	Phosphatidylserine decarboxylase proenzyme 3	31.78	7.00E-26	118
comp344164_c3_seq8	Q3ZCB2	Placenta-specific gene 8 protein	66.3	5.00E-24	105
comp180272_c0_seq1	P58171	Polcalcin Syr v 3	54.76	4.00E-48	169
comp354148_c1_seq1	Q7TN88	Polycystic kidney disease protein 1-like 2	36.74	1.00E-93	345
comp349680_c0_seq1	Q8WPW2	Probable pyridoxine biosynthesis SNZERR	73.87	8.00E-140	439
comp340860_c1_seq1	Q9SXS2	Probable sulfate transporter 3.3	31.25	1.00E-28	128
comp343191_c0_seq2	Q5VRN0	Probable UMP/CMP kinase 1	58.49	9.00E-123	412
comp419940_c0_seq1	Q9ZW35	Proliferating cell nuclear antigen 2	56.92	1.00E-15	81.3
comp341389_c1_seq1	Q6TMK8	Protein slowmo homolog 2	52.54	2.00E-55	192
comp237585_c0_seq1	F4ICD9	Protein transport protein SEC31 homolog A	41.67	7.00E-27	122
comp331913_c1_seq1	Q94BZ1	Protein ZINC INDUCED FACILITATOR-LIKE 1	35.28	4.00E-54	199
comp339880_c0_seq4	Q10462	Putative carbonic anhydrase 5	58.33	2.00E-25	112
comp348833_c2_seq1	P01122	Ras-like GTP-binding protein RHO	73.77	2.00E-19	92.8
comp292097_c0_seq1	Q13637	Ras-related protein Rab-32	58.97	2.00E-36	136
comp330575_c0_seq1	P79733	Ribonucleoside-diphosphate reductase subunit M2	79.39	0	545
comp350091_c0_seq4	Q7T3I7	RNA-binding protein 38	68.63	5.00E-14	83.6
comp337513_c3_seq1	Q61474	RNA-binding protein Musashi homolog 1	67.54	1.00E-71	251

comp337349_c3_seq2	P26686	Serine-arginine protein 55	71.7	3.00E-15	85.9
comp338208_c0_seq1	Q28728	Sodium/myo-inositol cotransporter 2	44.26	3.00E-146	454
comp337740_c0_seq1	Q8N695	Sodium-coupled monocarboxylate transporter 1	43.74	3.00E-133	421
comp350925_c2_seq1	Q9DBP0	Sodium-dependent phosphate transport protein 2B	56.85	3.00E-139	459
comp321028_c0_seq2	Q8BGF8	Solute carrier family 35 member D3	32.96	2.00E-23	108
comp321028_c0_seq1	Q8BGF8	Solute carrier family 35 member D3	32.96	2.00E-23	108
comp333933_c0_seq1	Q6AZV0	Succinate dehydrogenase [ubiquinone] cytochrome b small subunit B, mitochondrial	50	9.00E-36	135
comp354523_c0_seq1	Q96AY4	Tetratricopeptide repeat protein 28	25.24	1.00E-42	174
comp352754_c0_seq1	Q96AY4	Tetratricopeptide repeat protein 28	31.16	2.00E-37	156
comp328348_c0_seq2	Q96AY4	Tetratricopeptide repeat protein 28	38.98	5.00E-16	83.2
comp347842_c0_seq1	P19966	Transgelin	43.56	7.00E-36	139
comp333537_c0_seq1	O46629	Trifunctional enzyme subunit beta, mitochondrial	78.25	0	669
comp322399_c0_seq1	Q6IRU2	Tropomyosin alpha-4 chain	40.66	1.00E-34	143
comp331922_c0_seq1	P81902	Trypsin inhibitor	42.11	1.00E-14	81.6
comp353371_c0_seq5	P02556	Tubulin beta chain	53.98	3.00E-42	149
comp352325_c0_seq1	Q9HAV5	Tumor necrosis factor receptor superfamily member 27	41.86	6.00E-16	92.8
comp337674_c0_seq1	Q55909	TVP38/TMEM64 family membrane protein slr0305	46.43	2.00E-27	112
comp343899_c1_seq1	P17713	Tyrosine-protein kinase STK	64.86	0	677
comp327632_c0_seq2	A7MTX1	Ubiquinone/menaquinone biosynthesis C-methyltransferase UbiE	32.86	3.00E-31	129
comp352876_c0_seq1	P0DJ25	Ubiquitin-60S ribosomal protein L40	62.76	2.00E-100	318
comp352876_c0_seq3	P0DJ25	Ubiquitin-60S ribosomal protein L40	62.76	9.00E-100	316
comp322412_c1_seq3	Q5BL31	Uncharacterized protein C6orf106 homolog	38.68	3.00E-16	81.6
comp350393_c0_seq2	B7WFQ1	Uncharacterized skeletal organic matrix protein 2	40.35	6.00E-39	155
comp325048_c0_seq1	Q63358	Unconventional myosin-Ixb	44.12	0	849
comp346845_c0_seq1	B9GCH9	Urease	62.99	0	1051
comp336298_c0_seq1	A7RJI7	Vacuolar fusion protein CCZ1 homolog	75.38	0	722
comp345834_c2_seq1	Q9Z1Q9	Valine--tRNA ligase	65.42	0	1377
comp300418_c0_seq2	Q2EJA0	Yorkie homolog	37.5	5.00E-56	206
comp354617_c2_seq1	G8HTB6	ZP domain-containing protein	32.4	1.00E-32	136
comp324516_c0_seq1	G8HTB6	ZP domain-containing protein	28.32	1.00E-31	130

Supplementary Table 2: List of all annotated differentially expressed genes included in network analyses, grouped by final module assignment.

Module	Locus	spID	Annotation	Log_2fold Change
1	comp347148_c1_seq1	P00919	Carbonic anhydrase 2	-1.34987
1	comp304916_c0_seq1	A7RFT2	Cell division cycle protein 123 homolog	1.50788
1	comp345684_c0_seq1	Q7TQA3	Epidermal retinol dehydrogenase 2	1.8319
1	comp329150_c0_seq1	D3ZAT9	Failed axon connections homolog	3.37911
1	comp336017_c0_seq1	Q13480	GRB2-associated-binding protein 1	0.974539
1	comp222097_c0_seq1	P07746	High mobility group-T protein	-3.89122
1	comp347496_c0_seq1	P27615	Lysosome membrane protein 2	1.16751
1	comp341853_c3_seq1	A8PWF6	Myosin-1	2.10988
1	comp351722_c4_seq1	Q6UXZ4	Netrin receptor UNC5D	1.03543
1	comp354212_c0_seq1	Q3UQ28	Peroxidasin homolog	1.68936
1	comp354148_c1_seq1	Q7TN88	Polycystic kidney disease protein 1-like 2	2.60597
1	comp321028_c0_seq2	Q8BGF8	Solute carrier family 35 member D3	3.47399
1	comp321028_c0_seq1	Q8BGF8	Solute carrier family 35 member D3	2.65378
1	comp352754_c0_seq1	Q96AY4	Tetratricopeptide repeat protein 28	1.52801
1	comp322399_c0_seq1	Q6IRU2	Tropomyosin alpha-4 chain	-1.15595
1	comp353371_c0_seq5	P02556	Tubulin beta chain	2.24672
1	comp352325_c0_seq1	Q9HAV5	Tumor necrosis factor receptor superfamily member 27	2.78302
1	comp327632_c0_seq2	A7MTX1	Ubiquinone/menaquinone biosynthesis C-methyltransferase UbiE	2.21581
1	comp346845_c0_seq1	B9GCH9	Urease	-1.13272
2	comp343799_c0_seq4	Q70VZ7	2-acylglycerol O-acyltransferase 1	1.1995
2	comp333208_c0_seq1	Q2KHS5	2-acylglycerol O-acyltransferase 2-A	1.8375
2	comp339880_c0_seq3	P00920	Carbonic anhydrase 2	-1.20149
2	comp347593_c1_seq2	O43854	EGF-like repeat and discoidin I-like domain-containing protein 3	1.2882
2	comp333547_c0_seq1	Q2KIG0	Electron transfer flavoprotein-ubiquinone oxidoreductase, mitochondrial	1.56029
2	comp352569_c2_seq1	Q5S1U6	Interferon-related developmental regulator 1	1.04715
2	comp337689_c0_seq1	O60488	Long-chain-fatty-acid--CoA ligase 4	1.32518

2	comp353127_c5_seq1	B3EWY9	Mucin-like protein	3.31381
2	comp331913_c1_seq1	Q94BZ1	Protein ZINC INDUCED FACILITATOR-LIKE 1	3.66925
2	comp350091_c0_seq4	Q7T3I7	RNA-binding protein 38	2.03321
2	comp354523_c0_seq1	Q96AY4	Tetratricopeptide repeat protein 28	1.23941
2	comp352876_c0_seq1	P0DJ25	Ubiquitin-60S ribosomal protein L40	2.07207
2	comp352876_c0_seq3	P0DJ25	Ubiquitin-60S ribosomal protein L40	1.3711
2	comp350393_c0_seq2	B7WFQ1	Uncharacterized skeletal organic matrix protein 2	1.56919
3	comp346081_c0_seq1	A4YI89	3-hydroxypropionyl-coenzyme A dehydratase	-1.48711
3	comp352569_c0_seq1	P62484	Abl interactor 2	-1.62162
3	comp149645_c0_seq1	Q39596	Actin	-1.32723
3	comp226382_c0_seq1	Q8NCT1	Arrestin domain-containing protein 4	-1.53906
3	comp339880_c0_seq2	P00920	Carbonic anhydrase 2	-1.6768
3	comp345652_c0_seq1	P52826	Carnitine O-acetyltransferase	2.09946
3	comp353029_c1_seq1	P35224	Catenin beta	-2.2234
3	comp348632_c0_seq1	Q26636	Cathepsin L	1.1321
3	comp340734_c1_seq1	P58465	CTD small phosphatase-like protein	-2.00792
3	comp340439_c2_seq2	P56101	Cysteine string protein	-1.8161
3	comp349461_c2_seq1	Q0MQ97	Cytochrome c oxidase subunit NDUFA4	-1.53096
3	comp345160_c1_seq4	Q29496	Cytochrome P450 3A24	2.94683
3	comp345160_c1_seq2	Q29496	Cytochrome P450 3A24	3.91371
3	comp343301_c0_seq1	Q92506	Estradiol 17-beta-dehydrogenase 8	-1.0969
3	comp337451_c1_seq1	O18728	Fascin-2	-1.85246
3	comp351548_c0_seq5	Q8K385	Ferric-chelate reductase 1	2.19765
3	comp353272_c0_seq1	P32674	Formate acetyltransferase 2	-1.80438
3	comp319875_c0_seq1	Q9U6Y3	GFP-like fluorescent chromoprotein cFP484	-1.63436
3	comp346920_c0_seq5	P30676	Guanine nucleotide-binding protein G(i) subunit alpha	-1.23133
3	comp337279_c0_seq1	Q5ZJH9	H/ACA ribonucleoprotein complex subunit 4	-1.29148
3	comp315290_c1_seq1	O54879	High mobility group protein B3	-1.77629
3	comp354666_c0_seq1	Q96JM4	Leucine-rich repeat and IQ domain-containing protein 1	-1.46844
3	comp346945_c0_seq1	Q6NUT3	Major facilitator superfamily domain-containing protein 12	1.6363
3	comp354720_c2_seq1	O47497	NADH-ubiquinone oxidoreductase chain 4	-1.38225
3	comp346397_c0_seq2	O14111	Phosphatidylserine decarboxylase proenzyme 3	-1.19072

3	comp344164_c3_seq8	Q3ZCB2	Placenta-specific gene 8 protein	-1.63797
3	comp339880_c0_seq4	Q10462	Putative carbonic anhydrase 5	-1.91286
3	comp330575_c0_seq1	P79733	Ribonucleoside-diphosphate reductase subunit M2	-1.11285
3	comp337513_c3_seq1	Q61474	RNA-binding protein Musashi homolog 1	-1.02791
3	comp333933_c0_seq1	Q6AZV0	Succinate dehydrogenase [ubiquinone] cytochrome b small subunit B, mitochondrial	-1.44888
3	comp328348_c0_seq2	Q96AY4	Tetratricopeptide repeat protein 28	2.41877
3	comp347842_c0_seq1	P19966	Transgelin	-0.932793
3	comp343899_c1_seq1	P17713	Tyrosine-protein kinase STK	-2.15285
3	comp300418_c0_seq2	Q2EJA0	Yorkie homolog	-1.28156
3	comp354617_c2_seq1	G8HTB6	ZP domain-containing protein	-1.77989
4	comp351374_c0_seq1	D9IQ16	Galaxin	-1.51452
4	comp352047_c3_seq1	Q9K9H0	Isocitrate lyase	2.07042
4	comp353177_c0_seq1	B3EWZ6	MAM and LDL-receptor class A domain-containing protein 2	1.3609
4	comp353741_c0_seq1	Q9Z2Z6	Mitochondrial carnitine/acylcarnitine carrier protein	1.36537
4	comp337740_c0_seq1	Q8N695	Sodium-coupled monocarboxylate transporter 1	1.7103
5	comp341857_c4_seq1	Q6PBI4	Histone deacetylase 9-B	-2.53624
5	comp317412_c0_seq1	Q96HA9	Peroxisomal membrane protein 11C	2.12545
5	comp333537_c0_seq1	O46629	Trifunctional enzyme subunit beta, mitochondrial	1.01722
5	comp341607_c0_seq1	Q8VC30	Triokinase/FMN cyclase	-1.28775
5	comp345834_c2_seq1	Q9Z1Q9	Valine--tRNA ligase	1.71644
6	comp351374_c3_seq3	Q6DJI4	39S ribosomal protein L41-A, mitochondrial	1.20963
6	comp348081_c0_seq1	Q6GLK2	Acyl-coenzyme A thioesterase THEM4	2.8307
6	comp320404_c0_seq1	P11617	Adenosine receptor A2a	2.19892
6	comp353972_c3_seq1	Q8NKE2	Alternative oxidase, mitochondrial	3.66223
6	comp317101_c0_seq1	Q28BT4	Calumenin	1.22948
6	comp347368_c7_seq1	Q60HG9	Carnitine O-palmitoyltransferase 2, mitochondrial	1.49649
6	comp349474_c2_seq1	Q9Y2D1	Cyclic AMP-dependent transcription factor ATF-5	1.26443
6	comp332277_c2_seq1	P30043	Flavin reductase	1.69135
6	comp352047_c2_seq1	P95329	Malate synthase	1.6996
6	comp263105_c1_seq1	B3EWY9	Mucin-like protein	-1.9242
6	comp343191_c0_seq2	Q5VRN0	Probable UMP/CMP kinase 1	2.18567

6	comp348833_c2_seq1	P01122	Ras-like GTP-binding protein RHO	1.84994
7	comp345898_c2_seq1	Q90593	78 kDa glucose-regulated protein	0.956723
7	comp343594_c0_seq1	Q8JZN5	Acyl-CoA dehydrogenase family member 9, mitochondrial	2.52372
7	comp308661_c0_seq1	Q9U943	Apolipophorins	1.44498
7	comp352412_c0_seq1	P41233	ATP-binding cassette sub-family A member 1	0.960787
7	comp346166_c0_seq2	Q99758	ATP-binding cassette sub-family A member 3	1.5379
7	comp337569_c0_seq1	Q6DFB7	Centrosomal protein POC5	2.35184
7	comp354557_c0_seq1	Q9UGM3	Deleted in malignant brain tumors 1 protein	1.27496
7	comp345134_c0_seq1	Q9UJA9	Ectonucleotide pyrophosphatase/phosphodiesterase family member 5	1.37276
7	comp320510_c0_seq1	Q9GKT2	Fatty acid hydroxylase domain-containing protein 2	1.85124
7	comp224925_c0_seq1	Q8JHF0	Gamma-secretase subunit PEN-2	1.71257
7	comp342432_c0_seq1	Q7Z6J2	General receptor for phosphoinositides 1-associated scaffold protein	1.18889
7	comp333471_c0_seq1	P02516	Heat shock protein 23	3.60243
7	comp349241_c4_seq1	P06756	Integrin alpha-V	2.07558
7	comp332278_c0_seq1	Q9NPA2	Matrix metalloproteinase-25	0.987664
7	comp347668_c1_seq1	P24610	Paired box protein Pax-3	-1.24569
7	comp341389_c1_seq1	Q6TMK8	Protein slowmo homolog 2	2.24003
7	comp337349_c3_seq2	P26686	Serine-arginine protein 55	1.90822
7	comp338208_c0_seq1	Q28728	Sodium/myo-inositol cotransporter 2	-2.03809
7	comp350925_c2_seq1	Q9DBP0	Sodium-dependent phosphate transport protein 2B	1.37285
7	comp331922_c0_seq1	P81902	Trypsin inhibitor	1.22895
7	comp325048_c0_seq1	Q63358	Unconventional myosin-Ixb	1.02536
7	comp324516_c0_seq1	G8HTB6	ZP domain-containing protein	1.18039
8	comp347198_c0_seq1	B3EWY9	Mucin-like protein	1.82072
8	comp345211_c1_seq1	Q864R9	Multidrug resistance-associated protein 1	2.86064

CHAPTER THREE

LIFE OR DEATH- DISEASE TOLERANT CORAL SPECIES ACTIVATE AUTOPHAGY FOLLOWING IMMUNE CHALLENGE[1]

Lauren E. Fuess[a], Jorge H. Pinzón C[a,1], Ernesto Weil[b], Robert D. Grinshpon[a], Laura D. Mydlarz[a]

Fuess LE, Pinzon JHC, Weil E, Grinshpon RD, Mydlarz LD. 2017 Life or death- Disease tolerant coral species activate autophagy following immune challenge. Proc R Soc B 284: 20170771; doi: 10.1098/rspb.2017.0771

[a] Department of Biology, University of Texas Arlington, Arlington, Texas, United States of America
[b] Department of Marine Sciences University of Puerto Rico, Mayagüez, Puerto Rico, United States of America
[1]**Present Address:** University of Texas Southwestern Medical Center, Dallas, Texas, United States of America

[1] Used with permission of the publisher, 2018

ABSTRACT

Global climate change has increased the number and strength of stressors affecting species, yet not all species respond equally to these stressors. Organisms may employ cellular mechanisms such as apoptosis and autophagy in responding to stressful events. These two pathways are often mutually exclusive, dictating whether a cell adapts or dies. In order to examine differences in cellular response to stress, we compared the immune response of four coral species with a range of disease susceptibility. Using RNA-seq and novel pathway analysis we were able to identify differences in response to immune stimulation between these species. Disease susceptible species, *Orbicella faveolata*, activated pathways associated with apoptosis. In contrast, disease tolerant species *Porites porites* and *Porites astreoides* activated autophagic pathways. Moderately susceptible species *Pseudodiploria strigosa* activated a mixture of these pathways. These findings were corroborated by apoptotic caspase protein assays, which indicated increased caspase activity following immune stimulations in susceptible species. Our results indicate that in response to immune stress, disease tolerant species activate cellular adaptive mechanisms such as autophagy, while susceptible species turn on cell death pathways. Differences in these cellular maintenance pathways may therefore influence the organismal stress response. Further study of these pathways will increase understanding of differential stress response and species survival in the face of changing environments.

INTRODUCTION

In a rapidly changing environment where both natural and anthropogenic stressors have become more common, organisms are forced to adapt or die (Chevin *et al.* 2010;Foden *et al.* 2013;Hoffmann&Sgro 2011;Somero 2010). Human impacts on the environment such as climate change, pollution, and deforestation have impacted a wide variety of taxa and lead to widespread extinctions (Bellard *et al.* 2012;Murphy&Romanuk 2014;Pimm *et al.* 2014). Yet not all organisms are equally affected. Certain species or groups of species may adapt more rapidly therefore persisting or even flourishing, while others experience catastrophic declines under the same pressures (Domisch *et al.* 2011;Somero 2010;van Woesik *et al.* 2011). However what makes the so-called 'winners' and 'losers' in an era of global change is still poorly understood.

Apoptotic and autophagic processes are essential parts of cellular responses to stress in all organisms (Maiuri *et al.* 2007). These two processes are uniquely and complexly intertwined, predominantly acting as mutually exclusive processes during a wide range of cellular responses including cell death, stress, and starvation (Kroemer *et al.* 2010;Maiuri *et al.* 2007;Marino *et al.* 2014). Apoptosis is an essential regulatory pathway that results in controlled cell death (Assefa *et al.* 2005;Fulda *et al.* 2010;Greijer&van der Wall 2004;Verheij *et al.* 1996;Vicencio *et al.* 2008;Walter&Ron 2011;Xu *et al.* 2005). Additionally, apoptosis is an important component of organismal responses to stress (Fulda *et al.* 2010;Walter&Ron 2011) and pathogenic infection (Allam *et al.* 2014;Man&Kanneganti 2016;Yang *et al.* 1998). Initially, controlled apoptosis of infected cells may serve to prevent further infection of an organism (Allam *et al.* 2014;Man&Kanneganti 2016;Yang *et al.* 1998). However, 'runaway' apoptosis during stress events or pathogenic infection may result in extensive cell death and tissue damage, potentially

contributing to organismal death rather than adaptation (Ainsworth *et al.* 2007;Libro&Vollmer 2016;Liu *et al.* 2005). Therefore, while often initially beneficial, excessive apoptosis is often characteristic of an organism's failure to adapt to stress, potentially resulting in death (Ainsworth *et al.* 2007;Libro&Vollmer 2016;Liu *et al.* 2005).

In contrast to apoptosis, autophagy is known an essential component of cellular adaptation, rather than death, during sub-lethal levels of stress (Maiuri *et al.* 2007). While at times autophagy may corroborate apoptotic processes (Kroemer&Levine 2008;Shen&Codogno 2011), most often this process is an alternative to cell death, allowing for adaptation in response to stressors (Eisenberg-Lerner *et al.* 2009;Marino *et al.* 2014). Furthermore, autophagy is essential to response to pathogens, serving as one of the most ancestral forms of immunity (Levine *et al.* 2011;Tang *et al.* 2012). Cells may employ xenophagy, a specific form of autophagy, to destroy intracellular bacteria (Deretic&Levine 2009;Levine&Yuan 2005). This can occur independent of canonical immune recognition events (Yano *et al.* 2008), or can be triggered by the binding of pattern recognition molecules such as Toll-like receptors (TLRs) to bacterial or viral compounds (Cooney *et al.* 2010;Delgado *et al.* 2008;Nakamoto *et al.* 2012;Shi&Kehrl 2008;Xu *et al.* 2013;Xu *et al.* 2007). Autophagy therefore serves as a crucial first step in the survival response of a cell to a pathogen, promoting a positive immune response.

Coral reefs around the globe are experiencing rapid declines as a result of the loss of formative scelaractinian, or reef-building corals (Baker *et al.* 2008;De'ath *et al.* 2012;Hoegh-Guldberg *et al.* 2007;Hughes *et al.* 2007;Pandolfi *et al.* 2003;Pratchett *et al.* 2013). Stressors such as climate change (Harvell *et al.* 2002;Hoegh-Guldberg&Bruno 2010;Hughes *et al.* 2003) and pollution (Bruno *et al.* 2003;De'ath&Fabircius 2010;Edinger *et al.* 1998;Vega Thurber *et al.* 2014) have driven massive die-offs of these organisms. However, increasing disease prevalence

has arguably been one of the largest drivers of coral declines worldwide (Croquer&Weil 2009;Daszak *et al.* 2001;Harvell *et al.* 1999;Sutherland *et al.* 2004;Weil *et al.* 2009a;Weil&Rogers 2011). Diseases do not impact all coral species equally and some species have been significantly less affected by disease (Grottoli *et al.* 2014;Roff&Mumby 2012;van Woesik *et al.* 2011). Cellular-level differences in immunity many contribute to these observed differences. For example, corals have a diverse and varied repertoire of innate immune receptors including multiple TLRs, TLR-like molecules and downstream effectors (Mydlarz *et al.* 2016;Poole&Weis 2014;Shinzato *et al.* 2011). However, despite increasing knowledge of coral immunity, it is still unclear why certain species are flourishing under increasing disease pressure, while others are experiencing rapid population declines.

Our hypothesis is that differences in immunity and cellular response pathways, including potential variation in receptor repertoire, may underscore patterns of disease susceptibility and tolerance. We used bacterial pathogen-associated molecular patterns (PAMPs) to stimulate immunity in four coral species and analyzed transcriptomic and protein activity changes. This approach allows for insight into species level differences in host response to a proxy for bacterial pathogensis. Comparison of the immune responses of these four species revealed that apoptotic and autophagic pathways might have a significant impact on the susceptibility of corals to disease.

METHODS

Sample Collection

Four species of coral with ranging disease susceptibility were used for this study: *Orbicella faveolata*, *Pseudodiploria strigosa*, *Porites porites*, and *Porites astreoides*. Disease prevalence was based on analysis in Pinzon et al. 2014 , and includes disease prevalence to

all relevant surveyed diseases for these species (e.g. Black Band, White Band, White Plague, and Yellow Band). Disease prevalence in the two disease susceptible species ranges from 20% in *O. faveolata* to 6% in *Ps. strigosa*. Prevalence is less than 1% in each of the *Porites* genus species, herein classified as tolerant species. Coral fragments of each species were collected in July of 2012 from five randomly selected colonies of *O. faveolata, Ps. strigosa,* and *P. porites,* and four randomly selected *P. astreoides* colonies. All samples were collected from on Media Luna reef (17˚ 56.096 N; 67˚ 02.911 W) near La Parguera, Puerto Rico. Six small fragments (5 x 5 cm) were chipped off from each colony with a hammer and chisel for a total of 30 fragments per species for *O. faveolata, Ps. strigosa,* and *P. porites* and 24 total fragments for *P. astreoides*. Upon collection, the fragments were placed in labeled zip-lock bags and transported in ambient seawater to an indoor running saltwater facility at the Dept. of Marine Sciences (University of Puerto Rico – Mayagüez in Isla Magueyes). At the facility, fragments from each colony were randomly assigned to one of the two treatment groups (control or PAMP exposure).

Five fragments from the same treatment and species (four in the case of *P. astreoides*) were placed in one of six large plastic containers. Each container was aerated using an electric air pump and supplied with continuous flow of seawater. To control for temperature, the water was initially contained in a 500 gallon barrel where the temperature was maintained at 26°C using electric heaters and chillers when needed. Overhead lamps were used to maintain a 12 hour light/dark cycle. Fragments were maintained in these conditions for seven days prior to experimentation to allow for acclimatization. During this time, control fragments from *Ps. strigosa* colony one perished, reducing control replication for this species to n=4.

Experimental Design

Following the acclimatization period, continuous water flow and aeration were ceased and water levels in each of the large containers reduced to 3L. A piece of PVC pipe (6.35 cm high and 5.08 cm wide) was placed around each coral fragment, making a temporary microenvironment. Using a micropipette, 1 mL of 7.57 mg/mL lippopolysaccharides (LPS), a PAMP, from *Escherichia coli* 0127:B8 (Sigma-Aldrich L3129-100MG) was added just above the surface of each treatment fragment. Final concentration of LPS in the container was 10 μg/mL spread over the fragments on each PAMP exposure container. Control fragments received 1 mL of sterile seawater used in preparation of the LPS solution. Microbial mimics such as PAMPs were used this experiment as they have been used extensively as an immune stimulators in vertebrate, invertebrate and plant immunology including corals (Palmer *et al.* 2011;Weiss *et al.* 2013). Furthermore, PAMPs such as LPS are a proxy for immune stimulation and trigger an authentic immune response that is not complicated by pathogen-host interactions (Tang *et al.* 2012). Another advantage is that we can challenge the coral immune response in a standardized manner. Since each of these 4 coral species are susceptible to different diseases, live bacterial inoculations have the potential to confound the results.

Exposure conditions were maintained for 30 minutes to ensure the LPS was taken into the coral, after which the aeration was resumed. Then the fragments were then maintained in continuous flow for an additional 4 hours before being removed and frozen in liquid nitrogen. All samples were shipped on dry ice to the University of Texas at Arlington where they were stored at -80°C until tissues were collected.

RNA Extraction, Sequencing, and Transcriptome Assembly

RNA was extracted from a small fragment (~3-5 μg) of tissue and skeleton using the RNAaqueous Kit with DNAse step kit (Life Technologies AM1914). Each fragment was first ground in a 2 mL microcentrifuge tube with 800 μL of Lysis Buffer for 2 minutes. Next, the tube was centrifuged on an AccuSpin Micro (Fisher Scientific) after witch 700 μL of the supernatant were removed and placed in a new tube along with 700 μl of 64% Ethanol solution. This solution was then passed through the column provided with the kit and washed with the wash one solution and twice with the wash two solution. The column was spun dry for 2 minutes and RNA eluted with 50 μL elution solution. Potential contaminating DNA was removed from samples by mixing 25 μL final extract with 2.95 μL of Master Mix and 1.6 μL DNase solution. This mixture was incubated at 37 °C for 1 hour and then incubated at room temperature for 2 minutes with 2.95 μL inactivation reagent. The final extract (~30 μL) was then passed to a new tube and stored at -80°C.

Following extraction the three replicates from each species and colony within a treatment were pooled for RNA library sequencing, due to budgetary constraints (n = 4-5 per treatment and species). Quality of combined extracts was assessed at the University of Texas at Arlington Genomics Core facility using an Agilent BioAnalyzer 2100. Samples with RIN numbers (quality values) higher than 8 were processed for cDNA library creation using an Illumina TruSeq RNA with Poly-A selection libraries kit (Illumina). Pooled samples were then sent to the University of Texas Southwestern Medical Center Genomics Core facility where library construction and sequencing occurred. Samples were sequenced in two separate lines with 20 samples each. The second lane was completed with samples from a separate project.

Following sequencing, RNA-seq libraries were sorted and the quality of reads was assessed. The Trimmomatic v. 3 software package was used to remove adaptors and low quality reads (Lohse et al. 2012). Non-host sequences were filtered out using methods described in (Pinzon *et al.* 2015). Alignments were performed using BLAT (parameters: 90% identity and e-value < 0.000001). Duplicate hits were removed and coral-only sequences were identified using cdbfasta/dcbyank (http://sourceforge.net/projects/cdbfasta/). For three of the four species studied, a new reference transcriptome was composed from the sequences libraries. Libraries for *P. strigosa*, *P. asteroides*, and *P. porties* were each assembled *de novo* into transcriptomes using the Trinity software package (Grabherr *et al.* 2011;Haas *et al.* 2013). The existing *O. faveolata* reference transcriptome was used for analyses of that species' reads (Pinzon *et al.* 2015).

The Cufflinks software package, v. 2.2.1, was used to conduct differential expression analyses (Trapnell *et al.* 2013). Analyses were run separately for each species. Read counts for each transcript within a species were obtained by aligning coral only reads to either the newly generated reference transcriptomes (for *P. strigosa*, *P. asteroides*, and *P. porties*), or the existing reference transcriptome in the case of *O. faveolata* (Pinzon *et al.* 2015). Default parameters were used for this step. Next, normalized expression values were generated in the Cuffdiff package with the default parameters (Trapnell *et al.* 2013). Average $\log_2$fold change per transcript was estimated by comparing normalized expression values between treatments within a species. Significantly differentially expressed transcripts were identified based on $\log_2$fold change (adjusted $p < 0.05$) across treatments.

Transcriptome Annotation and Gene Ontology (GO) Analyses

Following assembly of the four species transcriptomes, sequences were annotated against the UniProtKB/Swiss-Prot database (blastx algorithm, 1.0E-5 e-value threshold). GO analyses and comparisons of all differentially expressed transcripts for each species were conducted using the online PANTHER database (Thomas *et al.* 2003).

Ingenuity Pathway Analysis

Ingenuity Pathway Analysis (IPA) software was used to identify significantly activated canonical pathways in each of the four species of coral (IPA©, QIAGEN Redwood City, www.quiagen.com/ingenuity). Analyses were conducted using UniProt accession numbers and fold-change values for all annotated transcripts within a species. The Ingenuity Knowledge Base was used as a reference set to identify activated pathways. For each pathway, IPA generates a measure of activation or inactivation for each pathway known as a z-score and assesses the significance of that pathway using a Fisher's exact test and Benjamini-Hochberg-adjusted p-values (significance set at $padj < 0.05$). However, when transcripts do not follow patterns expected (based on what is known regarding the pathways in humans), no z-score is generated. Significant pathway overlap between species was determined by comparing lists of significantly activated pathways between species.

Apoptotic Caspase Activity Assay

Coral tissues were removed from the colony skeleton over ice using a Paansche airbrush (Chicago, IL, USA) with coral extraction buffer (50 mmol tris buffer, pH 7.8, with 0.05 mmol dithiothreitol). Tissues were then homogenized using a Power Gen 125 tissue homogenizer with a medium saw tooth generator (Fisher Scientific, Pittsburgh, PA, USA) for 60 seconds on ice. Samples were then left on ice for 10 minutes and the remaining volume was then centrifuged for 5 minutes at 4°C and 3500 RPM in an Eppendorf centrifuge 5810R.

The resulting supernatant, or whole cell coral protein extract, was split into two ~2 mL aliquots mL which were frozen in liquid nitrogen and stored at -80°C (Mydlarz & Palmer 2011). Total protein concentration in each sample was determined using the Red_{660} protein assay (G Biosciences, St. Louis, MO) standardized to BSA. This assay was run in duplicate on 96 well plates using a Synergy two multi-detection microplate reader and Gen5 software (Biotek Instruments, Winooski, VT, USA). Caspase activity results were standardized by protein concentration.

In order to determine the proteolytic activity of caspases per sample, a PTI (Photon Technology Internationl, Edison, NJ) fluorometer was used to detect the generation of free AFC (7-amino-4-trifluoromethylcoumarin) from a general fluorogenic tetrapeptide substrate for caspases, typically involved in apoptotic processes, AC-DEVD-AFC (acetyl-Asp-Glu-Val-Asp-AFC – purchased from Enzo Life Sciences). The excitation and emission wavelengths were set to 400 nm and 505 nm respectively. The activity buffer (50mM sodium chloride, 150 mM Tris-HCL, 1% sucrose at pH 7.5) for the reaction was also used to prepare a 200uM AC-DEVD-AFC stock. The reaction mixture had a final volume of 200uL; including a final concentration of 10 mM DTT (dithiothreitol), 0.1% CHAPS (3-[(3-cholamidopropyl) dimethylammonio]-1-propanesulfonate), and 60 uM AC-DEVD-AFC. The reaction was initiated with the addition of 60 uL of the coral cell lysate, and DEVDase activity was monitored for five minutes. A standard curve of free AFC was generated to determine the amount of free AFC generated per second during the assay.

The caspase activity data was square root transformed to adjust for normality and analyzed in SPSS using a 2-way ANOVA with ‘species identity’ and ‘LPS exposure’ as factors and with Tukey post-hoc comparisons to identify significant differences.

Additionally, to increase the sensitivity and reduce noise generated by biological variation, t-tests were conducted to specifically detect the effects of LPS exposure within each individual species. T-tests were corrected for multiple comparisons by Bonferroni correction (p value multiplied by number of comparisons, 4; significance determined as *padj*<0.05).

RESULTS

Transcriptome Assemblies

Sequencing of *O. faveolata*, *Ps.strigosa*, *P. porites* and *P. astreoides* samples yielded 120,020,664; 216,462,496**;**237,844,572 and 76,949,972 paired end reads respectively. Raw sequencing reads are available for download on NCBI (SRA Accession #SRP094633). Alignment of these reads to their respective species transcriptomes and filtering resulted in 31,958, 44,534, 6,640, and 26,556 expressed coral only contigs and N50 values of 1928, 2308, 3291, and 927 bps for *O. faveolata*, Ps. *strigosa***,** *P. porites* and *P. astreoides* respectively. Annotation of the final transcriptomes with the UniProtKB/Swiss-Prot database yielded annotations for 10,638 (~33%) of *O. faveolata*, 11,759 (~26%) of *Ps. strigosa* transcripts, 5,241 (~20%) of *P. porites* transcripts and 4,977 (~75%) of *P. astreoides* transcripts.

Differential Expression Analyses

Differential expression varied greatly between species following immune challenge. In *O. faveolata*, 371 transcripts were differentially expressed, 111 downregulated and 260 upregulated. Of those 371 transcripts, 149 could be assigned annotations. In comparison, 79 *P. astreoides* transcripts were differentially expressed: 31 downregulated and 48 upregulated. 53 *P. astreoides* differentially expressed transcripts could be assigned annotations. Finally, there were no *Ps. strigosa* or *P. porites* transcripts were significantly differentially expressed.

Gene ontology classification of differentially expressed genes for *O. faveolata* and *P. astreoides* also varied greatly (**Supplementary Figure 1**). *O. faveolata* had a higher proportion of differentially expressed transcripts involved in apoptosis, while *P. astreoides* had a higher proportion of transcripts associated with metabolic processes.

Pathway Analyses

Analysis of each of the four species of corals using IPA software yielded 231 unique pathways that were significantly activated ($padj < 0.05$) in one or more coral species. The number of significantly activated pathways per species ranged from 113 in *Ps. strigosa* to 35 in *O. faveolata*. The number of significantly activated pathways which could be assigned a z-score varied from 12 (*O. faveolata*) to 49 (*Ps. strigosa*). Of these significantly activated pathways with z-scores, between 7 (*O. faveolata* and *P. astreoides*) and 18 (*Ps. strigosa*) could be identified as involved in stress or immune responses (**Figure 1**).

While many pathways were unique to a single species, there were also numerous pathways that were activated in one or more species (**Figure 2, Supplementary Table 1**). Three pathways were significantly activated in all four species: protein ubiquitination pathway, pyrimidine deoxyribonucleotides de novo biosynthesis I pathway, and superpathway of inositol phosphatase compounds. Furthermore, several pathways were shared between just susceptible or tolerant coral species. Many pathways involving the cell cycle and cell death were activated in both *O. faveolata* and *Ps. strigosa*. This included the death receptor signaling pathway and numerous cancer pathways. *O. faveolata* alone activated apoptotic pathways such as NF-κB signaling, TWEAK signaling and retinoic acid mediated apoptosis signaling. In contrast, *P. porites* and *P. astreoides* both activated pathways that were involved in protein turnover (isoleucine degradation I and valine

degradation I). Autophagy-related pathways (autophagy signaling, AMPK signaling, phagosome maturation) were commonly activated in all species except the most susceptible, *O. faveolata*.

Apoptotic Pathways

Pathways involved in apoptosis including apoptotic signaling, death receptor signaling, and TWEAK signaling were activated in multiple species. Z-scores of all three of these pathways decreased with disease susceptibility (**Table 1**). Additionally, genes involved in both the death receptor signaling and TWEAK signaling pathways demonstrated more pronounced downregulation (negative $\log_2$fold change) in disease tolerant *Porites* species as compared to disease susceptible species **(Supplementary Figure 2**).

Apoptotic Caspase Activity

Caspase activity varied significant between coral species but no significant effect of LPS treatment was observed (2-way ANOVA; 'species identity' effect $F_{3,29} = 8.814$, $p = 2.61e\text{-}4$ and 'LPS exposure' effect $F_{1, 29} = 0.0293$, $p = 0.763$). Specifically, the two disease susceptible species, *O. faveolata* and *Ps. Strigosa*, showed higher caspase higher activity compared to the two disease tolerant species, *P. porites* and *P. astreoides* (Tukey post-hoc comparisons: *O. faveolata* vs. *P. porites* $p = 0.007$, *O. faveolata* vs. *P. astreoides* $p = 0.022$, *Ps. strigosa* vs. *P. porites* $p = 0.002$, *Ps. strigosa* vs. *P. astreoides* $p = 0.006$). While there was no effect of LPS exposure as a factor in the 2-way ANOVA, caspase activity following immune stimulation did significantly increase and decrease in *O. faveolata* and *P. porites* respectively (t-test, *padj*= 0.016 and 0.0004 respectively; **Figure 3**).

Autophagy Pathways

Two pathways involved in autophagy: autophagy and AMPK signaling were activated in the study coral species. Z-score patterns varied for each pathway. No z-scores were generated for the autophagy-specific pathway. However, z-scores for the AMPK signaling pathway were fairly consistent across all four species. (**Table 1**) Patterns of log_2fold change varied within each pathway, due to overlap in contigs between regulatory pathways (**Supplementary Figure 3**). Autophagy inhibitor mTOR was upregulated in disease susceptible *O. faveolata* and downregulated in tolerant *Porites* species. In contrast autophagy activator AMPK was most downregulated (lowest log_2fold change) in *O. faveolata* (**Supplementary Figure 4**).

DISCUSSION

While diseases are driving unprecedented coral mortality events (Daszak *et al.* 2001;Harvell *et al.* 1999;Sutherland *et al.* 2004), not all species seem to be effected similarly (Grottoli *et al.* 2014;Roff&Mumby 2012;van Woesik *et al.* 2011). Differences in disease susceptibility between coral species could have important implications for the future ecological functioning of reefs. Here we use bacterial PAMPs such as LPS to stimulate immunity in four coral species. LPS is one of many virulence factors that initiates host response, primarily through activation of TLR4 in humans (Chow *et al.* 1999;Lu *et al.* 2008). It is evident that corals possess a variety of TLR receptors, some of which are analogous to TLR4, although the variation of TLR receptors within specific species of corals is still unknown (Mydlarz *et al.* 2016;Poole&Weis 2014;Shinzato *et al.* 2011). This potential diversity of TLR receptors may have contributed in part to the variation of host immune responses observed here and therefore may have significant ecological consequences.

Apoptosis is Activated in Disease Susceptible Species

Our findings highlight two major processes that may be contributing to variable immunity in corals: apoptosis and autophagy. Apoptosis has complex and multi-faceted roles in innate immunity, severing as both a crucial aspect of immediate immune response (Allam *et al.* 2014;Man&Kanneganti 2016;Yang *et al.* 1998) and as a last-resort (i.e. cell death) response (Ainsworth *et al.* 2007;Libro *et al.* 2013) depending on the circumstances and stage of infection. Apoptosis of infected cells is part of the innate immune responses that promotes organismal survival (Allam *et al.* 2014). In contrast, apoptosis in corals infected with white disease is characteristic of tissue loss and organismal death (Ainsworth *et al.* 2007;Libro *et al.* 2013). These contrasting observations suggest that while immediate apoptosis may be beneficial in combating pathogenic immune response, prolonged upregulation of apoptotic pathways may in fact signal the demise of the organism.

Changes in gene expression and activation (log_2fold change and z-scores) of apoptotic pathways were lower in tolerant species when compared to disease susceptible ones. Additionally, the susceptible coral *O. faveolata* had a higher proportion of significantly differentially expressed genes involved in apoptotic processes and higher apoptotic caspase activity compared to tolerant coral *P. astreoides*. Disease tolerant corals reduced expression of apoptotic pathways to a greater extent than their susceptible counterparts, as evidenced by both pathway expression and caspase activity, which may contribute to resilience to stress. Corals that recover post temperature stress and bleaching are characterized by inhibition of apoptotic pathways, while those that experience mortality following these events are marked by increased apoptotic activity (Tchernov *et al.* 2011). In other invertebrates, apoptosis is the last resort under stressful conditions, and if stress continues, death results due to excessive cell death (Chiarelli *et al.* 2016). Furthermore, in shrimp infected with white-spot syndrome

virus, inhibition of apoptosis decreases mortality, suggesting that excessive apoptosis associated with infection can lead to increased disease susceptibility and mortality (Rijiravanich *et al.* 2008). Increased activation of apoptosis in susceptible coral species may be a significant factor contributing to the susceptibility of these species to disease-related mortality.

Autophagy is Key in Disease Tolerant Coral Species

Tolerant corals uniquely activated pathways involved in autophagy (autophagy and AMPK signaling) following immune challenge. Induction of autophagy following immune challenge benefits hosts in two ways. First, autophagy of non-essential cell components can quickly provide new sources of macromolecules to fuel biochemical reactions (Maiuri *et al.* 2007). Tolerant corals therefore may be able to quickly mobilize resources during an immune challenge due to their activation of autophagy immediately following immune challenge. Second, autophagy is one of the most ancient forms of innate immune response (Tang *et al.* 2012). Autophagy is often triggered by canonical immune receptors such as toll-like and NOD receptors (Cooney *et al.* 2010;Delgado *et al.* 2008;Nakamoto *et al.* 2012;Shi&Kehrl 2008;Xu *et al.* 2013;Xu *et al.* 2007). Triggering of autophagy by these receptors can result in the elimination of intracellular bacteria (Levine *et al.* 2011;Moy&Cherry 2013;Nakagawa *et al.* 2004;Watson *et al.* 2012;Yano *et al.* 2008) and viruses (Levine *et al.* 2011;Moy&Cherry 2013;Nakamoto *et al.* 2012;Shelly *et al.* 2009). Therefore activation of autophagic proteins by tolerant corals likely allows for a more rapid response to, and elimination of, potential pathogens. In comparison, susceptible corals, which either do not activate, or delay activation of, autophagic pathways, may experience more disease-related mortality as a result of slower pathogen clearance.

Tolerant corals also uniquely activated the AMPK signaling pathway, which regulates autophagy (Alers *et al.* 2012;Kim *et al.* 2011;Mihaylova&Shaw 2011). Under normal conditions within a cell, mTOR will negatively regulate autophagic pathways. However, during cellular starvation or other stressful events, the AMPK pathway becomes active, blocking mTOR and activating autophagy (Gomes&Dikic 2014;Kim *et al.* 2011). Z-score patterns for the AMPK pathways did not follow a clear pattern, likely due to the many functions of this pathway. In contrast, patterns of expression of just mTOR and AMPK subunits provides a clear picture of increased activation of autophagy in tolerant corals. Decreasing expression of mTOR and increasing expression of AMPK by tolerant corals would promote increased autophagy during infection, allowing for a more rapid pathogen response.

Autophagy vs. Apoptosis: A Spectrum Affecting Disease Resistance?

Close examination of the results of this study offers a potential new paradigm describing the cellular mechanisms driving variation in disease susceptibility in corals. The results presented here suggest that susceptibility may be determined by cellular maintenance responses . We found that corals that are characterized as disease susceptible are marked by an apoptotic response, while tolerant species display an autophagic response. In fact, these two processes are more often than not mutually exclusive (Kroemer *et al.* 2010;Maiuri *et al.* 2007;Marino *et al.* 2014), and often times activation of one pathway over another can mean the difference between an adaptive or death response (Baehrecke 2005;Chiarelli *et al.* 2016;Marino *et al.* 2014).

Our results demonstrated a clear activation of apoptosis over autophagy in our susceptible coral species, likely triggered by excessive immune stress (Chiarelli *et al.* 2016;Marino *et al.*

2014). The induction of apoptosis over autophagy is possibly a result of the inability of susceptible corals to respond to the stressor and/or limited plasticity in their response. This inability to resist stress results in the increased susceptibly of these species to pathogens and high levels of disease-related mortality. In contrast, tolerant corals were characterized by activation of autophagic pathways. Autophagy is a pathway of survival under various stressful circumstances (Deretic&Levine 2009;Levine&Yuan 2005;Mizushima&Komatsu 2011;Ogata *et al.* 2006), including during infection (Liu *et al.* 2005). Additionally, autophagic pathways can be used as a mechanism of cellular adaptation, or plasticity, during stress (Baehrecke 2005;Gomes&Dikic 2014;Maiuri *et al.* 2007;Marino *et al.* 2014), which may explain the activation of autophagic pathways by tolerant corals. Increased expression of autophagy, and in particular cellular plasticity during immune challenge, likely allows tolerant corals to avoid cellular death. Therefore, we propose a new framework for the effects of apoptosis and autophagy on coral disease resistance shown in **Figure 4**. Likely the promotion of apoptosis over autophagy or vice versa plays a significant role in determining disease and stress response outcomes on coral reefs.

CONCLUSIONS

Decades of ecological survey data have established that coral species respond differently to disease (Grottoli *et al.* 2014;Roff&Mumby 2012;van Woesik *et al.* 2011). However, the cellular mechanisms underlying these patterns have been poorly described. Here we demonstrate the importance of apoptosis and autophagy in the response of multiple coral species to immune challenge. The contribution of these pathways to disease resistance in numerous species, including corals has been largely understudied. Indeed, cellular maintenance may play a much larger role in coral immune response than previously thought and examination of these pathways

in more species will only continue to increase our understanding of how autophagy and apoptosis impact immune variation.

ACKNOWLEDGEMENTS

The authors would like to acknowledge the Department of Marine Sciences, University of Puerto Rico Mayagüez (UPRM) for partial funding for boat and diving, logistical support and laboratory space. Additionally, the authors would like to thank Duane Sanabria, Luis Rodriguez, and Derek Soto for support in the field and the staff of the Genetics Core Facility (UTA) and the Castoe lab at the University of Texas for assistance with laboratory and bioinformatic work respectively. The analyses were run on a server provided by the UTA Office of Information Technology.

FIGURES AND TABLES

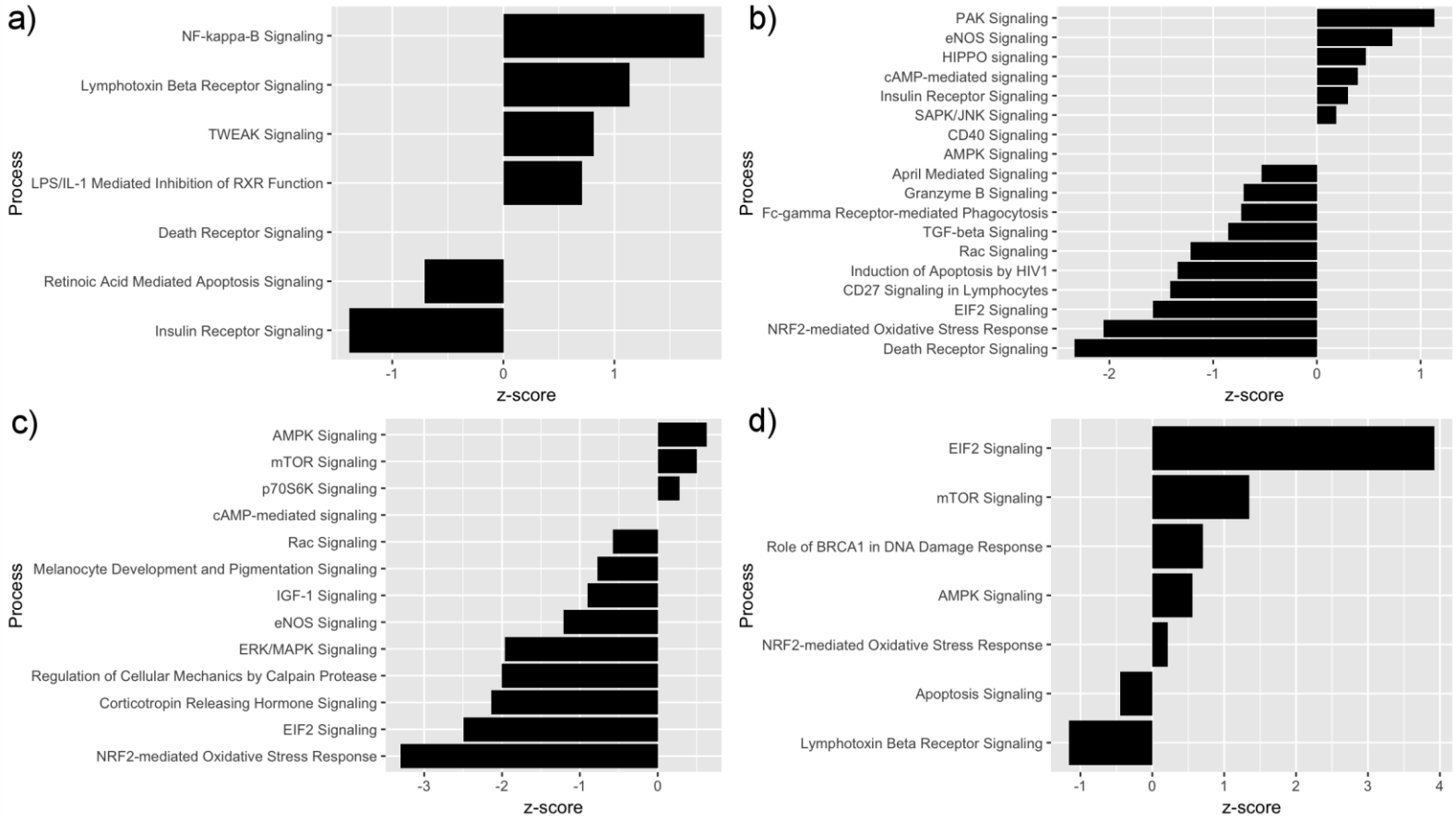

Figure 1: IPA analysis results for selected immune pathways. Bars indicate z-scores (measure of activation/inactivation). a) O. faveolata, b) Ps. strigosa c) P. porites d) P. astreoides

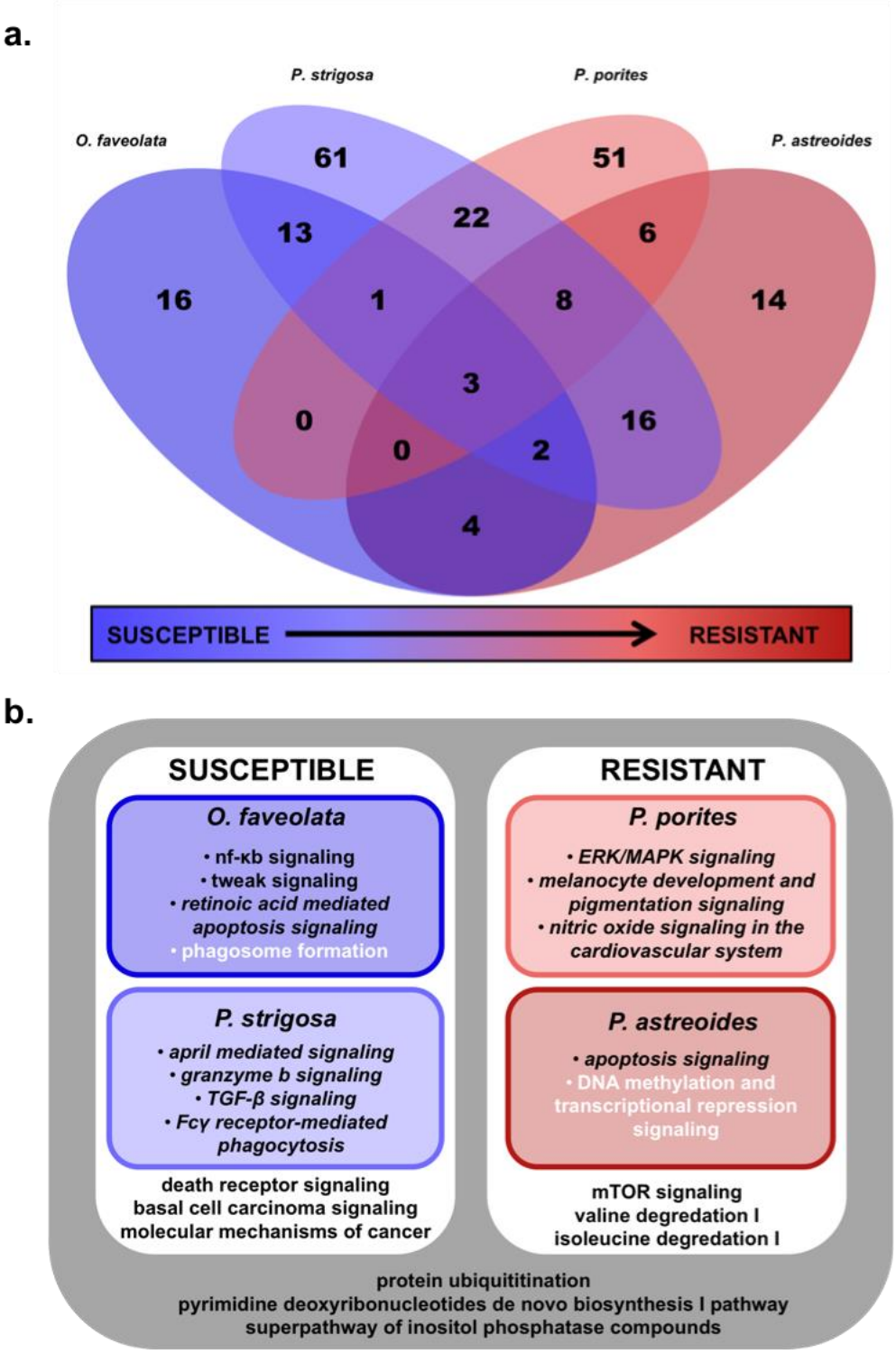

Figure 2: Venn diagrams displaying overlap of activated pathway for each of the four species. a) Numerical distribution of activated pathways for all four species, including overlap between species. Species are listed in order of increasing disease resistance from left to right. b) Venn diagram highlighting specific pathways of interest as well as pathways shared between susceptible or tolerant species and activated pathways shared by all four species. Bolded pathways are those that were activated, italicized pathways were inactivated. Shared pathways had differing patterns of activation between species.

Table 1 Pathway Statistic Summary: Summary of z-scores and p-values for relevant autophagy and apoptosis pathways (* indicates $p < 0.05$, ** $p < 0.01$)

Pathway	*O. faveolata*		*Ps. strigosa*		*P. porites*		*P. astreoides*	
	z-score	**p-value**	**z-score**	**p-value**	**z-score**	**p-value**	**z-score**	**p-value**
Autophagy	NaN	0.143	NaN	0.00741**	NaN	0.0126*	NaN	9.55E-5**
AMPK	0.707	0.0776	0	5.62E-6**	0.626	4.07E-4**	0.557	1.95E-5**
Apoptosis	-0.378	0.236	-0.200	0.122	-0.707	0.305	-0.447	0.0102*
Death Receptor Signaling	0	6.17E-4**	-2.34	0.00832**	-2.12	0.0891	-1.21	0.337
TWEAK Apotosis	0.816	0.0110*	0	0.213	N.A	N.A	-0.707	0.0692

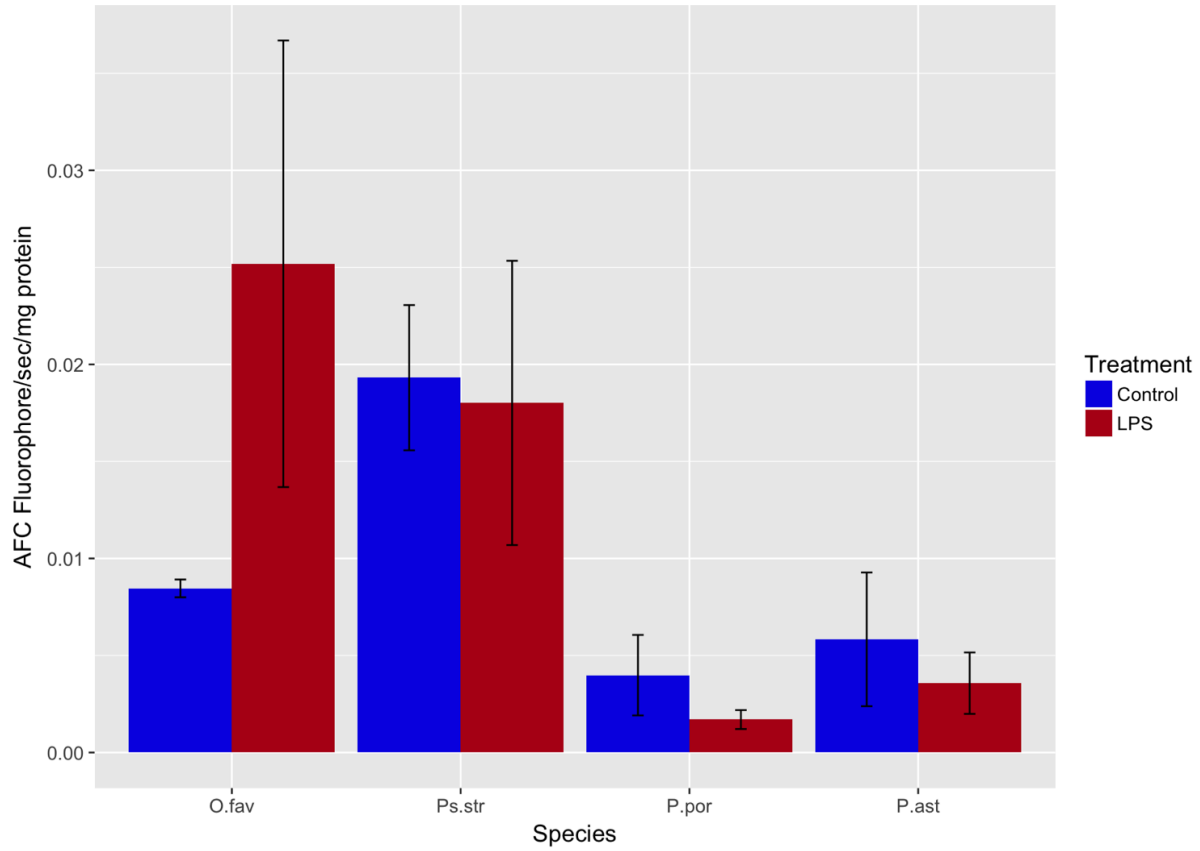

Figure 3: Caspase activity assay results for each species and treatment (n=4-5 individuals). Data is in AFC fluorophores released per second (estimate of caspase cleaving activity), adjusted for protein concentration. Species effect was significant ($p < 0.001$), and individual t-tests between treatment groups within species indicated significant differences for O. faveolata ($p=0.016$), and P. porites ($p=0.004$).

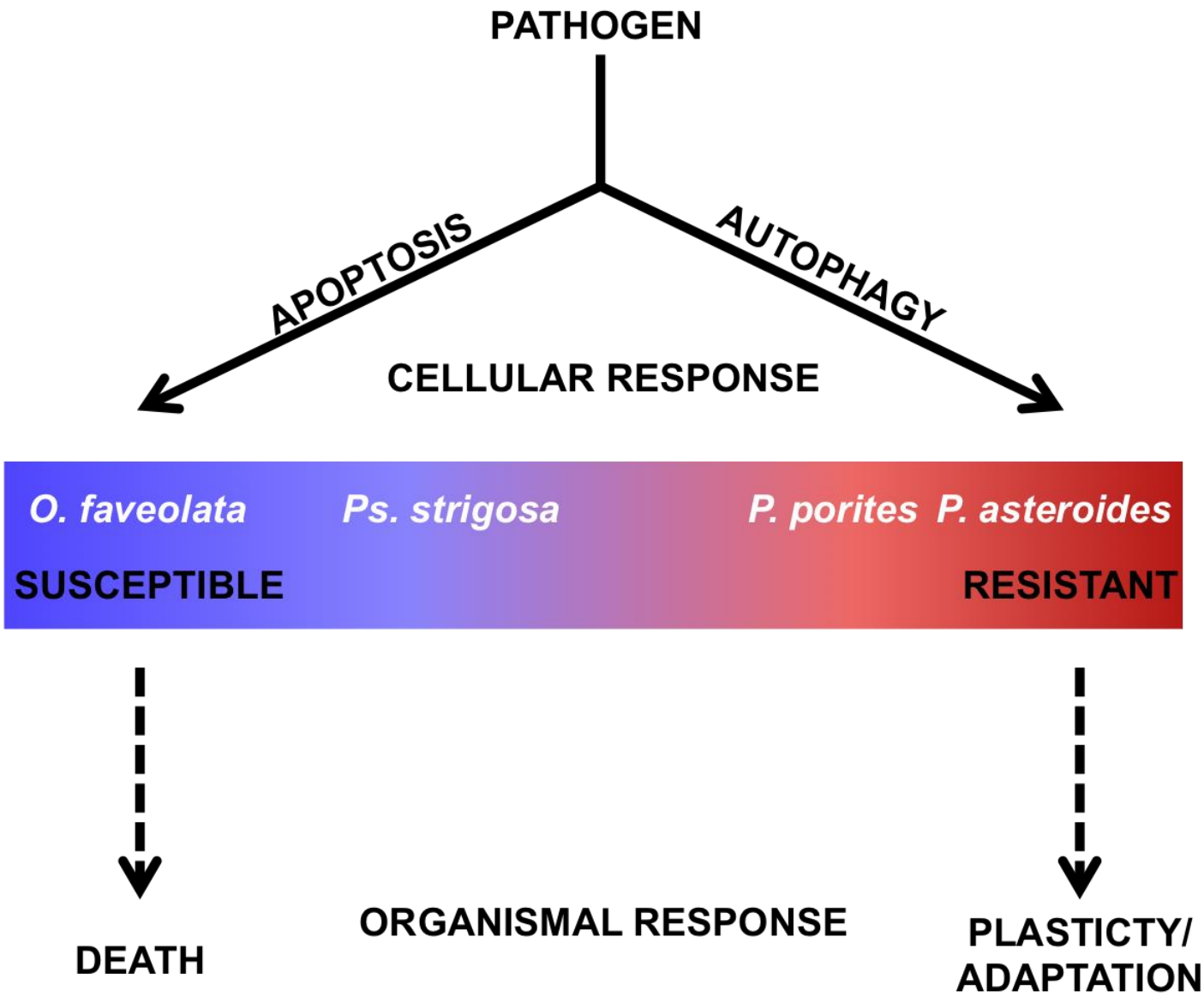

Figure 4: Working model of disease resistance as suggested by our findings. Upon pathogenic infection, an organism may favor apoptosis or autophagy, which contributes to the overall result of the infection. Susceptible species favor apoptosis, which results in organismal death, while tolerant species favor autophagy that results in plasticity and organismal adaptation. Responses exist on a spectrum with a mix of apoptosis and autophagic responses being possible.

Table 1 Pathway Statistic Summary: Summary of z-scores and p-values for relevant autophagy and apoptosis pathways (* indicates $p < 0.05$, ** $p < 0.01$)

Pathway	*O. faveolata*		*Ps. strigosa*		*P. porites*		*P. astreoides*	
	z-score	**p-value**	**z-score**	**p-value**	**z-score**	**p-value**	**z-score**	**p-value**
Autophagy	NaN	0.143	NaN	0.00741**	NaN	0.0126*	NaN	9.55E-5**
AMPK	0.707	0.0776	0	5.62E-6**	0.626	4.07E-4**	0.557	1.95E-5**
Apoptosis	-0.378	0.236	-0.200	0.122	-0.707	0.305	-0.447	0.0102*
Death Receptor Signaling	0	6.17E-4**	-2.34	0.00832**	-2.12	0.0891	-1.21	0.337
TWEAK Apotosis	0.816	0.0110*	0	0.213	N.A	N.A	-0.707	0.0692

SUPPLEMENTARY FIGURES AND TABLES

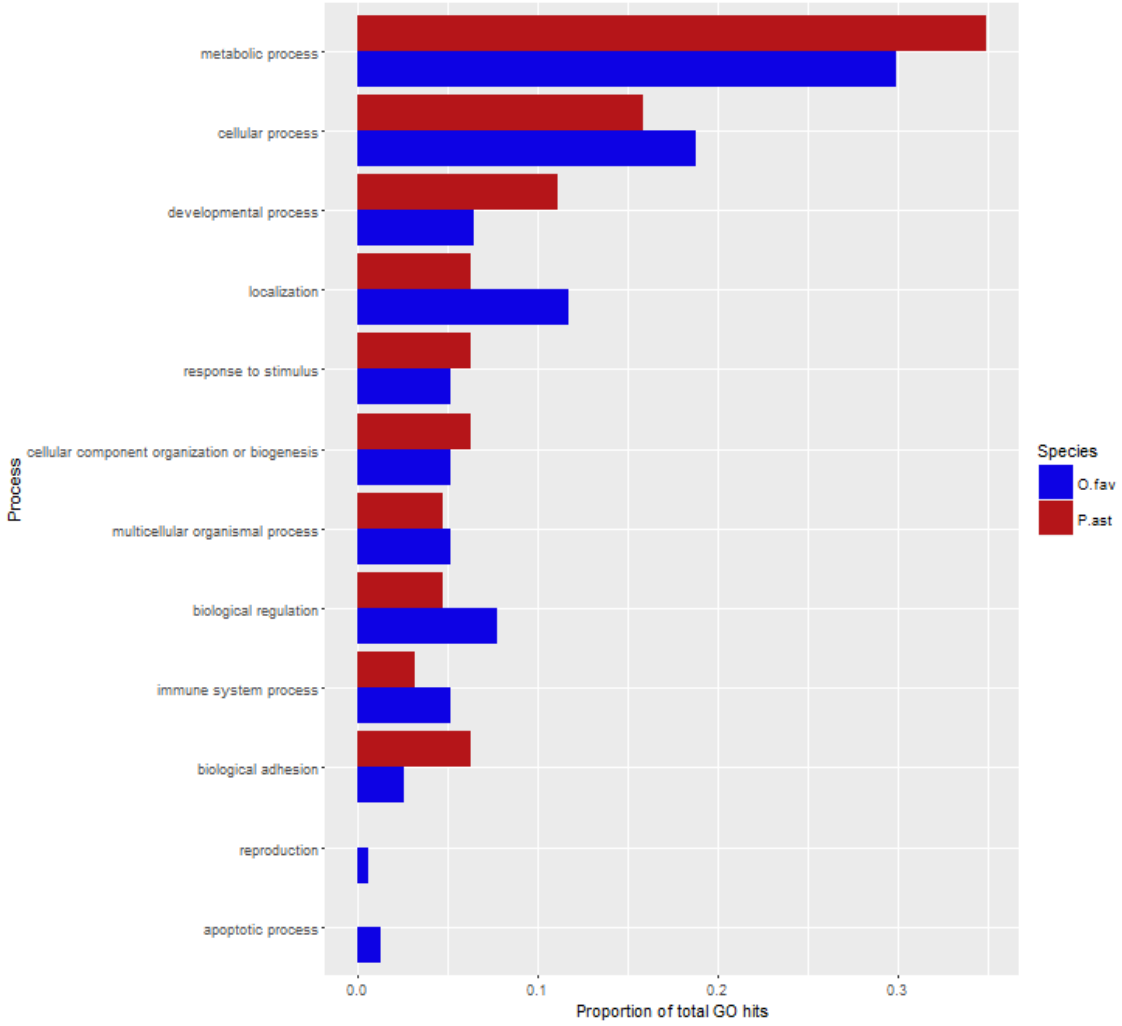

Supplementary Figure 1: Tier 1 Biological Process Gene Ontology term breakdown of differentially expressed genes for *Orbicella faveolata* (O.fav) and *Porites asteroides* (P.ast). Data shown as ratio of terms in a category out of the total number of GO terms for that species.

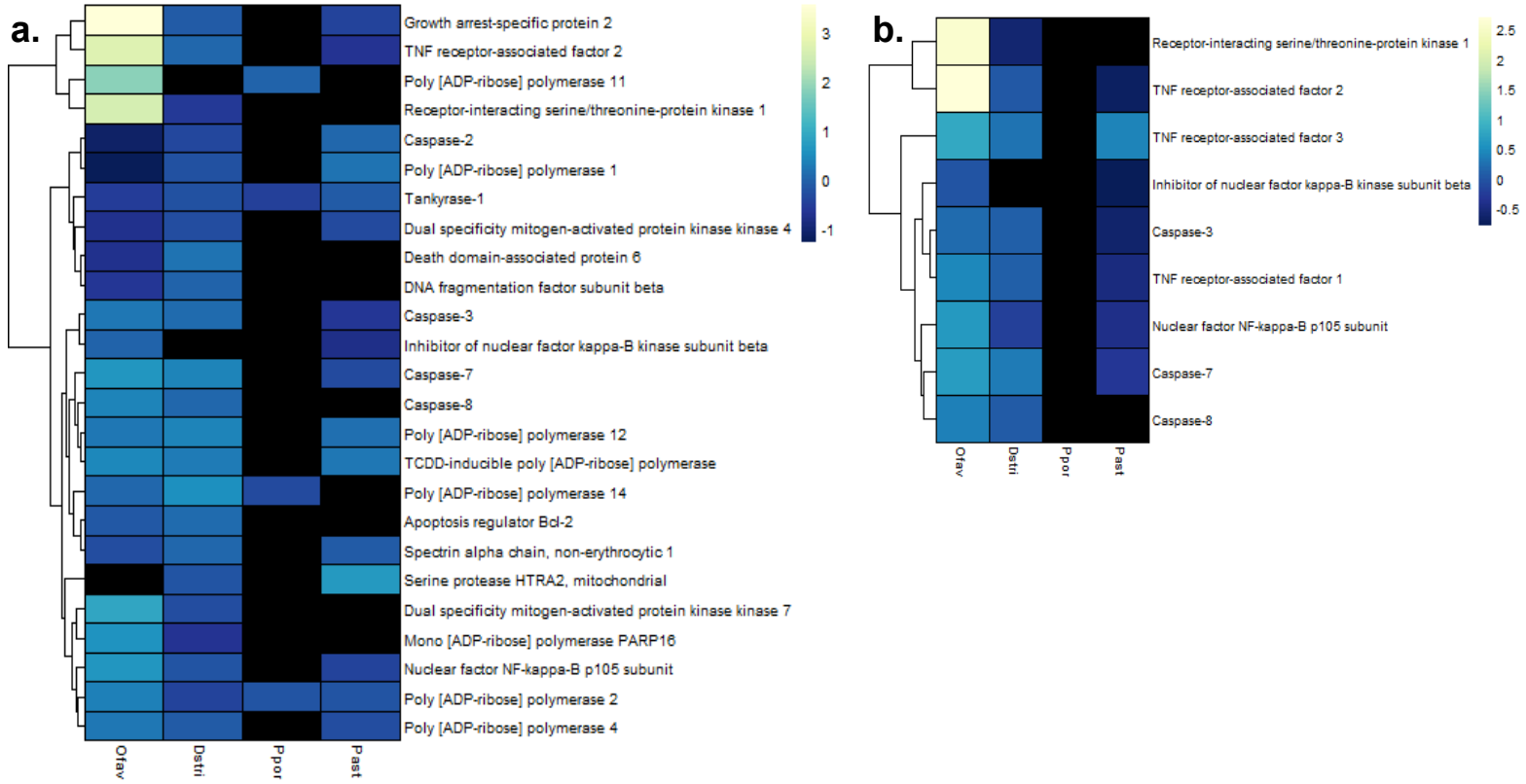

Supplementary Figure 2: Log2fold change per species of a) death receptor signaling b) TWEAK apoptosis. Black fill indicates gene was not present in the species in question. Log2fold values for annotation with multiple gene copies were averaged and the averaged values used to create the heat maps. Genes found in only one of four species not listed.

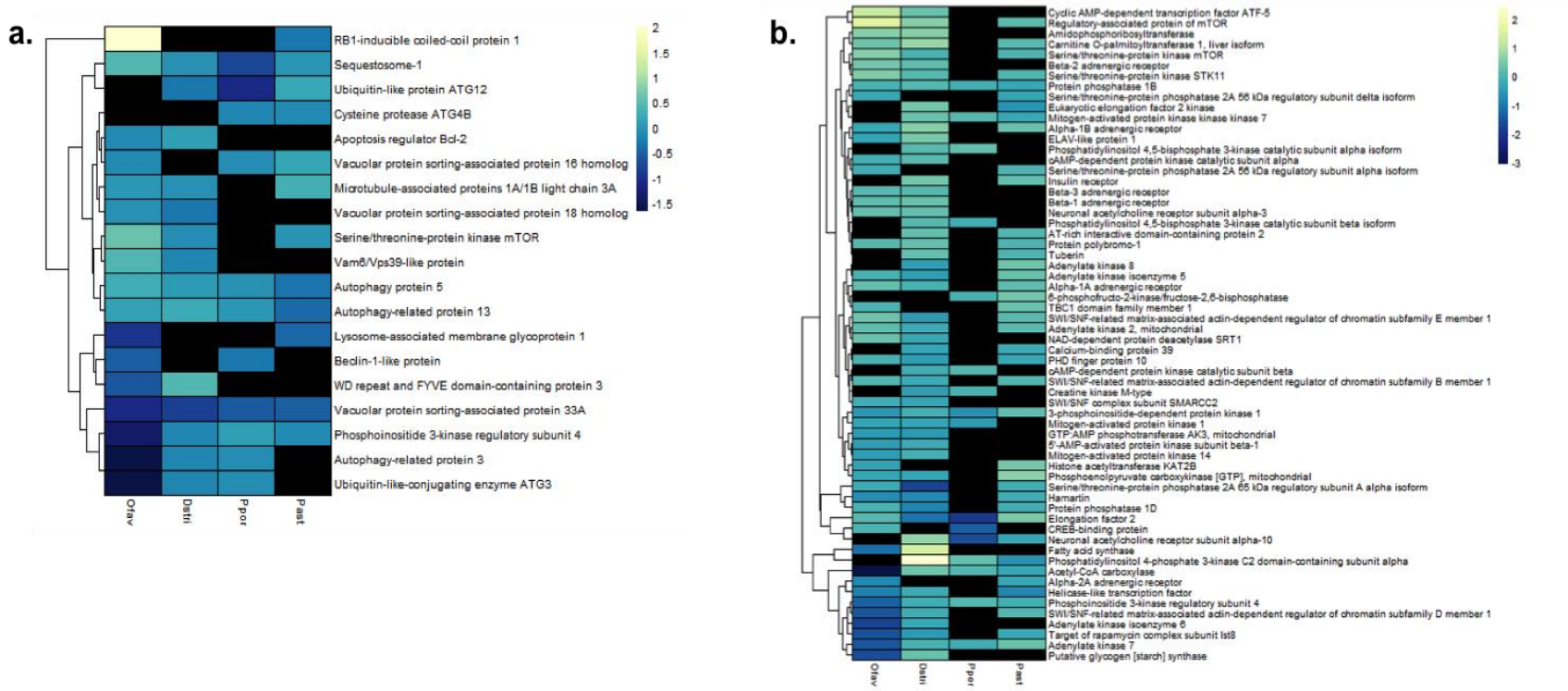

Supplementary Figure 3: Log2fold change per species of a) autophagy and b) AMPK. Black fill indicates gene was not present in the species in question. Log2fold values for annotation with multiple gene copies were averaged and the averaged values used to create the heat maps. Genes found in only one of four species not listed.

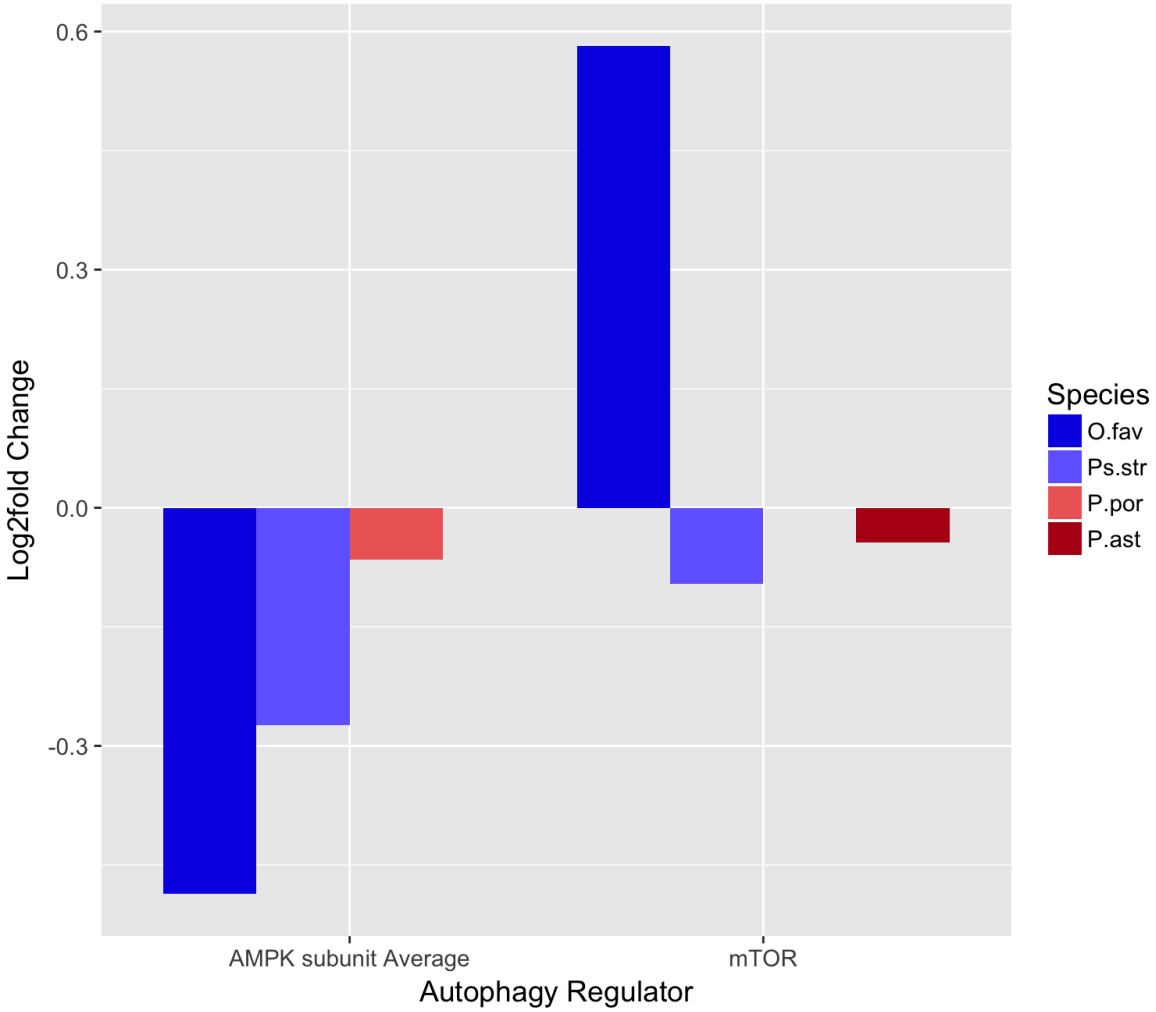

Supplementary Figure 4: Log2fold-change of autophagy regulations AMPK (promoter) and mTOR (inhibitor) by species.

Supplementary Table 1: Comparison of significant pathways across all four species. All pathways which were significant in at least one species are listed. Data presented is z-score and p-value for each pathway. * indicates a pathway is significant at $p < 0.05$, ** $p < 0.01$.

Pathway	*O. fav*		*Ps. stri*		*P. por*		*P. ast*	
	z-score	**p-value**	**z-score**	**p-value**	**z-score**	**p-value**	**z-score**	**p-value**
1D-myo-inositol Hexakisphosphate Biosynthesis II (Mammalian)	NaN	0.291	NaN	0.014*			NaN	0.232
2-ketoglutarate Dehydrogenase Complex			NaN	0.637	NaN	0.028*	NaN	0.431
3-phosphoinositide Biosynthesis	NaN	0.171	NaN	0.005**	NaN	0.008**	NaN	4.47E-04**
3-phosphoinositide Degradation	NaN	0.036*	NaN	0.001**	NaN	0.100	NaN	1.12E-04**
Acetate Conversion to Acetyl-CoA			NaN	0.037*			NaN	0.431
Acetyl-CoA Biosynthesis I (Pyruvate Dehydrogenase Complex)			NaN	0.049*	NaN	0.406	NaN	0.231
Actin Cytoskeleton Signaling	-1.604	0.238	0.674	0.011*				
Actin Nucleation by ARP-WASP Complex	0.816	0.013*	-0.728	0.032*			-0.632	0.193
Adipogenesis pathway	NaN	0.136	NaN	0.002**			NaN	0.106
Aldosterone Signaling in Epithelial Cells	-1.134	0.089	0.756	1.00E-07**	-0.302	0.000	-0.333	0.023*
AMPK Signaling	0.707	0.078	0	5.62E-06**	0.626	4.07E-04**	0.557	1.95E-05**
Amyloid Processing	NaN	0.324	-2.236	0.346	NaN	0.003**	NaN	0.124
Amyotrophic Lateral Sclerosis Signaling			NaN	0.343	NaN	0.004**	NaN	0.138
Androgen Signaling			-0.277	0.003**	-1.667	0.013*	1.000	0.085
Angiopoietin Signaling	0	0.315	1.000	0.049*	NaN	0.515	NaN	0.085
Apoptosis Signaling	-0.378	0.236	-0.200	0.122	-0.707	0.305	-0.447	0.010*
April Mediated Signaling	2.236	0.060	-0.535	0.030*			-1.890	0.224

Assembly of RNA Polymerase II Complex	NaN	0.541	NaN	1.62E-05**	NaN	0.485	NaN	3.47E-05**
Autophagy	NaN	0.143	NaN	0.007**	NaN	0.013*	NaN	9.55E-05**
Axonal Guidance Signaling	NaN	0.196	NaN	4.27E-05**				
B Cell Activating Factor Signaling	2.236	0.072	-0.258	0.021*			-1.414	0.146
B Cell Receptor Signaling	-0.302	0.393	0.429	0.043*			-1.000	0.344
Basal Cell Carcinoma Signaling	0	0.049*	1.091	0.039*				
BER pathway	NaN	0.501	NaN	0.007**	NaN	0.008**	NaN	0.062
Bile Acid Biosynthesis, Neutral Pathway	NaN	0.033*	NaN	0.327				
Biotin-carboxyl Carrier Protein Assembly	NaN	0.160	NaN	0.128	NaN	0.015*	NaN	0.047*
BMP signaling pathway	NaN	0.257	0.302	0.001**	NaN	0.301		
Breast Cancer Regulation by Stathmin1	NaN	0.515	NaN	0.065	NaN	5.37E-04	NaN	0.452
Calcium Signaling			0.200	0.248	-0.894	0.017	0.535	0.476
cAMP-mediated signaling			0.397	0.045*	0	9.12E-05**		
Cardiac Hypertrophy Signaling	0.277	0.492	0.775	0.010*	-0.229	0.121	-0.577	0.471
Cardiac β-adrenergic Signaling			0.426	0.512	0	1.95E-07**	1.291	0.212
CD27 Signaling in Lymphocytes	1.342	0.168	-1.414	0.030*			-1.265	0.136
CD40 Signaling	1.342	0.304	0	0.022*			-1.732	0.138
Cell Cycle Regulation by BTG Family Proteins			NaN	0.537	NaN	0.036*	NaN	0.493
Cell Cycle: G2/M DNA Damage Checkpoint Regulation	NaN	0.527	1.291	0.063	1.000	0.002*	-0.333	0.186
Cellular Effects of Sildenafil (Viagra)	NaN	0.444	NaN	0.521	NaN	1.20E-04**		
Choline Biosynthesis III	NaN	0.530			NaN	0.238	NaN	0.020*
Chondroitin Sulfate Biosynthesis	NaN	0.089	NaN	0.013*	NaN	0.359		
Chondroitin Sulfate Biosynthesis (Late Stages)	NaN	0.124	NaN	0.045*				

Chondroitin Sulfate Degradation (Metazoa)	NaN	0.581	NaN	0.032*	NaN	0.087	NaN	0.604
Citrulline-Nitric Oxide Cycle			NaN	0.311	NaN	0.045*		
Cleavage and Polyadenylation of Pre-mRNA	NaN	0.027*	NaN	0.001**	NaN	0.210	NaN	0.014*
CNTF Signaling			0.577	0.505	0	0.030*		
Coenzyme A Biosynthesis			NaN	0.532			NaN	0.047*
Colanic Acid Building Blocks Biosynthesis	NaN	0.185	NaN	0.021*			NaN	0.100
Corticotropin Releasing Hormone Signaling			0.200	0.430	-2.138	0.006		
Creatine-phosphate Biosynthesis					NaN	0.045*	NaN	0.505
CREB Signaling in Neurons			1.976	0.066	-0.447	0.001*		
Cysteine Biosynthesis III (mammalia)			NaN	2.34E-05**	NaN	2.24E-04**	NaN	0.463
D-myo-inositol (1,3,4)-trisphosphate Biosynthesis	NaN	0.089	NaN	0.014*			NaN	0.463
D-myo-inositol (1,4,5,6)-Tetrakisphosphate Biosynthesis	NaN	0.192	NaN	0.014*	NaN	0.078	NaN	2.34E-04**
D-myo-inositol (1,4,5)-trisphosphate Degradation			NaN	9.12E-03	NaN	0.373	NaN	0.203
D-myo-inositol (3,4,5,6)-tetrakisphosphate Biosynthesis	NaN	0.192	NaN	0.014*	NaN	0.078	NaN	2.34E-04**
D-myo-inositol-5-phosphate Metabolism	NaN	0.195	NaN	0.015*	NaN	0.156	NaN	0.001**
Death Receptor Signaling	0	6.17E-04**	-2.335	8.31E-03**	-2.121	0.337	-1.213	0.089
Dermatan Sulfate Biosynthesis	NaN	0.107	NaN	5.25E-03**	NaN	0.402		
Diphthamide Biosynthesis			NaN	0.128	NaN	0.200	NaN	2.24E-03**
DNA Double-Strand Break Repair by Non-Homologous End Joining	NaN	0.185	NaN	5.01E-03**	NaN	0.015*	NaN	0.100
DNA Methylation and			NaN	0.058			NaN*	0.038

Transcriptional Repression Signaling								
Dolichyl-diphosphooligosaccharide Biosynthesis			NaN	1.74E-03**	NaN	0.157	NaN	0.133
Dopamine Receptor Signaling			0	0.281	-0.707	0.023*	0	0.323
Dopamine-DARPP32 Feedback in cAMP Signaling			0.667	0.110	-1.043	7.76E-05**		
EGF Signaling			0	0.016*			-1.000	0.310
EIF2 Signaling			-1.581	7.59E-05	-2.496	3.16E-03**	3.922	1.66E-06**
Endoplasmic Reticulum Stress Pathway	NaN	0.112	NaN	0.029*	NaN	0.450	NaN	1.32E-04**
eNOS Signaling			0.730	0.043*	-1.213	6.92E-05**	-0.229	0.114
Ephrin A Signaling	NaN	0.285	NaN	5.37E-03**	NaN	0.453	NaN	0.290
Ephrin Receptor Signaling	-1.134	0.521	0.493	0.019*				
Epithelial Adherens Junction Signaling			NaN	0.042*				
ERK/MAPK Signaling			1.021	0.120	-1.961	3.80E-04		
Estrogen Receptor Signaling	NaN	0.296	NaN	4.17E-03**			NaN	2.04E-03**
Factors Promoting Cardiogenesis in Vertebrates	NaN	0.074	NaN	0.015*				
FAK Signaling	NaN	0.219	NaN	0.012*	NaN	0.093	NaN	0.100
Fatty Acid β-oxidation III (Unsaturated, Odd Number)			NaN	0.218	NaN	0.028*	NaN	0.431
Fcγ Receptor-mediated Phagocytosis in Macrophages and Monocytes	-2.828	0.154	-0.730	0.018*	-0.707	0.348	-2.183	0.095
FGF Signaling	0.378	0.203	0.756	0.016*				
FLT3 Signaling in Hematopoietic Progenitor Cells			NaN	0.494	NaN	0.016*		
G-Protein Coupled Receptor Signaling	NaN	0.372	NaN	0.083	NaN	0.017*		

Gap Junction Signaling	NaN	0.377	NaN	0.068	NaN	3.55E-03**		
GDNF Family Ligand-Receptor Interactions	-1.890	0.037*	0.500	0.344			-0.707	0.543
Germ Cell-Sertoli Cell Junction Signaling			NaN	0.015*			NaN	0.272
Glioblastoma Multiforme Signaling	-0.277	0.036	2.137	0.122				
Glioma Signaling			1.000	0.089	-1.155	0.022*	-0.302	0.410
Glucocorticoid Receptor Signaling			NaN	2.19E-04**			NaN	0.015*
Glutaryl-CoA Degradation	NaN	0.144	NaN	0.033*	NaN	8.13E-03**	NaN	0.062
Glutathione Biosynthesis	NaN	9.12E-03	NaN	0.128	NaN	0.200	NaN	0.047*
Glutathione Redox Reactions II	NaN	0.207	NaN	0.218	NaN	2.63E-05	NaN	0.431
Glycine Betaine Degradation			NaN	0.011*	NaN	0.525	NaN	5.50E-03**
Glycine Cleavage Complex	NaN	0.041*	NaN	0.130			NaN	0.570
Glycine Degradation (Creatine Biosynthesis)					NaN	5.13E-03**	NaN	0.245
Glycoaminoglycan-protein Linkage Region Biosynthesis	NaN	0.334	NaN	0.049*	NaN	0.085	NaN	0.627
Glycogen Biosynthesis II (from UDP-D-Glucose)	NaN	0.294	NaN	0.025*			NaN	0.180
GNRH Signaling	-1.414	0.444	-0.169	0.116	-1.807	0.043*		
GPCR-Mediated Nutrient Sensing in Enteroendocrine Cells					NaN	0.037*		
Granzyme B Signaling	NaN	0.227	-0.707	0.014*				
Growth Hormone Signaling	NaN	0.551	0	0.369	-0.905	0.010*		
Gustation Pathway	NaN	0.374			NaN	5.62E-03		
Gαs Signaling			0.928	0.012*	-1.667	0.023*		
Heme Biosynthesis from Uroporphyrinogen-III I			NaN	0.037*			NaN	0.085
Heme Biosynthesis II			NaN	0.031*	NaN	0.132	NaN	0.103

Heme Degradation	NaN	0.018	NaN	0.037*	NaN	0.257	NaN	0.085
Heparan Sulfate Biosynthesis	NaN	4.90E-03**	NaN	2.24E-03**			NaN	0.498
Heparan Sulfate Biosynthesis (Late Stages)	NaN	7.24E-03**	NaN	0.011*			NaN	0.511
Hereditary Breast Cancer Signaling	NaN	0.304	NaN	3.89E-04	NaN	0.213	NaN	2.34E-03**
HGF Signaling	-1.265	0.072	1.061	0.011*	-1.265	0.219		
HIF1α Signaling			NaN	0.022*	NaN	0.113		
HIPPO signaling	NaN	0.023*	0.471	0.019*	NaN	0.420	0.707	0.233
Human Embryonic Stem Cell Pluripotency	NaN	0.019*	NaN	0.026*				
Huntington's Disease Signaling	0	0.060	1.333	8.91E-04**	-1.134	0.208	0.243	0.023*
Hypoxia Signaling in the Cardiovascular System			-1.342	0.120	NaN	0.321	NaN	0.019*
Hypusine Biosynthesis			NaN	0.532			NaN	0.047*
IGF-1 Signaling	-1.342	0.469	0.426	0.242	-0.905	0.044*		
Induction of Apoptosis by HIV1	0.447	0.249	-1.342	0.017*			-1.155	0.087
Inhibition of Matrix Metalloproteases	NaN	0.378	NaN	2.51E-03**			NaN	0.245
Inosine-5'-phosphate Biosynthesis II			NaN	0.011*			NaN	2.24E-03**
Insulin Receptor Signaling	-1.387	0.035*	0.302	1.32E-03**	-0.535	0.091	-0.447	0.140
Integrin Signaling	-1.291	0.125	-0.802	2.57E-03**	-1.414	0.106	-1.219	0.068
Isoleucine Degradation I	NaN	0.556	NaN	0.071	NaN	0.015*	NaN	0.028*
L-carnitine Biosynthesis	NaN	9.12E-03**	NaN	0.011*			NaN	0.344
Leptin Signaling in Obesity	NaN	0.238	0.707	0.494	0	6.03E-03**		
LPS/IL-1 Mediated Inhibition of RXR Function	0.707	0.024*	-0.447	0.192	1.134	0.408		
Lymphotoxin β Receptor Signaling	1.134	0.031*	0.500	0.078	0	0.089	-1.155	0.020*

Mechanisms of Viral Exit from Host Cells	NaN	0.199	NaN	0.437	NaN	7.76E-03**	NaN	0.014*
Melanocyte Development and Pigmentation Signaling			0	0.416	-0.775	8.51E-04**		
Melatonin Signaling			0.392	1.58E-03**	-0.832	3.80E-04**		
Methionine Degradation I (to Homocysteine)			NaN	3.02E-05**	NaN	9.77E-05**		
Methionine Salvage II (Mammalian)			NaN	0.128	NaN	0.015*	NaN	0.344
Mevalonate Pathway I	NaN	0.164	NaN	0.049*	NaN	0.619	NaN	0.079
Mismatch Repair in Eukaryotes			NaN	0.014*			NaN	4.17E-04**
Mitochondrial Dysfunction	NaN	0.104	NaN	5.37E-06**	NaN	0.341	NaN	0.023*
Mitotic Roles of Polo-Like Kinase			-2.324	6.76E-03**	-0.447	0.019*	0	0.022*
Molecular Mechanisms of Cancer	NaN	2.88E-03**	NaN	2.95E-05**	NaN	0.459	NaN	0.394
mTOR Signaling	-0.302	0.257	0.686	0.065	0.500*	0.027	1.347	6.92E-05
N-acetylglucosamine Degradation I	NaN	0.160	NaN	0.532			NaN	0.047*
N-acetylglucosamine Degradation II	NaN	0.018*	NaN	0.637			NaN	0.085
Netrin Signaling	NaN	0.175	NaN	0.078	NaN	0.019*		
Neuropathic Pain Signaling In Dorsal Horn Neurons			1.826	0.046*	0.866	7.76E-05**		
Neuroprotective Role of THOP1 in Alzheimer's Disease	NaN	0.394			NaN	6.61E-03		
NF-κB Signaling	1.807	0.034*	1.732	0.051				
NGF Signaling	-1.134	0.150	1.219	8.71E-03	-0.577	0.042*	-1.213	0.103
Nitric Oxide Signaling in the Cardiovascular System			1.569	0.159	-1.043	4.57E-07		
nNOS Signaling in Neurons			0	0.353	NaN	0.017*		
Notch Signaling	NaN	0.363	1.667	0.030*			1.000	0.054
NRF2-mediated Oxidative Stress	-0.378	0.437	-2.058	6.92E-05**	-3.300	1.66E-07**	0.218	3.39E-03

Response								
Nucleotide Excision Repair Pathway	NaN	0.132	NaN	8.71E-06**	NaN	2.82E-03**	NaN	2.95E-04**
Oxidative Phosphorylation			NaN	9.55E-04			NaN	0.179
P2Y Purigenic Receptor Signaling Pathway					-0.775	0.011*		
p70S6K Signaling			0.500	0.062	0.277	0.046*	0.905	4.27E-03**
PAK Signaling			1.134	0.017*	-0.378	0.456		
Paxillin Signaling	-2.121	0.116	-0.928	0.019*			-1.387	0.456
PCP pathway	-1.667	2.63E-03**	1.528	3.93E-03**				
Pentose Phosphate Pathway	NaN	0.441	NaN	0.011*	NaN	0.525	NaN	0.133
Pentose Phosphate Pathway (Oxidative Branch)	NaN	0.207	NaN	0.037*			NaN	0.085
phagosome formation	NaN	0.044*	NaN	0.480	NaN	0.524		
phagosome maturation	NaN	0.519	NaN	2.00E-03**	NaN	8.71E-04**	NaN	2.31E-03**
Phenylalanine Degradation I (Aerobic)			NaN	2.51E-03**	NaN	0.257	NaN	0.431
Phosphatidylethanolamine Biosynthesis II	NaN	0.407	NaN	0.120	NaN	0.022*		
Phototransduction Pathway					NaN	3.98E-03**		
Protein Kinase A Signaling	0.229	0.423	1.584	6.17E-05**	0.156	1.66E-05**		
Protein Ubiquitination Pathway	NaN	0.018*	NaN	5.01E-16**	NaN	1.23E-07*	NaN	2.00E-14**
PTEN Signaling	-0.632	0.129	-1.480	0.015*			-1.147	0.201
Purine Nucleotides De Novo Biosynthesis II	NaN	0.125	NaN	0.076	NaN	0.184	NaN	1.29E-03
PXR/RXR Activation	NaN	0.315	NaN	0.206	NaN	6.76E-03**		
Pyridoxal 5'-phosphate Salvage Pathway			NaN	0.063	NaN	1.74E-03**		
Pyrimidine Deoxyribonucleotides De Novo Biosynthesis I	NaN	0.032*	NaN	3.80E-05**	NaN	0.018*	NaN	0.019*

Pyrimidine Ribonucleotides De Novo Biosynthesis	NaN	0.095	NaN	1.26E-03**	NaN	0.179	NaN	0.103
Pyrimidine Ribonucleotides Interconversion	NaN	0.223	NaN	5.13E-04	NaN	0.344	NaN	0.076
Rac Signaling			-1.219	1.45E-03**	-0.577	0.035*	-2.324	0.286
RAN Signaling	NaN	0.605	NaN	6.46E-04**	NaN	5.75E-04**	NaN	0.148
RAR Activation	NaN	0.118	NaN	6.92E-04**	NaN	0.054	NaN	0.055
Regulation of Cellular Mechanics by Calpain Protease	NaN	0.217	0	0.188	-2.000	0.019*		
Regulation of eIF4 and p70S6K Signaling			0.500	0.062	0.378	0.100	0.905	4.27E-03*
Regulation of IL-2 Expression in Activated and Anergic T Lymphocytes	NaN	0.461	NaN	0.020*			NaN	0.340
Regulation of the Epithelial-Mesenchymal Transition Pathway	NaN	0.344	NaN	0.035*				
Relaxin Signaling					NaN	8.51E-05**		
Remodeling of Epithelial Adherens Junctions			-2.530	0.107	-0.447	0.112	-0.333	0.013*
Renal Cell Carcinoma Signaling	-1.342	0.210	1.000	0.018*	-0.816	0.066	-1.134	0.457
Renin-Angiotensin Signaling			0.365	0.081	-1.387	0.048*		
Retinoate Biosynthesis I	NaN	0.036*	NaN	0.048*	NaN	0.028*		
Retinoic acid Mediated Apoptosis Signaling	-0.707	0.021*	-1.069	0.385	-2.449	0.270		
Role of BRCA1 in DNA Damage Response			-1.732	8.91E-03**			0.707**	2.14E-03
Role of CHK Proteins in Cell Cycle Checkpoint Control			-2.673	0.089	-0.378	0.095	1.000	0.010*
Role of NANOG in Mammalian Embryonic Stem Cell Pluripotency	NaN*	0.022	0.333	0.143				
Role of NFAT in Cardiac Hypertrophy			0.590	0.047*	-0.853	2.19E-03**		

S-adenosyl-L-methionine Biosynthesis			NaN	0.128	NaN	3.63E-04**	NaN	0.344
Salvage Pathways of Pyrimidine Ribonucleotides			NaN	0.018*	NaN	2.40E-03**	NaN	0.449
SAPK/JNK Signaling	-0.333	0.083	0.186	0.020*			-1.732	0.465
Small Cell Lung Cancer Signaling	NaN	0.046*	NaN	0.033*	NaN	0.134	NaN	0.076
Sperm Motility	-1.134	0.243	2.335	0.013*	-0.218	1.26E-09**		
STAT3 Pathway	0	0.229	0.784	6.76E-03**				
Stearate Biosynthesis I (Animals)					NaN	0.041*		
Superpathway of Cholesterol Biosynthesis	NaN	0.474	NaN	0.032*	NaN	0.324	NaN	0.152
Superpathway of D-myo-inositol (1,4,5)-trisphosphate Metabolism	NaN	0.151	NaN	9.12E-03**	NaN	0.521	NaN	0.388
Superpathway of Geranylgeranyldiphosphate Biosynthesis I (via Mevalonate)	NaN	0.068	NaN	0.065	NaN	0.347	NaN	0.017*
Superpathway of Inositol Phosphate Compounds	NaN	0.046*	NaN	6.17E-04**	NaN	0.036*	NaN	0.002**
Superpathway of Methionine Degradation			NaN	5.50E-04**	NaN	5.13E-05**	NaN	0.412
Synaptic Long Term Potentiation			1.768	0.098	-0.447	1.02E-04**		
Telomere Extension by Telomerase	NaN	0.581	NaN	0.095	NaN	3.09E-03**	NaN	0.313
Tetrapyrrole Biosynthesis II			NaN	0.311	NaN	0.045*	NaN	0.505
TGF-β Signaling	-1.000	0.366	-0.853	0.022*				
The Visual Cycle	NaN	0.049*	NaN	0.230	NaN	0.292	NaN	0.604
Thiosulfate Disproportionation III (Rhodanese)	NaN	9.12E-03**	NaN	0.128			NaN	0.344
Triacylglycerol Degradation	NaN	0.044*	NaN	0.279	NaN	0.245		
tRNA Splicing	NaN	0.132	NaN	0.139	NaN	1.20E-04**	NaN	0.493
TWEAK Signaling	0.816	0.011*	0	0.213			-0.707	0.069

Tyrosine Biosynthesis IV			NaN*	0.011	NaN	0.200		
Ubiquinol-10 Biosynthesis (Eukaryotic)	NaN	0.033*					NaN	0.020*
UDP-D-xylose and UDP-D-glucuronate Biosynthesis	NaN	0.110	NaN	0.050			NaN	0.017*
UDP-N-acetyl-D-galactosamine Biosynthesis II	NaN	0.012*			NaN	0.488	NaN	0.103
UDP-N-acetyl-D-glucosamine Biosynthesis II	NaN	0.041*			NaN	0.360	NaN	0.180
Unfolded protein response	NaN	0.363	NaN	7.08E-04**	NaN	0.187	NaN	1.10E-4**
UVA-Induced MAPK Signaling	-0.333	0.060	-0.730	3.98E-03**	-1.000	4.68E-04**	-0.832	0.260
Valine Degradation I	NaN	0.270	NaN	0.085	NaN	7.24E-03**	NaN	1.12E-03**
Vitamin-C Transport	NaN	0.581	NaN	0.230	NaN	0.019*	NaN	0.037*
Xenobiotic Metabolism Signaling	NaN	0.275	NaN	1.62E-03**	NaN	0.021*		
α-Adrenergic Signaling	0	0.548	-0.243	0.292	-1.069	1.23E-03**	-0.302	0.473
γ-glutamyl Cycle	NaN	8.32E-03**	NaN	0.095	NaN	0.292	NaN	0.037*

CHAPTER FOUR

TRANSCRIPTIONAL ANALYSES PROVIDE NEW INSIGHT INTO THE LATE STAGE IMMUNE RESPONSE OF A DISEASED CARIBBEAN CORAL[3]

Lauren E Fuess[1], Whitney T Mann[1], Lea R Jinks[1], Vanessa Brinkhuis[2], Laura D Mydlarz[1,*]

Fuess LE, Mann WT, Jinks LR, Brinkhuis V, Mydlarz LD. (*in press*) Transcriptional analyses provide new insight into the late stage immune response of a diseased Caribbean coral. *Royal Society Open Science*. (doi: 10.1098/rsos.172062)

[1] Department of Biology, University of Texas Arlington, Arlington, Texas, United States of America
[2] Florida Fish and Wildlife Conservation Commission, Fish and Wildlife Research Institute, 100 8th Ave SE, St. Petersburg, FL 33701

[3] Used with permission of the publisher, 2018

ABSTRACT

Increasing global temperatures due to climate change have resulted in respective increases in the severity and frequency of epizootics around the globe. Corals in particular have faced rapid declines due to disease outbreaks. Understanding the immune response and associated potential life history trade-offs is therefore a priority. In the fall of 2011, a novel disease of octocorals of the genus *Eunicea* was first documented in the Florida Keys. Termed Eunicea Black Disease (EBD), the disease is easily identified by the dark appearance of affected tissue, caused by a strong melanization response on the part of the host. In order to better understand the response of corals to EBD, we conducted full transcriptome analysis of 3 healthy and 3 diseased specimens of *E. calyculata* collected from offshore southeast Florida. Differential expression and protein analyses revealed a strong, diverse immune response to EBD characterized by phagocytosis, adhesion, and melanization on the part of the host. Furthermore, coexpression network analyses suggested this might come at the cost of reduced cell cycle progression and growth. This is in accordance with past histological studies of naturally infected hard corals, suggesting that potential tradeoffs during infection may affect post-outbreak recovery of reef ecosystems by reducing both organismal growth and fecundity. Our findings highlight the importance of considering factors beyond mortality when estimating effects of disease outbreaks on ecosystems.

INTRODUCTION

Increasing global temperatures as well as other anthropogenic stressors have resulted in dramatic increases in the prevalence, frequency, and severity of disease outbreaks (Burge *et al.* 2014;Hoegh-Guldberg&Bruno 2010). Increases in disease have necessitated subsequent increases in our understanding of organismal immune systems and the physiological consequences of mounting an immune response (Daszak *et al.* 2001;Ghosh *et al.* 2011;Magnadóttir 2006;Palmer&Traylor-Knowles 2012). These efforts have given rise to the field of ecological immunity, which is primarily concerned with understanding how immune responses vary between individuals and species, the dynamics of life history-immune response trade-offs, and the consequences of immune response (Brock *et al.* 2014;French *et al.* 2009;Graham *et al.* 2011;Hawley&Altizer 2011;Martin *et al.* 2011). In particular, numerous studies focused on organismal level, reproductive consequences of immune response have been published in recent years (Adamo *et al.* 2001;Bascunan-Garcia *et al.* 2010;Carlton *et al.* 2014;Gwynn *et al.* 2005). Furthermore, many theories regarding the costs of immunity for individuals have also been developed (French *et al.* 2009;Graham *et al.* 2011;Lee 2006;Rolff&Siva-Jothy 2003;Sadd&Schmid-Hempel 2009). Still many gaps exist in our knowledge of immunity and the consequences of immune tradeoffs on community structures as a whole. Knowledge of the consequences of immune response on individuals and subsequently community structure is key to developing a robust understanding of how disease outbreaks shape community structure.

Marine ecosystems have arguably been the hardest hit by recent increases in epizootic outbreaks (Burge *et al.* 2014). These rises in disease outbreaks in ocean ecosystems have resulted in significant die offs of urchins (Hughes 1994), corals (Burge *et al.* 2012), and shellfish (Mann

et al. 2009). Furthermore, many of these vulnerable invertebrate species are also essential to ecosystem function. Corals in particular form the structural and trophic basis of diverse coral reef ecosystems (Sebens 1994) and provide many important ecosystem services, such as serving as coastal protection and supporting fishing industries (Spurgeon 1992). However, despite these grim predictions of increasing disease threat, and the importance of affected species, many gaps still exist in our knowledge of marine diseases. These include lack of information regarding the origins and spread of marine diseases, infectious stages and host ranges, and immune responses of host organisms (Harvell *et al.* 2004).

Invertebrates possess a robust innate immune system consisting of three main processes: pathogen recognition, signaling pathways, and effector responses (Palmer&Traylor-Knowles 2012). Yet, while extensive research has revealed a framework for invertebrate immunity (Iwanaga&Lee 2005;Rolff&Siva-Jothy 2003), many questions of host response, and potential trade-offs still remain. While it is clear that immunity comes at a cost, organisms cannot maintain optimal fecundity or longevity while also maintaining a robust immune system (Lee 2006), few studies have investigated these tradeoffs in vulnerable marine invertebrates. In part this is because the species most affected by disease outbreaks are non-model organisms such as corals (Burge *et al.* 2012) and echinoderms (Fuess *et al.* 2015), for which there are limited existing resources (Dheilly *et al.* 2013;Palmer&Traylor-Knowles 2012). Therefore, it is essential to increase efforts to understand immune function, and trade-offs between immunity and life history in these groups so as to better predict future ecosystem structures under rapid global change.

In the fall of 2011, a novel disease (Eunicea Black Disease; EBD) causing a heavily melanized appearance was observed affecting gorgonian corals of the genus *Eunicea* off the

coast of Florida. To date EBD has been documented along the Florida Reef Tract (FRT) from the Dry Tortugas National Park to offshore southeast Florida with prevalence ranging from 12 to 86% within the *Eunicea* community (Brinkhuis&Lunz 2015). While the etiological agent of this disease remains unknown, the disease is easily identifiable due to the darkening of affected tissue resulting from a strong melanization response **(Figure 1).** Additionally, since its first observation, the disease has been reported in multiple other locations throughout the Caribbean (personal observation). In order to document the response of these corals to this disease, and any potential trade-offs associated with the disease or immune-stimulated state, we conducted a transcriptional study of naturally affected *Eunicea calyculata* colonies. Here we document both the strong immune response of individuals to the disease that articulate the late stage or effector responses, and clear trade-offs with growth associated with the disease.

METHODS

Sample Collection

Sample Collection

During October 2013, fragments of *Eunicea calyculata* were collected from 7 healthy and 7 diseased colonies from Southeast Coral Reef Evaluation and Monitoring Project site DC3, an octocoral reef, near Miami, FL (25° 50.526’ -80° 05.286’). Samples were collected while working with the Florida Fish and Wildlife Conservation Commission in compliance with Chapter 68B-8.016 of the Marine Special Activity License program**.** Diseased corals were identified based on the presence of black tissue lesions and 3-5 cm fragments were cut from the affected areas. Fragments of the same size and approximate location were cut from normally pigmented colonies that did not show any signs of disease. Samples were immediately frozen in liquid nitrogen and shipped back to the University of Texas at

Arlington on dry ice and stored at -80 °C until processing for protein and transcriptomic analysis.

Protein Analyses

Prior to protein processing, two small pieces (approximately 0.5 cm^2) were removed from each sample and preserved for later RNA extraction. Proteins were extracted from all 14 samples by grinding the entire remaining sample in liquid nitrogen with a mortar and pestle. A small portion of this frozen powder was placed in a pre-weighed 1.5 mL centrifuge tube and reserved for melanin concentration analysis. Proteins were then extracted from the remaining powder on ice for approximately 45 minutes using approximately 2 mL of 100 mM sodium PBS, pH 7.8. The remaining volume was centrifuged for 10 minutes at 4°C and 3500 RPM in an Eppendorf centrifuge 5810R. The resulting coral extract, was divided between 2 mL aliquots, flash frozen in liquid nitrogen, and stored at -80°C (Mydlarz & Palmer 2011).

Prophenoloxidase activity was estimated by diluting 20 µL of extract in 50 mM phosphate buffer, pH 7.0. Next, samples were incubated for 30 minutes in 25 µL of trypsin (0.1 mg/mL). Just prior to the assay, 30 µL of 10 mM L-1,3- dihydroxphenylalanine (L-dopa, Sigma-Aldrich) was added to each sample. Absorbance was then read every 20 minutes at 490 nm. PPO activity was calculated as the change in absorbance per minute at the steepest part of the curve. A Red660 protein assay (G Biosciences, St. Louis, MO) was used to determine total protein concentration in each sample. All colorimetric assays were run in duplicate on 96 well plates using a Synergy two multi-detection microplate reader and Gen5 software (Biotek Instruments, Winooski, VT, USA). The results of the PPO activity assay were then standardized by protein concentration as determined using a standard Red660

colorimetric assay (Mydlarz & Palmer 2011). Presented PPO activity results are representative of combined activity of proenzyme (PPO) activated with tyrpsin and existing active phenoloxidase within a sample.

In addition to PPO activity, total melanin concentration per sample was estimated using the portion of extract reserved for melanin analysis. The aliquot was lyophilized in a tarred two mL microcentrifuge tube overnight. At the end of this period, the total dry tissue weight in the aliquot was determined and a full spatula of glass beads (~200 uL in volume) was added to each. Samples were vortexed for 10 seconds, 400 μL of 10 M NaOH was added to each tube, and the samples were vortexed for another 20 seconds. Tubes were then incubated for 48 hours at room temperature in the dark and vortexed every 24 hours. Following incubation, tubes were centrifuged at 1000 RPM at room temperature for 10 minutes. 40 uL of supernatant was transferred to a ½ well UV plate (Costar, Corning Life Sciences, Lowell, MA, USA) and absorbance was recorded at 410 and 490 nm. Concentrations of melanin were estimated based on a standard curve of melanin dissolved in 10 M NaOH and are presented as mg of melanin per mg of tissue (Mydlarz & Palmer 2011).

Assay results were analyzed in SPSS software using standard ANOVAs with disease status as a factor. Protein data was tested for normality and outliers prior to statistical analysis. Data from both the prophenoloxidase and melanin assays were normally distributed and required no transformation. Significance was determined as $p < 0.05$.

RNA Extraction and Sequencing

Total RNA was extracted from approximately 0.5 cm^2 pieces of a subset of 3 fragments per group (healthy and diseased). Coral pieces were homogenized in Trizol (ThermoFisher) until all of the polyp tissue was removed from the gorgonin skeleton. Chloroform was added

to the solution, incubated for 2-3 min, and centrifuged at 12,000 x g at 4 °C for 15 min. The aqueous phase was transferred to an RNeasy spin column and the extraction was completed per the RNeasy protocol (Qiagen). RNA quality was assessed using the 2100 BioAnalyzer (Agilent) and samples with RIN values greater than 8.0 were submitted for sequencing. Extracted RNA was submitted to the University of Texas Genome Sequencing Facility that created total RNA libraries using the NEBNext® Ultra™ Directional RNA Library Prep Kit for Illumina® (New England Biolabs, #E7420S) with poly-A tail selection. Libraries were constructed according to the manufacturer's protocol, with modifications to add custom barcodes during the ligation step. Samples were then sequenced at this facility on a single lane using an Illumina HiSeq 2500 platform with 100 base pair paired end reads.

Transcriptome Assembly and Differential Expression Analyses

Using the Trimmomatic software package (Bolger *et al.* 2014) sequences were trimmed to remove adaptors and low quality reads. All sequences of 36 bp in length or less were discarded. Forward and reverse reads for all samples were concatenated together to create a reference forward and reverse read. Reference reads were fed into Trinity (Grabherr *et al.* 2011) for transcriptome assembly using default parameters. Non-host sequences were filtered out using methods described in (Pinzon *et al.* 2015). Briefly, symbiont reads were removed by BLAT (Kent 2002) comparison to a data file consisting of combined genomic and transcriptomic data from multiple species of *Symbiodinium*. The remaining transcriptome was filtered to obtain host only reads by BLAT comparison against a second meta-data file consisting of multiple cnidarian genomes (*O. favolata*, *Acropora digitifera* (Shinzato et al. 2011), *A. millepora* (http://genome.wustl.edu/genomes/detail/acropora-millepora/), and *Nematostella vectensis* (Putnam et al. 2007)). Transcriptome completeness of the resulting

host-only transcriptome was assessed via comparison to the publically available *Gorgonia ventalina* transcriptome (Burge *et al.* 2013). A tblastx comparison of the two transcriptomes was conducted with a minimum e-value cutoff of 1E-5.

Differentially expressed contigs were identified and normalized read counts generated using the Cufflinks software package with default parameters (Trapnell *et al.* 2013). Log_2fold change values for each contig were generated by comparing average normalized expression values between disease status groups. Significantly differentially expressed contigs were identified as those with an adjusted $p < 0.05$ between treatments.

Transcriptome Annotation and Gene Ontology Analyses

The full *E. calyculata* transcriptome generated from collected samples was annotated against the UniProtKB/Swiss-Prot and TrEMBL databases (blastx algorithm, 1.0E-5 e-value threshold). Gene ontology was first assessed using the online PANTHER database (Thomas *et al.* 2003) to determine relative abundance of gene ontology terms. Additionally, to identify enriched functional groups that were characteristic of differentially expressed contigs, we conducted Gene Ontology enrichment analysis using a Fisher's exact test with the R script GO MWU (Wright *et al.* 2015).

Coexpression Network Analysis

In order to identify groups of coexpressed contigs with potential correlation to disease status, the R package Weighted Gene Correlation Network Analyses (Langfelder & Horvath 2008) was used to analyze the full transcriptome. Normalized read counts for all contigs were log_2 transformed. Using these values for all six samples, a single, signed network was built with manual network construction methods (parameters: soft power=20, minimum module size = 180, deep split = 2, merged cut height = 0.25, minimum verbose = 3, cutHeight =

0.991). Module eigengene values (average expression of all contigs in a module) of each module were correlated to disease status, sample identity, and protein analysis data using a bicor correlation. Modules with significant correlations (p-value ≤ 0.05) were selected for further analyses. Gene Ontology enrichment analysis for each significant module was conducted using a Fisher's exact test with the R script GO MWU (Wright *et al.* 2015).

RESULTS

Protein Analyses

Prophenoloxidase activity was significantly reduced in diseased samples compared to those from healthy colonies (ANOVA, $p = 0.040$). In contrast, melanin concentration was significantly higher in diseased samples (ANOVA, $p = 0.031$, **Figure 2**).

Transcriptome Assembly

A total of 37,936,228 paired end reads were obtained from sequencing of all six samples (3 healthy and 3 diseased). Full reads are available for download from NCBI (SRA PRJNA407366). Reads were assembled into a *de novo* transcriptome consisting of 95,665 contigs with an N50 value of 1364. Comparison of the full transcriptome to the UniProtKB/Swiss-Prot database resulted in annotation of 29,409 (~31%) contigs.

Assessment of transcriptome completeness by comparison to the available *G. ventalina* transcriptome (Burge *et al.* 2013) suggested a robust transcriptome assembly. Blast results yielded 50,498 **(**52.8%) significant matches between the two transcriptomes. Furthermore, the two transcriptomes are relatively comparable in size, with the *G. ventalina* transcriptome consisting of 90,230 contigs, while our *E. calyculata* transcriptome was composed of 95,665 contigs. Finally both transcriptome assemblies had a similar N50 value, 1,149 and 1,364, for *G. ventalina* and *E. calyculata* respectively.

Differentially Expressed Contigs

Principle component analysis of patterns of expression among all six samples showed a clear division between healthy and diseased samples along the secondary principle component, and little division among the first principle component between samples. Disease status rather than colony identity appeared to be the primary factor contributing to sample variance in gene expression (**Supplementary Figure 1**). Differential expression analyses comparing diseased to healthy samples found 1,662 differentially expressed contigs: 1,124 (~68%) upregulated and 538 (~32%) downregulated. 554 (~33%) of the differentially expressed contigs were annotated (**Supplementary File 1**). A total of 37 contigs putatively involved in innate immune processes could be identified from this list (**Figure 3, Supplementary File 1**). This included contigs involved in multiple different processes such as Toll-like receptor (TLR) signaling, complement cascade, antiviral responses, and the encapsulation and destruction of pathogens.

Gene Ontology Enrichment Analyses

Top tier gene ontology breakdown of the 554 differentially expressed contigs revealed a large portion of contigs involved in response to stimulus, immune response, and biological adhesion processes (**Figure 4**). Gene ontology enrichment analyses of differentially expressed contigs found one significantly enriched term: biological adhesion. A total of 50 differentially expressed contigs were included in the biological adhesion GO term (**Figure 5**). This included contigs with potential immune function such as those related to interferon responses, techylectins, and integrins.

Coexpression Analyses

Coexpression analyses of all expressed contigs using WGCNA resulted in a network composed of 29 modules ranging in size from 190 to 3252 contigs each (**Supplementary File 2**). Of these 29 modules, 2 were significantly correlated to disease status, Modules 4 (r = -0.93, p = 0.008) and 19 (r = 0.98, p < 0.001) (**Supplementary Figure 2**). These two modules were significantly enriched for multiple biological process gene ontology terms, 50 terms for module 4 and 114 terms for module 19 ($p < 0.05$; **Figure 6, Supplementary File 3**). Module 4, which was negatively correlated to disease status, was significantly enriched with terms involved in RNA and DNA processing, as well as cell cycle progression (**Supplementary Figure 3**). Module 19, which was positively correlated to disease status, was significantly enriched with immune terms such as inflammatory response, regulation of MAPK cascade, receptor mediated endocytosis, and regulation of wound healing. Additionally this module was significantly enriched for terms involved in cell signaling such as G-protein coupled receptor signaling and regulation of intracellular signaling, as well as terms involved in cell adhesion such as cell-cell adhesion and biological adhesion (**Supplementary Figure 4**).

An additional four modules were correlated with either melanin concentration or prophenoloxidase activity (**Supplementary Figure 2**). Module 9 was significantly negatively correlated to melanin activity (p = 0.03, r = -0.83). This module was not significantly enriched for any biological process GO terms. Three modules were significantly correlated to prophenoloxidase activity: Module 12 (p = 0.03, r = 0.86), Module 14 (p = 0.02, r = 0.89), and Module 21 (p = 0.04, r = -0.84). Module 14 was also significantly correlated to Healthy Colony 8. Again, none of these modules were significantly enriched for any biological process GO terms.

DISCUSSION

Coastal ecosystems such as coral reefs have experienced rapid declines due to increasing global temperatures and other anthropogenic stressors (Burge *et al.* 2014; Hoegh-Guldberg & Bruno 2010). This outbreak of yet another novel coral disease is further evidence of rapidly declining ocean conditions and coral health. This disease in particular is clearly characterized by darkly pigmented tissue resulting from a strong immune response dominated by melanin deposition (**Figure 1**). The disease phenotype is in fact the result of a melanization response as evidenced by the results of our assays (**Figure 2**). Furthermore, patterns of gene expression among samples were predominately driven by disease status rather than colony identity (**Supplementary Figure 1**). Differential expression and gene ontology analyses reveal significant changes in numerous immune and adhesion contigs underlying these responses, Finally, coexpression analyses suggest that this response may come at the cost of reduced cell division and growth. Here we further examine the immune response and associated fitness trade-offs of the host *E. calyculata* using transcriptional analyses.

Infected *E. calyculata* mount a strong immune response characterized by melanization to an unknown pathogen

Black pigmented diseased tissue *E. calyculata* demonstrated a clear immune response as evidenced by both protein and gene expression data. Biochemical analysis of protein samples revealed that infected tissue had significantly lower prophenoloxidase activity than apparently healthy tissue. Consequently, infected tissue also had higher melanin concentration. This is as would be expected for a late stage immune response. Melanization is the end product of the prophenoloxidase cascade in invertebrates (Cerenius *et al.* 2010; Cerenius *et al.* 2008) and has been previously documented as an important component of the

cnidarian immune response (Mydlarz *et al.* 2008; Palmer *et al.* 2008). Therefore the observed response is likely indicative of previous rapid melanization and subsequent reduction in prophenoloxidase availability or activity. These findings here add to existing ecological observations and histology results that suggest that melanization in a key component of the response of *E. calyculata* to EBD.

Supporting our protein results, we found contigs representative of various components of innate immunity to be differentially expressed, including components of the Toll-like receptor signaling pathway, complement cascade, antiviral response, phagocytosis, and antioxidant activity. Toll-like receptor signaling is an important mechanism by which hosts detect pathogens and activate immune responses (Akira & Takeda 2004). Here we document 8 differentially expressed contigs involved in or downstream of this pathway, including two copies of the signaling protein deleted in malignant brain tumor protein 1 (DMBT1) which is regulated by TLR signaling and has roles in pathogen recognition (Rosenstiel *et al.* 2007). This protein has previously been shown to be an important part of the coral immune response in multiple studies and has been linked to host production of antimicrobial compounds (Fuess *et al.* 2016; Wright *et al.* 2017). Other TLR-related contigs we observed to be differentially expressed included tumor necrosis factor receptor-associated factor 6 (Kawai *et al.* 2004; Medzhitov *et al.* 1998), and contigs involved in the negative regulation of TLR signaling, E3 ubiquitin-protein ligase RNF31 (Bowman *et al.* 2015) and 4 copies of Ubiquitin carboxyl-terminal hydrolase CYLD (Yoshida *et al.* 2005). Additionally, we observed upregulation of the protein argonaute 2, an antiviral protein that has previously been described as part of the response of acroporid corals to white diseases (Libro *et al.* 2013).

In addition to differential expression of conventional immune contigs, the biological process GO term *biological adhesion* was significantly enriched in our data set. The enrichment of biological adhesion as a response to a pathogen is not surprising, as cellular adhesion is a basic component of multiple innate and adaptive immune responses (Evans *et al.* 2009; Lavine & Strand 2002; Liu *et al.* 2007; Tsirogianni *et al.* 2006). Specifically, cellular adhesion is an important characteristic of the prophenoloxidase activating system that results in the formation of melanin (Iwanaga & Lee 2005; Liu *et al.* 2007) that can be used to encapsulate pathogens for later phagocytosis (Nappi & Christensen 2005). Biological adhesion is also often associated with phagocytic response (Iwanaga & Lee 2005; Lavine & Strand 2002; Liu *et al.* 2007). Interestingly, the majority of immune-related differentially expressed contigs were in fact related to phagocytosis and antioxidant responses. This included several contigs involved in recognition and agglutination of pathogens for later phagocytosis such as MARCO, techylectin-5B, stabilin-1, fucolectin-1, and DMBT1 (Kawabata&Iwanaga 1999;Multerer&Smith 2004;Park *et al.* 2012;Rosenstiel *et al.* 2007;van der Laan *et al.* 1999), as well as lysozyme and peroxidase contigs which can be associated with phagocytosis. (Nauseef 2007). Upregulation of antioxidants and lysozymes, which are frequently associated with degradation of phagocytized particles, is further suggestion of ongoing phagocytic processes (Becker *et al.* 2004;Cheng *et al.* 1975;Forman&Torres 2002;Shimada *et al.* 2010). Together these patterns of expression strongly support our hypothesis that diseased samples are undergoing a late-stage immune response characterized by phagocytosis of melanized particles and pathogens. Therefore, despite our limited sample size, our combination of protein data and robust transcriptomic analyses provide a clear and unified picture of late stage immune responses in cnidarians.

Finally, it should be noted that the transcriptomic responses documented here share a great deal of overlap with a number of other transcriptomic studies of cnidarian immune responses (Fuess *et al.* 2017; Fuess *et al.* 2016; Libro *et al.* 2013; van de Water *et al.* 2018; Wright *et al.* 2017). Many of these studies document changes in a core subset of contigs that are shared across cnidarian species in response to both pathogenic challenge and immune stimulation. This suggests a common, conserved role of a robust innate immune response characterized by pathways such as the Toll-like receptor signaling pathway, in the cnidarian immune response.

E. calyculata undergo a fitness tradeoff during infection

Gene ontology enrichment analyses of the two modules that were significantly correlated to disease status demonstrated a trade-off associated with immune response. The module positively correlated to disease status was enriched with immune system and signaling processes, while the one negatively correlated to disease status was enriched with processes associated with cell cycle progression, including DNA and RNA processes. These findings were corroborated by examination of patterns of expression of contigs included in these two modules (**Figure 6**), suggesting that cellular division and growth may be impacted during a pathogenic infection of *E. calyculata*. Decreases in cell cycle and other like processes have the potential to detrimentally impact growth of the organism as a whole. As colonial organisms, octocorals such as *E. calyculata* undergo modular, iterative growth via replication of polyps through asexual budding (Lasker & Sanchez 2002; Sanchez & Lasker 2003). Furthermore, asexual reproduction is dependent on proliferative cells; therefore decreases in cellular growth may have impacts on the growth, size, and ultimately fitness of the whole organism (Campagna *et al.* 2016). However the effects of decreased cell cycle progression

may not only result in decreased size of the organism, but also potentially organism fecundity. Growth and size are an important determinant of fecundity, and therefore fitness, in colonial organisms such as gorgonian corals. Many gorgonian corals must maintain a certain colony size to reproduce (Bruno *et al.* 2011; Kapela & Lasker 1999), and larger colonies have larger reproductive outputs (Kapela & Lasker 1999). Subsequently, in theory, reduction in growth during disease would correspond to reduced long-term fecundity and fitness. While this is the first documentation of transcriptomic evidence of the potential consequences of disease on reproductive output in a cnidarian, it is in accordance with past observations reporting reduced fecundity (measured as amount of gravid polyps) in a hard coral infected with disease (Weil *et al.* 2009). Therefore our findings here provide new molecular context to previously published findings that disease comes at the cost of fecundity in corals.

It should be noted that samples used for transcriptomic analysis of diseased colonies were collected from heavily mealanized lesion locations. This leaves the potential that observed signals are the result of either death response or the cellular stress response. However, we observed little differential expression of apoptotic, death, or autophagic pathways in our analysis. Similarly we saw little evidence of the cellular stress response, particularly in comparison to other similar studies that document this as part of the cnidarian disease response (van de Water *et al.* 2018). Additionally these lesions often affect the majority of diseased colonies. Therefore we are confident that the trends discussed here are relevant and have important potential ecological consequences.

Our findings documented here point to an ecologically relevant potential trade-off. Increasing sea surface temperatures as a result of climate change have resulted in increases in

the prevalence of coral disease (Weil & Rogers 2011). During active infection, our findings suggest that *E. calyculata* may reduce cell cycle progression, growth, and fecundity. Therefore, as disease outbreaks become more common and individuals are more frequently infected, *E. calyculata* growth, and fecundity, may be impacted. This could have implications beyond individual corals as self-seeding is one of the most important sources of recruitment on a recovering reef (Bruno *et al.* 2011; Nishikawa *et al.* 2003). Regardless, as *Eunicea* corals are relatively slow growing under normal conditions (Brinkhuis 2009; Cary 1914), recovery times will be slow, and even slower still should our findings here regarding reduced expression of growth related processes following disease be corroborated by further investigation. Therefore, mortality of *Eunicea* and reduced growth of remaining colonies may lead to displacement of the species by faster growing species such as those from the genus *Antillogorgia* (Yoshioka 1994).

CONCLUSIONS

The results presented here are some of the first transcriptomic evidence to corroborate past field and histological observations of the growth and fecundity consequences of disease in cnidarians. Furthermore, our documentation of the response of *E. calyculata* to disease joins a growing body of literature reporting shared transcriptomic responses of cnidarians to pathogenic infection and immune stimulation. The severity of this disease, robustness of the associated immune response, and potential related fitness trade-offs cast a grim outlook for the future of *Eunicea* octocorals on Caribbean reefs. As climate change effects increase and with it the frequency of disease outbreaks affecting numerous species (Bruno *et al.* 2007), resilience of these communities may decrease, resulting in decreases or shifts in octocoral communities on reefs (Linares *et al.* 2008). Therefore it is essential to continue to explore our findings regarding

the consequences of disease on growth and fecundity of individual corals. Increasing understanding of these potential trade-offs will improve our ability to understand species and community level effects of disease beyond mortality. Our findings open the door to future research that will increase our ability to predict coral community trajectories under increasing pressure from disease and climate change.

ACKNOWLEDGEMENTS

The authors would like to thank the Florida Department of Environmental Protection for boat support in the field. Additionally we would like to thank Esther Peters, Jan Landsberg, Yasu Kiryu, Noretta Perry, and Yvonne Waters for assistance in obtaining the histopathology pictures shown in **Figure 1**. Finally, we would like to thank the staff of the Genetics Core Facility (UTA) for assistance with laboratory work and anonymous reviewers for edits to improve the manuscript. The analyses were run on a server provided by the UTA Office of Information Technology. Funding was provided by NSF grant IOS #1017458 to LDM. This material is based upon work supported by the National Science Foundation Graduate Research Fellowship under Grant #1144240 to LEF.

FIGURES AND TABLES

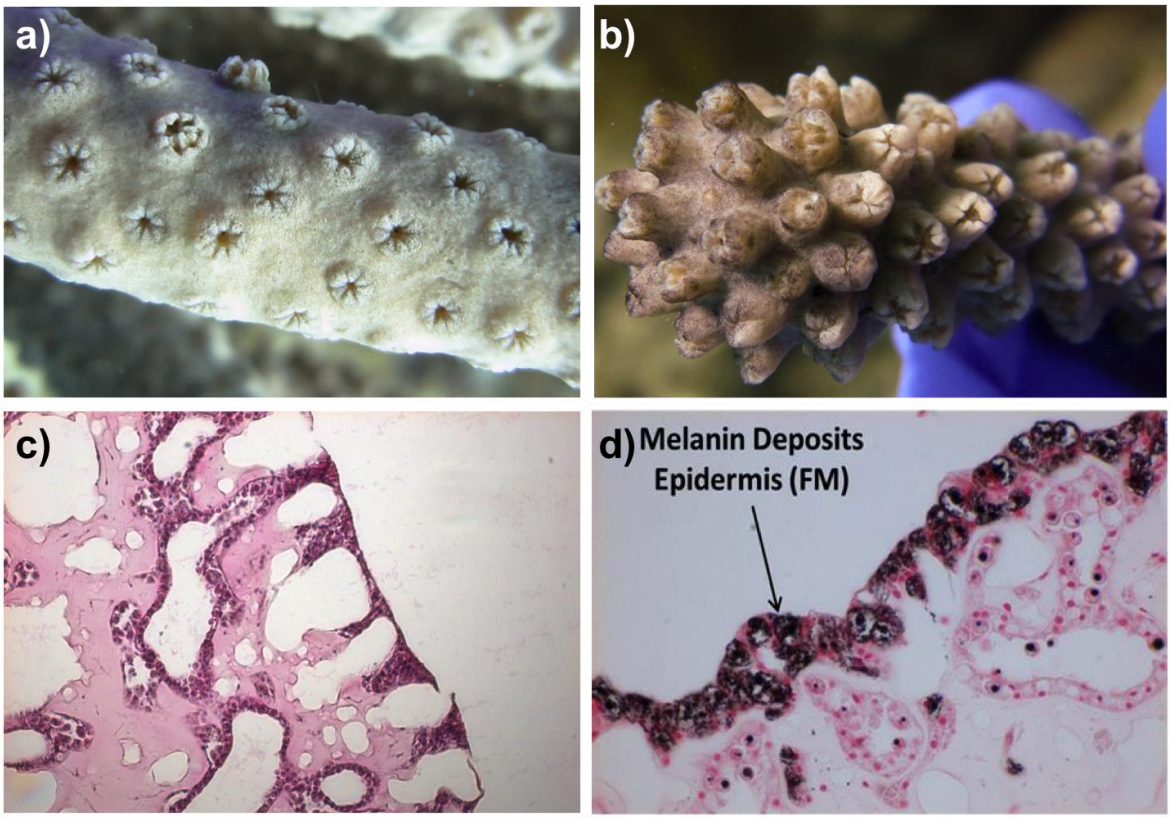

Figure 1: Macro and histological views of healthy (**a,c**) and diseased (**b,d**) *Eunicea*. **a)** close up of a healthy colony of *Eunicea* lacking any characteristic black pigmentation associated with the disease. **b)** close up of a colony of *Eunicea* infected with EBD; note the characteristic black pigmentation of the tissue. **c)** Standard hematoxylin and eosin stained histology slides of apparently healthy sample showing good tissue organization and normal staining characteristics (pink staining) **d)** slides of tissue from an infected colony stained with Fontana-Masson showing the epidermis with melanin deposition.

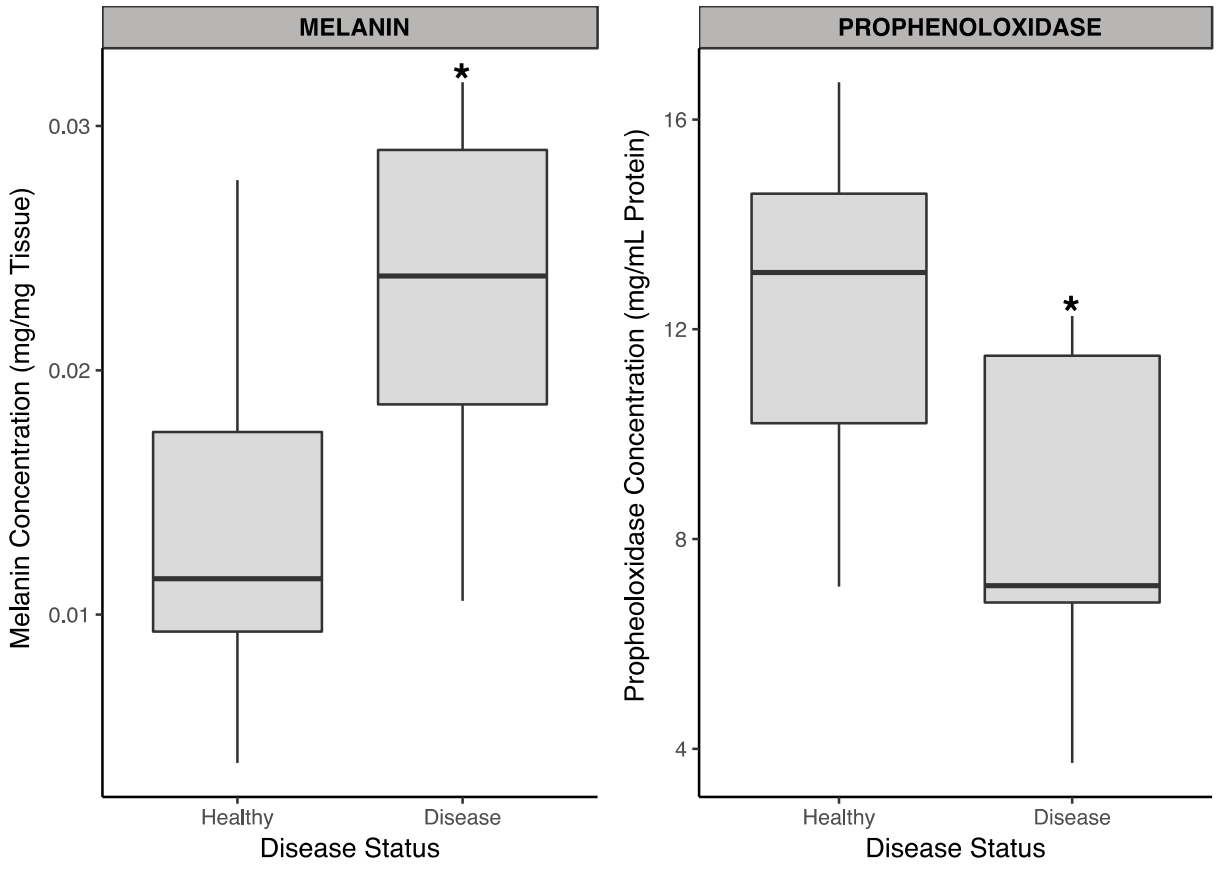

Figure 2: Results of biochemical assays measuring prophenoloxidase protein activity (standardized by protein concentration) and melanin concentration per mg tissue. Infected samples had significantly lower prophenoloxidase activity ($p = 0.040$), and significantly higher melanin concentration ($p = 0.031$).

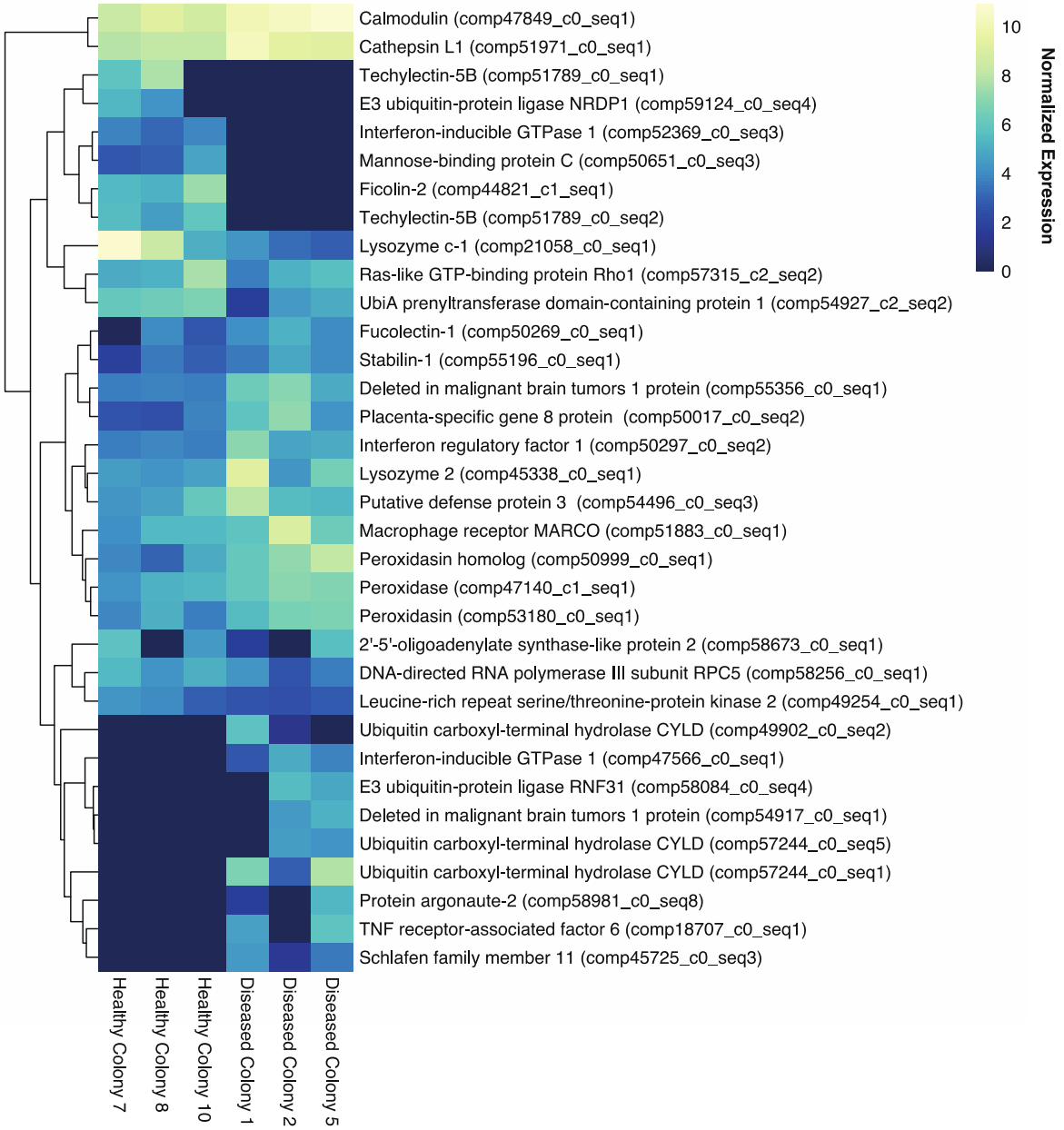

Figure 3: Heatmap of expression of all significantly differentially expressed immune contigs. Log2 transformed expression values are displayed for each sample. Colonies are ordered by treatment and contigs are clustered based on similarity in expression patterns. Contigs that were only expressed in one sample not shown.

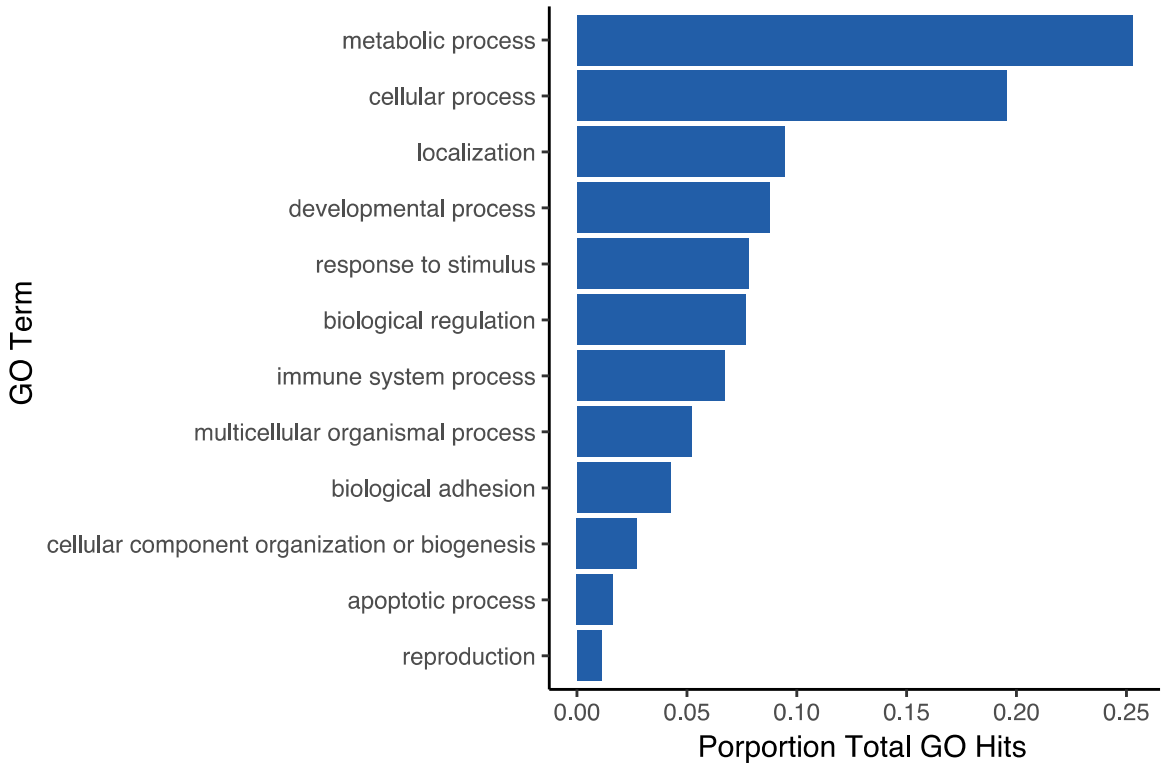

Figure 4: Top tier gene ontology breakdown of all annotated differentially expressed contigs. Shown as ratio of hits to total hits within a given category.

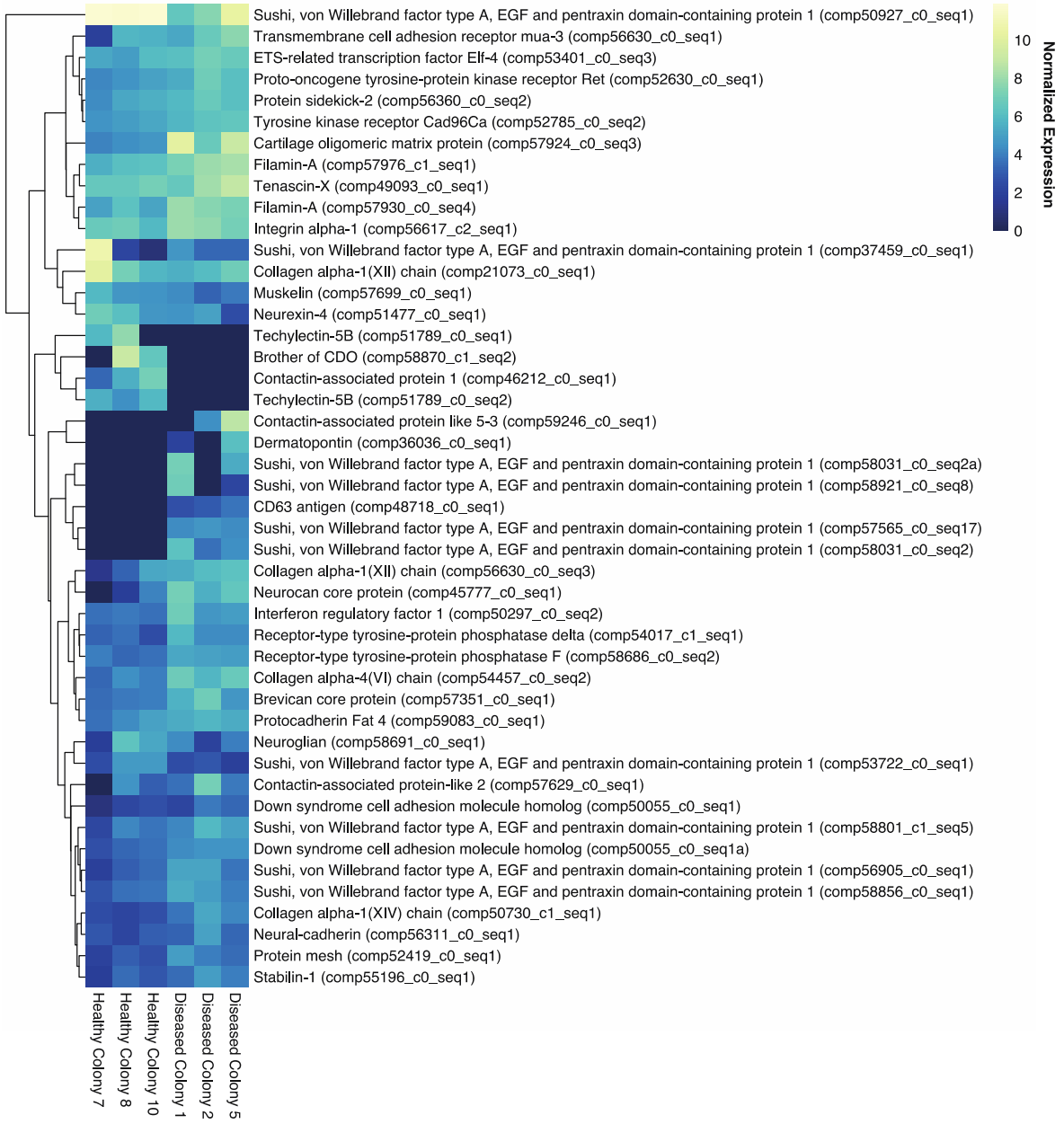

Figure 5: Heatmap of differentially expressed contigs that are involved in biological adhesion. Log2 transformed expression values are displayed for each sample. Colonies are ordered by treatment and contigs are clustered based on similarity in expression patterns. Contigs that were only expressed in one sample not shown.

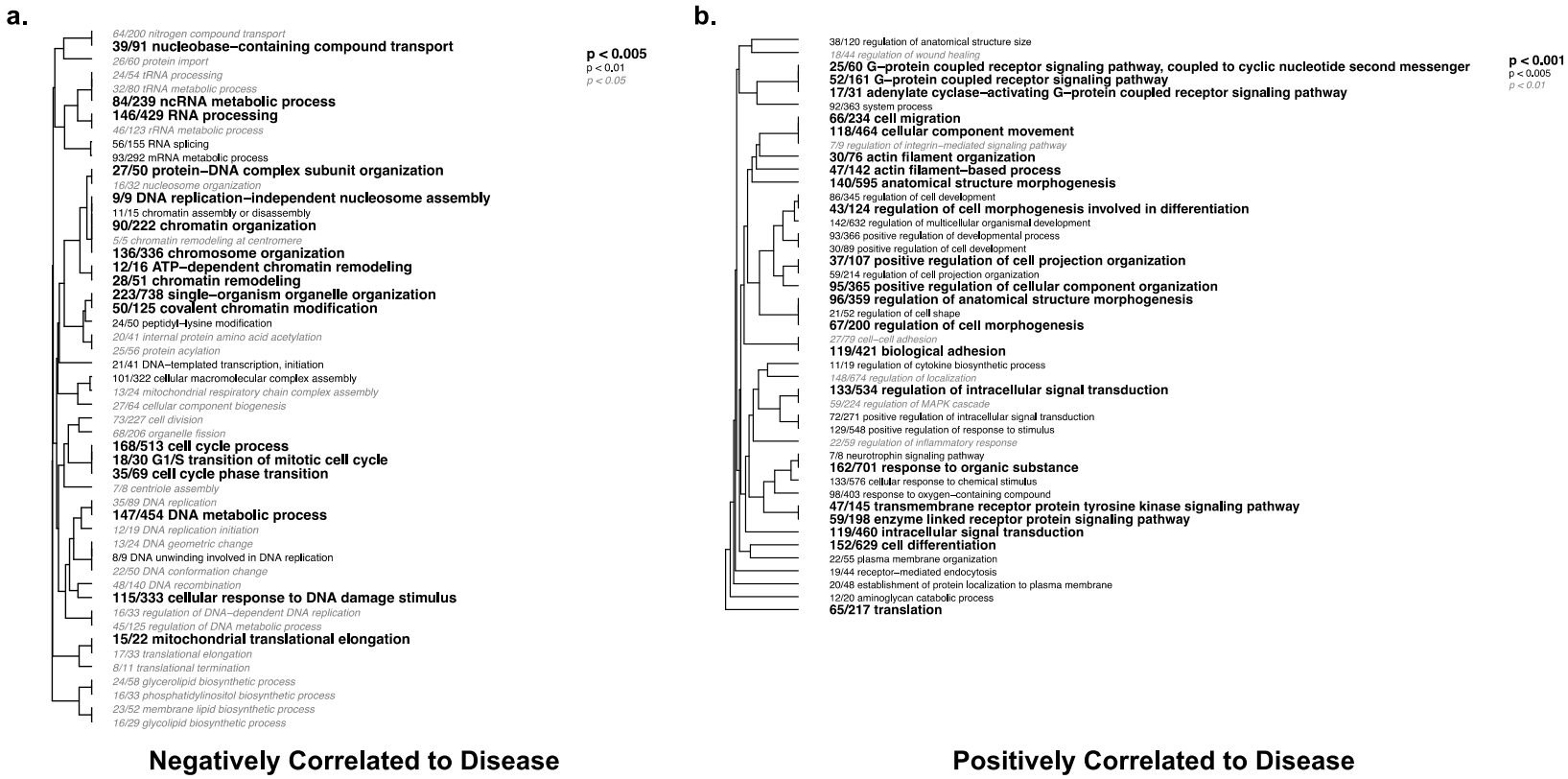

Figure 6: Hierarchical clustering of significantly enriched biological process gene ontology enrichment of the two modules correlated to disease status **a)** Module 4 (negatively correlated) and **b)** Module 19 (positively correlated)

SUPPLEMENTARY TABLES AND FIGURES

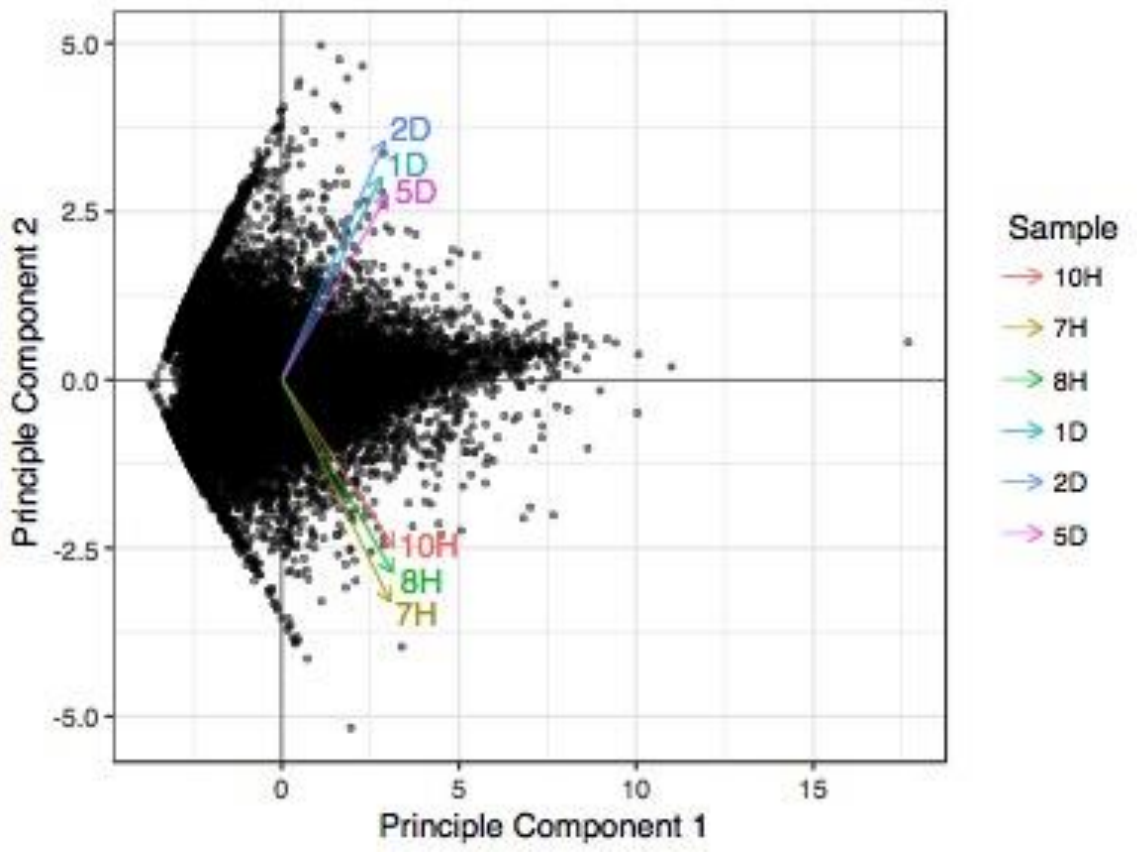

Supplementary Figure 1: Principle component analysis of patterns of gene expression in the six samples of *E. calyculata*.

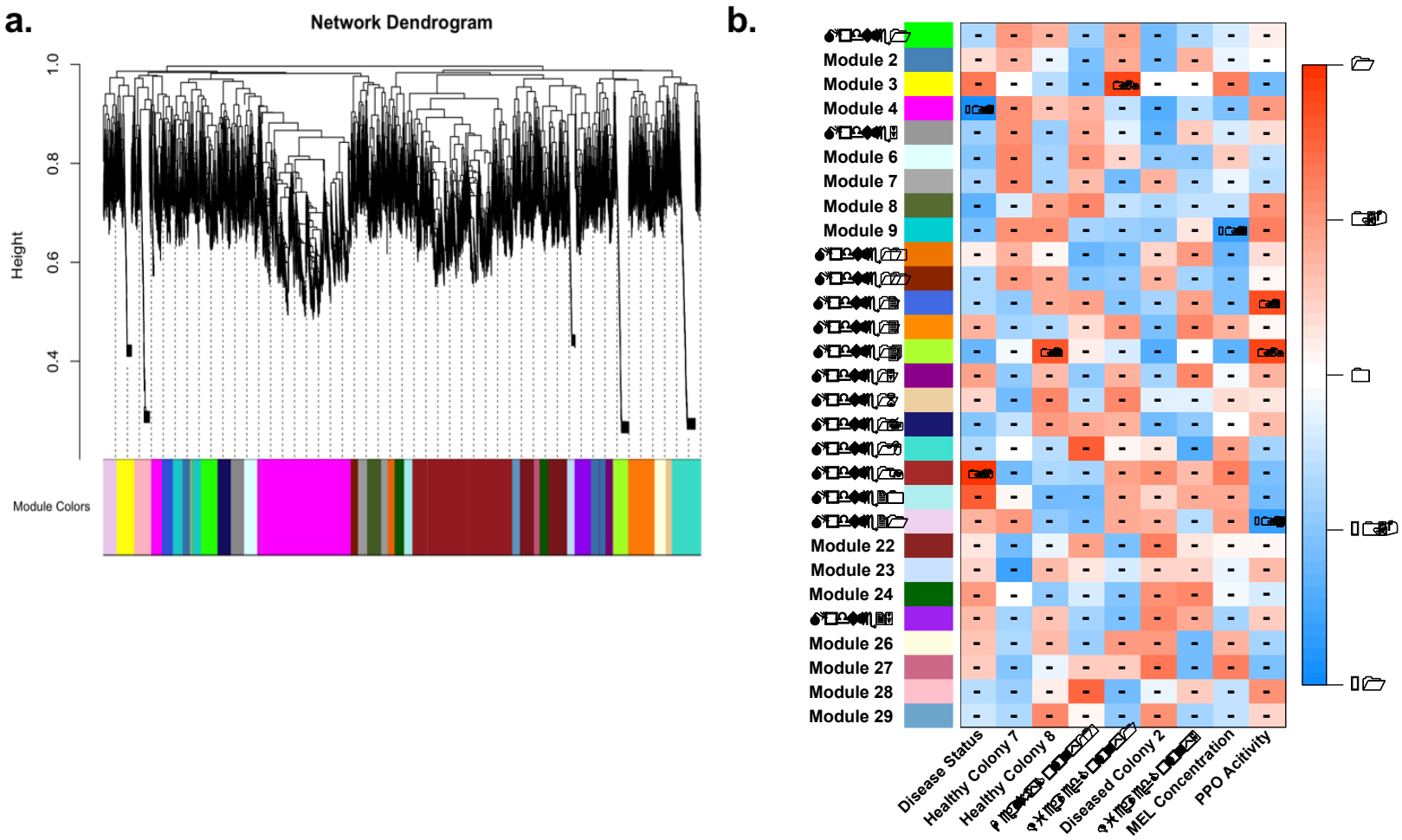

Supplementary Figure 4: WGCNA analysis results showing **a)** clustered network dendrogram and module colors and **b)** correlations between module eigengenes and disease status of each sample.

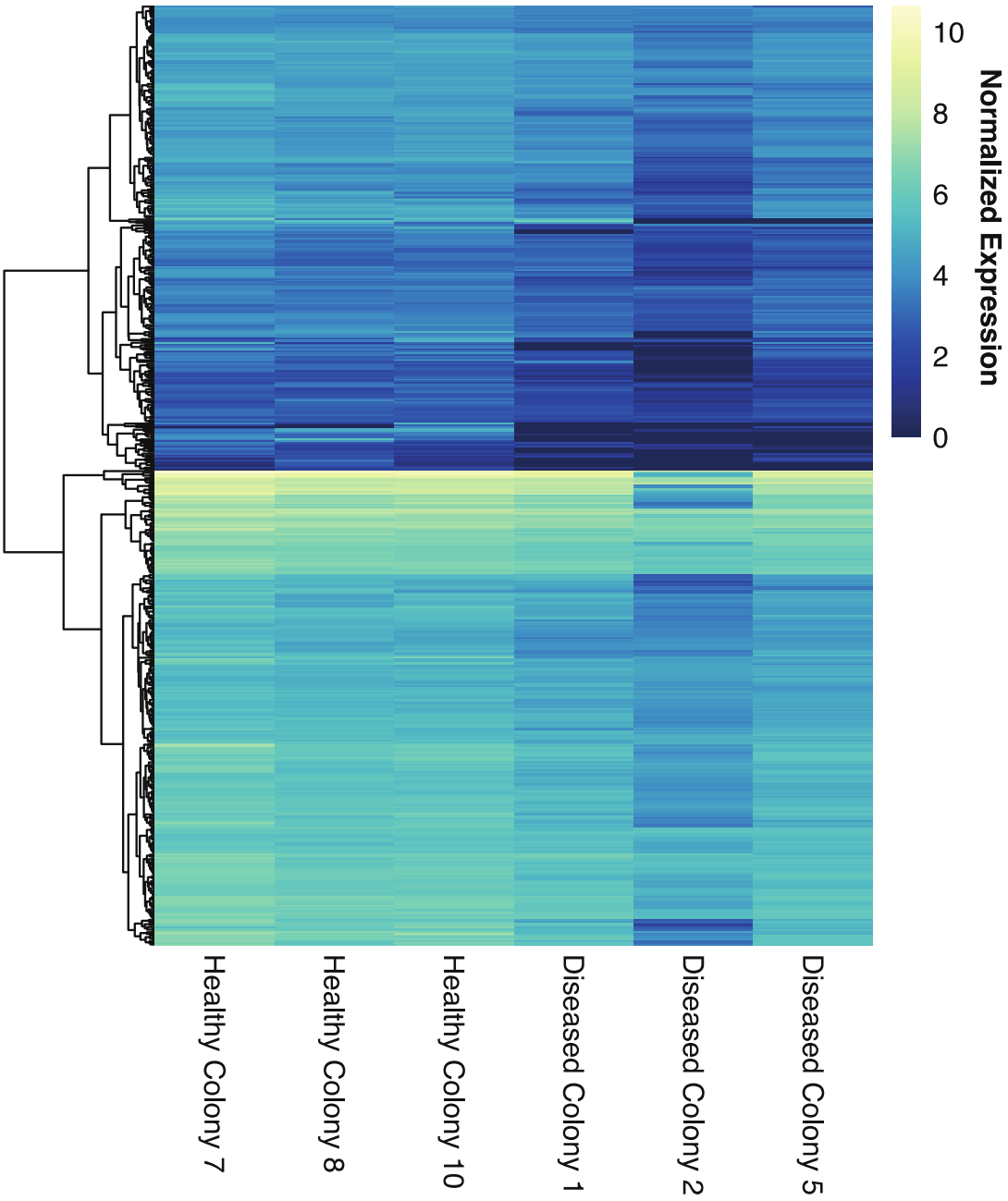

Supplementary Figure 3: Heatmap of contigs belonging to Module 4 that had GO annotations involved in DNA or RNA processing or a component of the cell cycle. Log2 transformed expression values are displayed for each sample. Colonies are ordered by treatment and contigs are clustered based on similarity in expression patterns. Contigs that were only expressed in one sample not shown.

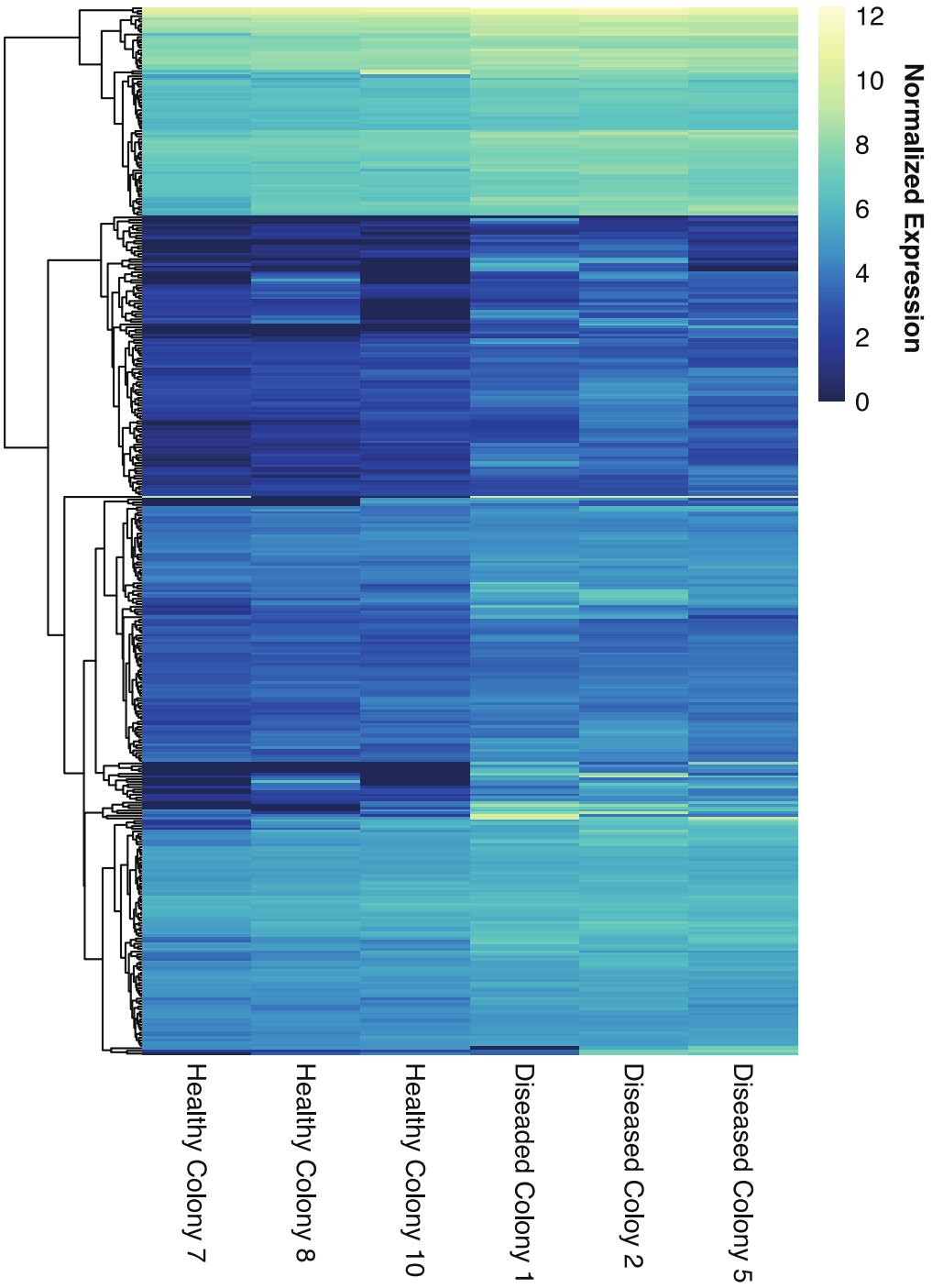

Supplementary Figure 4: Heatmap of contigs belonging to Module 19 that had GO annotations involved in immune response, signaling or adhesion. Log2 transformed expression values are displayed for each sample. Colonies are ordered by treatment and contigs are clustered based on similarity in expression patterns. Contigs that were only expressed in one sample not shown.

Supplementary Table 1: Table of differentially expressed genes involved in either immunity or biological adhesion.

Function	Locus	spID	Protein names	Evalue
Immune	comp18707_c0_seq1	P70196	TNF receptor-associated factor 6	5.00E-19
Immune	comp21058_c0_seq1	Q17005	Lysozyme c-1	3.00E-26
Biological Adhesion	comp21073_c0_seq1	Q99715	Collagen alpha-1(XII) chain	0.000001
Biological Adhesion	comp27753_c0_seq1	Q28IL6	60S ribosomal protein L22	3E-34
Biological Adhesion	comp36036_c0_seq1	P83553	Dermatopontin	2E-18
Biological Adhesion	comp37459_c0_seq1	A2AVA0	Sushi, von Willebrand factor type A, EGF and pentraxin domain-containing protein 1	3E-10
Biological Adhesion	comp41479_c0_seq2	Q94887	Neurexin-4	0.0000004
Immune	comp44821_c1_seq1	Q15485	Ficolin-2	8.00E-25
Immune	comp45338_c0_seq1	Q1XG90	Lysozyme 2	8.00E-30
Immune	comp45725_c0_seq3	Q7Z7L1	Schlafen family member 11	6.00E-20
Biological Adhesion	comp45777_c0_seq1	O14594	Neurocan core protein	2E-15
Biological Adhesion	comp46212_c0_seq1	P97846	Contactin-associated protein 1	0.00000001
Immune	comp47140_c1_seq1	Q01603	Peroxidase	2.00E-15
Immune	comp47566_c0_seq1	Q9QZ85	Interferon-inducible GTPase 1	2.00E-34
Immune	comp47849_c0_seq1	P62184	Calmodulin	2.00E-25
Biological Adhesion	comp48718_c0_seq1	P08962	CD63 antigen	8E-15
Biological Adhesion	comp49093_c0_seq1	P22105	Tenascin-X	0.000008
Immune	comp49254_c0_seq1	Q5S007	Leucine-rich repeat serine/threonine-protein kinase 2	0
Biological Adhesion	comp49650_c0_seq3	Q58EX2	Protein sidekick-2	0.00000007
Immune	comp49902_c0_seq2	Q80TQ2	Ubiquitin carboxyl-terminal hydrolase CYLD	3.00E-20
Biological Adhesion	comp49921_c0_seq2	Q70E20	Sushi, nidogen and EGF-like domain-containing protein 1	0.0000002
Immune	comp50017_c0_seq2	Q9NZF1	Placenta-specific gene 8 protein	3.00E-09
Immune	comp50269_c0_seq1	Q9I931	Fucolectin-1	9.00E-22
Biological Adhesion & Immune	comp50297_c0_seq2	Q90876	Interferon regulatory factor 1	1.00E-25

Immune	comp50651_c0_seq3	P08661	Mannose-binding protein C	4.00E-12
Biological Adhesion	comp50730_c1_seq1	P32018	Collagen alpha-1(XIV) chain	9E-20
Biological Adhesion	comp50803_c0_seq3	O35474	EGF-like repeat and discoidin I-like domain-containing protein 3	0.000000002
Biological Adhesion	comp50927_c0_seq1	P0C6B8	Sushi, von Willebrand factor type A, EGF and pentraxin domain-containing protein 1	3E-15
Immune	comp50999_c0_seq1	Q92626	Peroxidasin homolog	5.00E-89
Biological Adhesion	comp51477_c0_seq1	Q94887	Neurexin-4	1E-31
Biological Adhesion & Immune	comp51789_c0_seq1	Q9U8W7	Techylectin-5B	7.00E-20
Biological Adhesion & Immune	comp51789_c0_seq2	Q9U8W7	Techylectin-5B	6.00E-29
Immune	comp51883_c0_seq1	Q9WUB9	Macrophage receptor MARCO	2.00E-12
Immune	comp51971_c0_seq1	Q95029	Cathepsin L	5.00E-114
Immune	comp52369_c0_seq3	Q9QZ85	Interferon-inducible GTPase 1	5.00E-43
Biological Adhesion	comp52419_c0_seq1	Q0KHY3	Protein mesh	2E-79
Biological Adhesion	comp52630_c0_seq1	P07949	Proto-oncogene tyrosine-protein kinase receptor Ret	4E-32
Biological Adhesion	comp52785_c0_seq2	Q9VBW3	Tyrosine kinase receptor Cad96Ca	3E-67
Biological Adhesion	comp53006_c0_seq5	Q98919	Limbic system-associated membrane protein	2E-11
Immune	comp53180_c0_seq1	Q9VZZ4	Peroxidasin	3.00E-116
Biological Adhesion	comp53401_c0_seq3	Q9Z2U4	ETS-related transcription factor Elf-4	7E-23
Biological Adhesion	comp53722_c0_seq1	Q4LDE5	Sushi, von Willebrand factor type A, EGF and pentraxin domain-containing protein 1	2E-14
Biological Adhesion	comp54017_c1_seq1	Q64487	Receptor-type tyrosine-protein phosphatase delta	3E-76
Biological Adhesion	comp54457_c0_seq2	A2AX52	Collagen alpha-4(VI) chain	4E-11
Immune	comp54496_c0_seq3	Q0Q028	Putative defense protein 3	1.00E-12
Immune	comp54917_c0_seq1	Q4A3R3	Deleted in malignant brain tumors 1 protein	8.00E-29

Biological Adhesion & Immune	comp55196_c0_seq1	Q9NY15	Stabilin-1	5.00E-06
Immune	comp55356_c0_seq1	Q9UGM3	Deleted in malignant brain tumors 1 protein	2.00E-26
Biological Adhesion	comp56311_c0_seq1	O15943	Neural-cadherin	1E-134
Biological Adhesion	comp56360_c0_seq2	Q58EX2	Protein sidekick-2	4E-14
Immune	comp56426_c0_seq1	Q92626	Peroxidasin homolog	4.00E-06
Biological Adhesion	comp56617_c2_seq1	Q90615	Integrin alpha-1	0.00000002
Biological Adhesion	comp56630_c0_seq1	P34576	Transmembrane cell adhesion receptor mua-3	7E-26
Biological Adhesion	comp56630_c0_seq3	P13944	Collagen alpha-1(XII) chain	9E-28
Biological Adhesion	comp56905_c0_seq1	P0C6B8	Sushi, von Willebrand factor type A, EGF and pentraxin domain-containing protein 1	0
Immune	comp57244_c0_seq1	Q5RED8	Ubiquitin carboxyl-terminal hydrolase CYLD	3.00E-33
Immune	comp57244_c0_seq3	Q1RMU2	Ubiquitin carboxyl-terminal hydrolase CYLD	5.00E-17
Immune	comp57244_c0_seq5	Q80TQ2	Ubiquitin carboxyl-terminal hydrolase CYLD	2.00E-16
Immune	comp57315_c2_seq2	P48148	Ras-like GTP-binding protein Rho1	2.00E-46
Biological Adhesion	comp57351_c0_seq1	Q96GW7	Brevican core protein	1E-15
Biological Adhesion	comp57565_c0_seq17	P0C6B8	Sushi, von Willebrand factor type A, EGF and pentraxin domain-containing protein 1	0.0000002
Biological Adhesion	comp57629_c0_seq1	Q9UHC6	Contactin-associated protein-like 2	3E-24
Biological Adhesion	comp57699_c0_seq1	Q9UL63	Muskelin	0
Biological Adhesion	comp57924_c0_seq3	P35445	Cartilage oligomeric matrix protein	5E-158
Biological Adhesion	comp57930_c0_seq4	P21333	Filamin-A	1E-12
Biological Adhesion	comp57976_c1_seq1	P21333	Filamin-A	1E-112
Biological Adhesion	comp58031_c0_seq2	Q4LDE5	Sushi, von Willebrand factor type A, EGF and pentraxin domain-containing protein 1	2E-38
Biological Adhesion	comp58079_c0_seq3	O73792	Tyrosine-protein kinase receptor Tie-1	9E-42
Immune	comp58084_c0_seq4	Q924T7	E3 ubiquitin-protein ligase RNF31	7.00E-125
Immune	comp58256_c0_seq1	Q9CZT4	DNA-directed RNA polymerase III subunit RPC5	2.00E-95

Immune	comp58673_c0_seq1	Q5MYT9	2'-5'-oligoadenylate synthase-like protein 2	5.00E-28
Immune	comp58673_c0_seq8	P11928	2'-5'-oligoadenylate synthase 1A	1.00E-07
Biological Adhesion	comp58686_c0_seq2	A4IFW2	Receptor-type tyrosine-protein phosphatase F	2E-130
Biological Adhesion	comp58691_c0_seq1	P20241	Neuroglian	4E-11
Biological Adhesion	comp58801_c1_seq5	P0C6B8	Sushi, von Willebrand factor type A, EGF and pentraxin domain-containing protein 1	3E-128
Biological Adhesion	comp58856_c0_seq1	P0C6B8	Sushi, von Willebrand factor type A, EGF and pentraxin domain-containing protein 1	2E-32
Biological Adhesion	comp58870_c1_seq2	Q6AZB0	Brother of CDO	0.000000004
Biological Adhesion	comp58921_c0_seq8	A2AVA0	Sushi, von Willebrand factor type A, EGF and pentraxin domain-containing protein 1	7E-13
Immune	comp58981_c0_seq8	O77503	Protein argonaute-2	3.00E-82
Biological Adhesion	comp59083_c0_seq1	Q6V0I7	Protocadherin Fat 4	0
Immune	comp59124_c0_seq4	Q7ZW16	E3 ubiquitin-protein ligase NRDP1	6.00E-14
Biological Adhesion	comp59246_c0_seq1	Q0V8T4	Contactin-associated protein like 5-3	9E-10
Immune	comp60580_c0_seq1	Q9PU28	Lysozyme C	3.00E-13

Supplementary Table 2: List of significantly enriched gene ontology terms associated with Module 4 (negatively correlated to disease) and Module 19 (positively correlated to disease)

Module	Number of Sequences	Go Term	*padj*
Module 4	336	chromosome organization	2.89E-11
Module 4	222	chromatin organization	5.47E-07
Module 4	429	RNA processing	4.71E-06
Module 4	513	cell cycle process	5.60E-06
Module 4	738	single-organism organelle organization	3.33E-05
Module 4	333	cellular response to DNA damage stimulus	4.70E-05
Module 4	454	DNA metabolic process	6.75E-05
Module 4	69	cell cycle phase transition	6.75E-05
Module 4	51	chromatin remodeling	0.000123954
Module 4	50	protein-DNA complex subunit organization	0.000281456
Module 4	9	DNA replication-independent nucleosome assembly	0.000371437
Module 4	239	ncRNA metabolic process	0.000605182
Module 4	125	covalent chromatin modification	0.001145985
Module 4	22	mitochondrial translational elongation	0.001145985
Module 4	91	nucleobase-containing compound transport	0.001631956
Module 4	30	G1/S transition of mitotic cell cycle	0.001671693
Module 4	16	ATP-dependent chromatin remodeling	0.001900342
Module 4	15	chromatin assembly or disassembly	0.006138586
Module 4	9	DNA unwinding involved in DNA replication	0.006696824
Module 4	155	RNA splicing	0.006940178
Module	50	peptidyl-lysine modification	0.006940178

4			
Module 4	292	mRNA metabolic process	0.008479293
Module 4	322	cellular macromolecular complex assembly	0.008479293
Module 4	123	rRNA metabolic process	0.010594434
Module 4	29	glycolipid biosynthetic process	0.013511423
Module 4	19	DNA replication initiation	0.016820912
Module 4	56	protein acylation	0.01685111
Module 4	41	internal protein amino acid acetylation	0.016876191
Module 4	8	centriole assembly	0.017956912
Module 4	89	DNA replication	0.01897361
Module 4	206	organelle fission	0.019041444
Module 4	60	protein import	0.019239436
Module 4	33	translational elongation	0.019384428
Module 4	54	tRNA processing	0.019797857
Module 4	80	tRNA metabolic process	0.021111064
Module 4	64	cellular component biogenesis	0.022283265
Module 4	125	regulation of DNA metabolic process	0.022730076
Module 4	227	cell division	0.022730076
Module 4	52	membrane lipid biosynthetic process	0.025434114
Module 4	50	DNA conformation change	0.036421951
Module 4	11	translational termination	0.036847198
Module 4	32	nucleosome organization	0.036847198
Module 4	5	chromatin remodeling at centromere	0.038710809

Module 4	140	DNA recombination	0.042842037
Module 4	24	DNA geometric change	0.042842037
Module 4	24	mitochondrial respiratory chain complex assembly	0.042842037
Module 4	33	phosphatidylinositol biosynthetic process	0.048396432
Module 4	200	nitrogen compound transport	0.048396432
Module 4	33	regulation of DNA-dependent DNA replication	0.048396432
Module 4	58	glycerolipid biosynthetic process	0.049019253
Module 19	421	biological adhesion	1.53E-06
Module 19	200	regulation of cell morphogenesis	4.19E-06
Module 19	460	intracellular signal transduction	0.000141745
Module 19	629	cell differentiation	0.000162029
Module 19	534	regulation of intracellular signal transduction	0.000162029
Module 19	217	translation	0.000211938
Module 19	464	cellular component movement	0.000211938
Module 19	161	G-protein coupled receptor signaling pathway	0.000211938
Module 19	124	regulation of cell morphogenesis involved in differentiation	0.000211938
Module 19	359	regulation of anatomical structure morphogenesis	0.000211938
Module 19	142	actin filament-based process	0.000276097
Module 19	31	adenylate cyclase-activating G-protein coupled receptor signaling pathway	0.000347969
Module 19	76	actin filament organization	0.00038137
Module 19	145	transmembrane receptor protein tyrosine kinase signaling pathway	0.000399069
Module 19	701	response to organic substance	0.000399069
Module 19	365	positive regulation of cellular component organization	0.000399069

Module 19	198	enzyme linked receptor protein signaling pathway	0.000410913
Module 19	595	anatomical structure morphogenesis	0.000652167
Module 19	107	positive regulation of cell projection organization	0.000683681
Module 19	234	cell migration	0.000691588
Module 19	366	positive regulation of developmental process	0.001107151
Module 19	363	system process	0.001273516
Module 19	548	positive regulation of response to stimulus	0.001273516
Module 19	20	aminoglycan catabolic process	0.001843938
Module 19	271	positive regulation of intracellular signal transduction	0.002079783
Module 19	576	cellular response to chemical stimulus	0.002254652
Module 19	8	neurotrophin signaling pathway	0.002699206
Module 19	44	receptor-mediated endocytosis	0.00307077
Module 19	55	plasma membrane organization	0.00307077
Module 19	214	regulation of cell projection organization	0.00307077
Module 19	403	response to oxygen-containing compound	0.00307077
Module 19	120	regulation of anatomical structure size	0.003107698
Module 19	48	establishment of protein localization to plasma membrane	0.003188054
Module 19	345	regulation of cell development	0.003338258
Module 19	52	regulation of cell shape	0.003382327
Module 19	632	regulation of multicellular organismal development	0.003672011
Module 19	19	regulation of cytokine biosynthetic process	0.004451874
Module 19	89	positive regulation of cell development	0.004831996
Module 19	9	positive regulation of integrin-mediated signaling pathway	0.007273732

Module 19	674	regulation of localization	0.007587817
Module 19	59	regulation of inflammatory response	0.007802836
Module 19	79	cell-cell adhesion	0.007802836
Module 19	44	regulation of wound healing	0.008061013
Module 19	224	regulation of MAPK cascade	0.008939219
Module 19	211	regulation of growth	0.010385396
Module 19	160	endocytosis	0.010761169
Module 19	85	neuron differentiation	0.010761169
Module 19	53	homophilic cell adhesion	0.011568128
Module 19	61	cell junction organization	0.011841439
Module 19	78	establishment or maintenance of cell polarity	0.013502964
Module 19	153	regulation of neuron projection development	0.013502964
Module 19	28	actin cytoskeleton reorganization	0.013502964
Module 19	317	locomotion	0.013502964
Module 19	398	response to endogenous stimulus	0.013554206
Module 19	87	regulation of nucleoside metabolic process	0.014375747
Module 19	10	platelet-derived growth factor receptor signaling pathway	0.014562181
Module 19	245	regulation of locomotion	0.015807832
Module 19	22	regulation of smooth muscle contraction	0.016180283
Module 19	265	regulation of cellular component biogenesis	0.016180283
Module 19	261	membrane organization	0.017224241
Module 19	543	regulation of cell differentiation	0.018014854
Module 19	470	regulation of transport	0.018122371

Module 19	166	signaling	0.019356767
Module 19	98	response to peptide	0.019762391
Module 19	52	morphogenesis of a branching structure	0.019762391
Module 19	8	adrenergic receptor signaling pathway	0.020219575
Module 19	259	neurological system process	0.021538204
Module 19	23	ERBB signaling pathway	0.022615064
Module 19	30	vascular process in circulatory system	0.023048925
Module 19	61	aminoglycan metabolic process	0.023380037
Module 19	61	regulation of ERK1 and ERK2 cascade	0.023380037
Module 19	241	regulation of hydrolase activity	0.024372001
Module 19	587	regulation of phosphorus metabolic process	0.024947884
Module 19	87	regulation of cellular component size	0.024947884
Module 19	11	positive regulation of cytokine biosynthetic process	0.024947884
Module 19	34	positive regulation of developmental growth	0.024947884
Module 19	11	cardiac conduction	0.024947884
Module 19	237	positive regulation of cell differentiation	0.02503396
Module 19	6	respiratory system process	0.02566711
Module 19	50	positive regulation of neurogenesis	0.027946381
Module 19	97	regulation of actin filament-based process	0.029908008
Module 19	543	regulation of catalytic activity	0.029908008
Module 19	433	vesicle-mediated transport	0.030410292
Module 19	129	response to growth factor	0.030410292
Module 19	162	regulation of defense response	0.031029502

Module 19	497	response to external stimulus	0.032212622
Module 19	47	second-messenger-mediated signaling	0.033406504
Module 19	21	protein localization to plasma membrane	0.033406504
Module 19	144	positive regulation of MAPK cascade	0.033544202
Module 19	267	cell development	0.037293629
Module 19	9	positive regulation of inflammatory response	0.037293629
Module 19	117	negative regulation of transport	0.037293629
Module 19	9	cellular response to nerve growth factor stimulus	0.037293629
Module 19	15	platelet degranulation	0.040158725
Module 19	238	regulation of neurogenesis	0.040158725
Module 19	12	protein depolymerization	0.041004964
Module 19	224	positive regulation of transport	0.043042385
Module 19	137	negative regulation of intracellular signal transduction	0.043066307
Module 19	78	single-organism cellular localization	0.043811737
Module 19	142	positive regulation of hydrolase activity	0.043988686
Module 19	33	liver development	0.044477342
Module 19	133	regulation of nucleotide metabolic process	0.044477342
Module 19	22	striated muscle contraction	0.044477342
Module 19	33	axonogenesis	0.044477342
Module 19	245	regulation of response to external stimulus	0.044477342
Module 19	215	cellular response to oxygen-containing compound	0.044477342
Module 19	37	regulation of heart contraction	0.04517925
Module 19	83	regulation of developmental growth	0.04517925

Module 19	53	regulation of dendrite development	0.04517925
Module 19	191	positive regulation of multicellular organismal process	0.04517925
Module 19	88	negative regulation of protein phosphorylation	0.048702933
Module 19	26	protein polymerization	0.048943098
Module 19	19	formation of primary germ layer	0.049223045
Module 19	197	response to lipid	0.049234387

CHAPTER FIVE

MODULATION OF THE TGFβ PATHWAY AFFECTS IMMUNE RESPONSE IN A SCELARACTINIAN CORAL: POTENTIAL ECOLOGICAL IMPLICATIONS OF SYMBIOSIS

Lauren E Fuess[1], Caleb C Butler[1], Marlyn E Brandt[2], Laura D Mydlarz[1]

[1] Department of Biology, University of Texas Arlington, Arlington, Texas, United States of America
[2] Center for Marine and Environmental Studies, University of the Virgin Islands, St. Thomas, USVI, United States of America

ABSTRACT

Symbiotic relationships, found in many taxa across the earth, range from parasitic to mutualistic in nature. Despite their diversity, endosymbionts face similar problems in establishing relationships, namely the host's own immune response. Symbionts, regardless of parasitic or mutualistic nature, most somehow evade or suppress host immune responses designed to eliminate non-host entities. Many symbiotic organisms have evolved similar mechanisms to establish and maintain symbiosis, including manipulation of the host's own transforming growth factor-beta (TGFβ) pathway. Here we explore the functions of this pathway in scelaractinian corals, which are dependent on dinoflagellate *Symbiodinium* to meet their nutritional needs. Preliminary evidence suggests that *Symbiodinium* may manipulate host TGFβ to establish and maintain symbiosis. Using replicate cores of the coral, *Orbicella faveolata*, we explore the effects of inhibition and enhancement of this pathway on host transcriptomics under constitutive and immune challenge conditions. We demonstrate limited effects of enhancement or inhibition of this pathway on coral gene expression under constitutive conditions. However, manipulation of this pathway does significantly affect the subsequent ability of host corals to mount an immune response. Enhancement of the TGFβ pathway eliminates host coral immune response, while inhibition of the pathway increases the response. These findings suggest that while variation in TGFβ may have limited effects on corals under constitutive conditions, the implications are severe under disease pressure. This suggests a potentially important ecological trade-off between symbiosis and immunity that is particularly relevant under the relatively new selective pressure of increasing disease prevalence on reefs.

INTRODUCTION

Symbiotic relationships are present in a diversity of earth's ecosystems and involve a wide diversity of taxa (Brundrett 2009;Wang&Qiu 2006;Zeigler 2014). These relationships range from parasitic, where one partner benefits at the expense of another, to mutualistic, where both partners benefit (Hentschel *et al.* 2000;Johnson *et al.* 1997). Additionally these relationships take a variety of forms, ranging from macro relationships, such as those between plants and ants (Palmer&Brody 2013), to moderate scale relationships such as macro-parasitic infections (de Roij&MacColl 2012;Koprivnikar *et al.* 2012), to micro-, endosymbiotic relationships, such as those which comprise lichens (Perez-Ortega *et al.* 2010). Particularly in the case of parasitism and endosymbiotic interactions, establishment of these relationships presents a unique set of challenges for both partners.

One of the largest hurdles to the establishment and maintenance of both parasitic and endosymbiotic relationships is the host's immune response (Anbutsu&Fukatsu 2010;Chu&Mazmanian 2013;Molina-Cruz *et al.* 2013;Toth&Stacey 2015;Yasuda *et al.* 2016). Immunity has evolved over millions of years with the specific purpose of eliminating any detected non-host entities. Symbiotic partners, whether mutualistic or parasitic, are by nature non-self and therefore must find a way to be recognized by the host immune's system or otherwise suppress or evade these responses (Anbutsu&Fukatsu 2010;Molina-Cruz *et al.* 2013;Yasuda *et al.* 2016). While some mutualistic symbionts have developed complex recognition pathways to prevent elimination by the immune system and establish symbiosis, many other organisms have developed less savory techniques for accomplishing similar purposes. Parasites such as *Trypanosoma cruzi* and *Plasmodium falciparum* are known to manipulate the host's own TGFβ pathway to suppress host immune response and establish

symbiosis (Ndungu *et al.* 2005;Simmons *et al.* 2006;Waghabi *et al.* 2005). The TGFβ pathway is found throughout metazoans and is involved in many different processes including development, homeostasis, and immunity (Massague 1998). Binding of activated TGFβ to receptors activates members of the SMAD transcription factor family, which elicit changes in gene expression, including changes in expression of various immune genes (Detournay *et al.* 2012;Kulkarni *et al.* 1993;Letterio&Roberts 1998;Massague 1998). For example, mice deficient in TGFβ undergo excessive inflammatory responses, suggesting that loss of TGFβ results in impaired immune regulation (Kulkarni *et al.* 1993). Therefore by manipulating and increasing TGFβ activation, parasites and other symbionts may be capable of directly suppressing host immune response to avoid destruction.

Coral reefs, some of the most biodiverse ecosystems on the planet (Odum&Odum 1955;Roberts 1995;Sebens 1994), are comprised predominately of scelaractinian corals (Odum&Odum 1955). These coral hosts are largely dependent on endosymbiotic dinoflagellates known as *Symbiodinium* to meet their nutritional needs (Muscatine 1984, 1990;Muscatine&Porter 1977). Interestingly, there is considerable variation both within and between host species in both the identity (Cunning *et al.* 2015a;Silverstein *et al.* 2012;Stat *et al.* 2011) and density (Al-Sofyani&Floos 2013;Cunning&Baker 2014;Cunning *et al.* 2015b;Cunning *et al.* 2015c) of hosted symbionts. Additionally microhabitat variation may contribute to variation in symbiotic relationships (Cunning *et al.* 2015b;Cunning *et al.* 2015c). New findings in cnidarian models suggest that *Symbidoinium*, like parasites, manipulate the TGFβ pathway to establish and maintain symbiotic relationships (Berthelier *et al.* 2017;Detournay *et al.* 2012). However the mechanisms of this relationship are poorly understood.

Scelaractinian corals around the globe have experienced unprecedented declines due to rising sea surface temperatures and increases in the severity and prevalence of marine disease (Harvell *et al.* 1999;Hoegh-Guldberg *et al.* 2007;Hughes *et al.* 2003;Sutherland *et al.* 2004). However there is considerable variation within and between species in the susceptibility of organisms to these stressors (Barshis *et al.* 2013;Kenkel *et al.* 2013;Palmer *et al.* 2010;Palmer *et al.* 2011;Pinzon *et al.* 2014a;Pinzon *et al.* 2014b). Thermal stress in particular can cause breakdown of symbiotic relationships, resulting in eventual starvation and death of the host coral (Glynn 1993). Interestingly, variation in not only symbiont identity (Cunning *et al.* 2015a;LaJeunesse *et al.* 2010), but also density (Cunning&Baker 2013) has been linked to host bleaching tolerance. However little work has been done to investigate whether similar effects exist in the context of coral immune response and disease susceptibility (Berthelier *et al.* 2017;Detournay *et al.* 2012).

In order to increase understanding of the potential effects of symbiotic relationships and the TGFβ pathway on host coral immune response, we conducted a controlled immune challenge experiment. So as to mimic predicted effects of variation in symbiont density on TGFβ signaling, we directly inhibited or enhanced this pathway and measured subsequent effects on host gene expression under constitutive and immune challenge conditions. Our findings here provide significant evidence for the immune-regulatory role of the TGFβ pathway in corals and suggest that this pathway merits further study the in context of coral symbiotic relationships to increase understanding of potential immune-symbiosis tradeoffs in cnidarians.

METHODS

Sample Collection

Colonies of *Orbicella faveolata* were collected from Brewer's Bay (GPS coordinates: 18° 20′ 38.9, −64° 58′ 56.6), a fringing reef located in a shallow embayment on the south side of

St. Thomas Island, U.S. Virgin Islands. Each of the five colonies was collected using a hammer and chisel and transported in ambient seawater back to the University of the Virgin Islands Marine Laboratory facility. There, colonies were labeled and fragmented into roughly 5cm pieces. Each colony was fragmented into at least eight cores, with additional portions reserved for ongoing experiments. Fragmented corals were then placed in large water tables with flow through filtered seawater maintained at 27°C for the duration of the experiment. Tanks were covered with shade cloth to prevent stress due to ultraviolet radiation or excessive sunlight and samples were maintained in these conditions for approximately four days prior to experimentation.

Experimental Design

Prior to the experiment, eight fragments per colony were randomly selected and assigned to a treatment group (**Table 1**). Colonies were then placed in individual 4.7 L buckets that had been cleaned prior to experiment. Each bucket was filled with ambient seawater and supplied with continuous individual aeration though out the duration of the experiment. Individual buckets were than randomly distributed between two water tables, which were filled with flow through seawater to maintain temperature. Samples were allowed to acclimate to new conditions for approximately two hours prior to experimentation.

The experiment employed a full factorial design, combining one of four TGFβ treatments with one of two immune challenge treatments, for a single replicate per colony (n = 5). First, samples were inoculated with one of four TGFβ pre-treatments to mimic the effects of variation in symbiont density on TGFβ signaling. Samples were injected with 100uL of either .125 ug/mL recombinant TGFβ-3 expressed in *Escherichia coli* prepared in filtered seawater (TGFβ, Sigma-Aldrich, SRP3171), 10ug/mL anti-TGFβ, pan antibody produced in

rabbit and prepared in filtered seawater (anti- TGFβ, Sigma-Aldrich, T9429), or an appropriate vehicle control. Two controls were used for this portion of the experiment: a filtered seawater vehicle served as a control control for TGFβ inoculations while 10ug/mL normal rabbit IGG antibody in filtered seawater **(**Sigma-Aldrich, NIO1) was used as a control for the anti-TGFβ treatment. Inoculants were injected in equal amounts in 5 random locations across the coral fragment. Samples were then placed back into their individual containers and incubated with this treatment for approximately 2 hours.

Following incubation with a given TGFβ treatment, cores were again removed and injected with one of two immune challenge treatments. Samples received either a cocktail of bacteria lipopolysaccharides from *Escherichia coli* O127:B8 (LPS, Sigma-Aldrich, L3129) and peptidoglycan from *Staphylococcus aureus* (PGN, Sigma-Aldrich, 77140) prepared in filtered seawater (final concentration: .15 ug/uL LPS and .05 ug/uL PGN) or a vehicle (filtered seawater) control. Corals were injected with 100uL of inoculant in equal parts across five random locations on the coral fragment and then were placed back into their individual containers an additional two hour incubation.

At the conclusion of the experiment, samples were removed from their individual containers and processed for later analysis. Two small (~10 ug) portions of tissue were removed and placed in microcentrifuge tubes containing 1mL RNA-later (ThermoFisher, AM7021). RNA samples were then preserved according to manufactures instructions for later RNA extraction. The remaining core was then flash frozen in a liquid nitrogen dry shipper and stored at -80C for later protein extraction and analysis.

RNA Extraction and Sequencing

RNA was extracted from a small fragment of each sample using an RNAaqueous with DNAse step kit (Life Technologies AM1914) using a modified version of the manufacturer's instructions. Fragments with first homogenized with 800 µL of Lysis Buffer in a 2 mL microcentrifuge tube for approximately one minute. The tube was then centrifuged on an AccuSpin Micro (Fisher Scientific) and 700 µL of the supernatant was removed and processed using the manufacturer's instructions for RNA extraction. Final RNA was eluted twice with 50 µL elution solution for at total of 100 µL eluted RNA. In order to remove DNA contamination, eluted RNA was treated with an additional DNAse step. A 25 µL aliquot of final extract was combined with 1.5 µL DNase solution and 2.95 µL of Master Mix and incubated at 37°C for 1 hour. This solution was then incubated at room temperature for two minutes with 2.95 µL inactivation reagent. This process was repeated in triplicate to increase RNA yield. The final extracts (~30 µL per reaction) were combined and transferred to a new 1.5 µL tube, stored at -80°C.

Prior to sequencing, all samples were quality assessed using an Agilent BioAnalyzer 2100 at the University of Texas at Arlington Genomics Core facility. Samples with quality values (RIN number) greater than 5 were selected for library preparation and sequencing. Seven samples did not pass quality requirements and were therefore not sequenced (see **Table 1** for final *n* per treatment). Samples were then processed by the NovoGene Corporation for library construction and sequencing. A eukaryotic RNA-Seq library of total RNA extracts was constructed for each sample and libraries were sequenced on an Illumina Hiseq X with 150 base pair, paired end reads.

Transcriptome Analysis

Raw reads were obtained from NovoGene and filtered using the software package Trimmomatic, (v. 0.32) (Lohse et al. 2012). Adaptors and low quality reads were removed, and resulting sequences less than 36 base pairs in length were discarded. Sequences were then aligned to the reference *Orbicella faveolata* transcriptome (Pinzon *et al.* 2015) using the Tophat software package (v. 2.1.1; Trapnell *et al.* 2009) with default parameters. Read counts were obtained using the Cufflinks package (v 2.2.1; Trapnell *et al.* 2010) cufflinks and cuffmerge) and a read count matrix was generated from results using the htseq software package (v 0.6.1; Anders *et al.* 2015).

Differential expression was conducted using the R package DESeq2 (R v. 3.4.3; DESeq2 v. 1.18.1; Love *et al.* 2014). Outliers were assessed using PCA analyses, and none were detected. Prior to analysis, reads were variance stabilizing transformed to generate normalized read counts. Differential expression was modeled using treatment combination as a single effect. Average $\log_2$fold change per transcript was then generated for all relevant contrasts between treatment combinations (**Table 1**). Significantly differentially expressed transcripts were identified as those where $padj < 0.05$.

Transcriptome Annotation and Gene Ontology Analyses

The reference host transcriptome was re-annotated against the UniProtKB/Swiss-Prot database downloaded in January of 2018 prior to analysis of differentially expressed transcripts. A blastx algorithm with a minimum e-value threshold of 1.0E-5 was used for this analysis. The resulting annotations were used to conduct Gene Ontology analysis of the effects of each treatment using the R script GOMWU (Wright *et al.* 2015) with default parameters. Briefly, the script uses the 'stat' value and associated GO terms (if annotated) for

each transcript to generate a rank-based estimate of enriched GO terms. GO Terms were considered significant if their adjusted *p*-value was less than 0.05.

RESULTS

Differential Gene Expression Analysis

Full transcriptome sequencing resulted in a total of 833,787,572 combined reads for all 30 samples following initial quality control and prior to further trimming (approximate average of 25,266,290 reads per sample; minimum 20,000,000 reads per sample). Differential expression analysis of trimmed reads against the reference *O. faveolata* transcriptome resulted in a total of 73 unique contigs which were differentially expressed as a result of one or more contrasts of interest (**Table 1**). Manipulation of TGFβ pathway under control conditions had a limited effect on gene expression. Addition of exogenous TGFβ resulted in differential expression of 11 contigs, of which 2 were annotated. All contigs significantly affected by the addition of TGFβ were upregulated. In contrast, addition of anti-TGFβ resulted in the differential expression of six contigs when compared to rabbit antibody controls, and only one of these contigs was annotated. All of these contigs decreased in expression as a result of addition of anti-TGFβ.

In contrast, both immune stimulation, and the combination of manipulation of the TGFβ pathway and immune stimulation had significant effects on gene expression. Addition of immune stimulation inoculant alone (SCvSL) resulted in the differential expression of 41 contigs, of which 12 were annotated. This included a contig annotated as putative stress-response, protein dual specificity protein phosphatase 1B, and one annotated as putative immune protein, serine/threonine-protein phosphatase 5 (PP5). The group of contigs differentially expressed as a result of immune stimulation in specimens pre-treated with

rabbit antibody showed significant overlap with those contigs differentially expressed as a result of immune challenge alone (**Figure 1**). Addition of immune stimulant to corals treated with rabbit antibody controls resulted in differential expression of 48 contigs, of which 27 were also differentially expressed as a result of immune treatment alone (SCvSL). 15 contigs in this group were annotated, including PP5 and contigs annotated as putative immune and defense proteins (probable serine/threonine-protein kinase PBL18 and interferon regulatory factor 2-binding protein 1).

In contrast, there was limited effect of addition of immune stimulation to samples pretreated with TGFβ (TCvTL). Three contigs were differentially expressed as a result of this treatment, two of which were annotated including a histamine H2 receptor. Similarly, few contigs were differentially expressed as a result of immune stimulation to samples pretreated with anti-TGFβ (ACvAL). Only six contigs were differentially expressed as a result, of which one was annotated.

Gene Ontology Analyses

Gene ontology analysis confirmed that manipulation of the TGFβ had limited effects on host corals under control conditions. A total of three biological process GO terms were significantly enriched as a result of the addition of TGFβ (**Figure 2**). In contrast, no BP GO terms were differentially expressed as a result of addition of anti-TGFβ. It should be noted that the addition of rabbit antibody (SCvRC) did result in significant enrichment of six BP GO terms, none of which were involved in immune or stress response (**Supplementary Figure 1**).

By comparison, addition of immune challenge alone, and in combination with manipulation of host TGFβ pathway resulted in significant enrichment of many BP GO

terms, a large portion of which were significantly enriched as a result of multiple treatments (**Figure 3**). Immune challenge alone resulted in significant enrichment of 49 BP GO terms, all but two of which were positively enriched (**Figure 4**). This included two terms involved in apoptosis, and 20 terms involved in immune response, all of which were positively enriched. The combination of rabbit antibody and immune stimulation resulted in significant enrichment of 27 terms, many of which were involved in RNA processing (**Supplementary Figure 1**).

The combination of TGFβ pathway manipulation and immune challenge had significant effects on gene ontology enrichment. Immune challenge in samples pretreated with TGFβ (TCvTL) resulted in differential expression of 29 BP GO terms, only one of which was involved in immune response (**Figure 4**). An additional six terms involved in reactive oxygen processes were negatively enriched as a result of this treatment. In contrast, samples treated with anti-TGFβ (ACvAL) combined with immune stimulation demonstrated a preserved immune response, resulting in significant enrichment of 68 BP GO terms, of which only six were negatively enriched (**Figure 4**). Twenty-six of these terms were involved in immune response, all of which were significantly positively enriched.

In total, 36 immune related BP GO terms were significantly enriched as a result of immune stimulation in one or more pretreatment groups. This included a total of 1,397 contigs that were annotated as involved in one or more of these processes. Contigs in this group were involved in a variety of immune processes, including inflammation (**Figure 5**) and toll like receptor signaling processes (**Figure 6**). Many of these contigs, while not significantly differentially expressed, did show contrasting patterns of expression as a result of both immune challenge and manipulation of the TGFβ pathway.

Expression of Putative TGFβ Components

A total of 40 contigs with annotations involved in the TGFβ were expressed in one or more of our coral samples. This included 9 copies of various SMAD signaling molecules, 3 contigs annotated as a bone morphogenic protein, and two contigs annotated as thrombospondin-1 (**Supplementary Table 1**). None of these contigs were differentially expressed.

DISCUSSION

While it is well understood that there is considerable overlap between symbiosis and immunity in a variety of systems (Akamatsu *et al.* 2016;Toth&Stacey 2015;Yasuda *et al.* 2016), little effort has been spent investigating these potential relationships in cnidarians (Correa *et al.* 2009;Detournay *et al.* 2012;Detournay&Weis 2011). Here we document the effects of manipulating host TGFβ pathway, which has been implicated as an important mediator of host-symbiont relationships in cnidarians (Detournay *et al.* 2012;Detournay&Weis 2011), under constitutive and immune challenge conditions. We document the limited impact of manipulating this pathway under constitutive conditions, which is in stark contrast to the effects enhancing or inhibiting this pathway has on subsequent host immune response. Our findings indicate that variation in TGFβ pathway activity has significant effects on the coral immune response, and potentially subsequent disease susceptibility. Here we summarize our findings and highlight the potential associated ecological consequences of these results.

Manipulation of the TGFβ pathway has little constitutive effects

Addition of exogenous TGFβ or anti-TGFβ had limited effects on host coral gene expression under control conditions, as evidenced by the low number of significantly differentially expressed genes and few significantly enriched GO terms affected by these

changes. Enhancement of the pathway (by addition of TGFβ) predominantly increased microtubule and ciliary action. Interestingly, both microtubule networks and cilia may regulate TGFβ activity in different capacities (Batut *et al.* 2007;Christensen *et al.* 2017;Dong *et al.* 2000;Labour *et al.* 2016). Microtubule networks may serve to sequester SMAD molecules and thus reduce downstream TGFβ signaling (Dong *et al.* 2000). Other microtubule-associated proteins such as kinesin are necessary for the transport and activation of SMADs (Batut *et al.* 2007). Similarly, primary cilia have been implicated in many types of TGFβ signaling (Christensen *et al.* 2017;Labour *et al.* 2016). Therefore observed enrichment of these two processes is likely a result of increased downstream signaling and regulation following addition of exogenous TGFβ. In contrast, addition of anti-TGFβ to reduce or block TGFβ signaling resulted in almost no effects on host gene expression under constitutive conditions.

The limited effects of manipulation of the TGFβ pathway under constitutive conditions is particularly surprising considering the diverse functions of TGFβ signaling in metazoans (Massague 1998). However, it is possible that the dosage used and/or duration of the experiment was insufficient to observe significant effects of manipulation of this pathway under constitutive conditions. An additional explanation is that under control conditions corals are capable of adapting to variation in this pathway using moderate changes in diversity of genes. This type of response would be difficult to detect using common statistical approaches and therefore explains our lack of observed effect.

Immune response changes considerably following TGFβ pathway manipulation

While manipulation of the TGFβ signaling pathway had minimal effects on corals under constitutive conditions, its effects on subsequent immune response were considerable.

Control corals exposed to an immune challenge mounted a strong response marked by positive enrichment of multiple general and specific immune GO terms, including those involved with NF-κB signaling and apoptosis. Both NF-κB (Williams *et al.* 2018) and apoptotic (Fuess *et al.* 2017) signaling have been demonstrated to be key components of the cnidarian immune response. The responses of control coral to immune challenge are generally comparable to past studies of both *O. faveolata* and other scleractinian corals (Fuess *et al.* 2017;Fuess *et al.* 2016;van de Water *et al.* 2018;Wright *et al.* 2015;Wright *et al.* 2017).

Addition of exogenous TGFβ, enhancing downstream signaling, resulted in a complete reduction of this strong immune response, as evidenced by gene ontology analysis. Multiple invertebrate studies in other systems have found TGFβ to be a potent immune regulatory pathway (Letterio&Roberts 1998;Travis&Sheppard 2014). Similar patterns have been preliminarily reported in other model cnidarians (Detournay *et al.* 2012), but our results here are by far the most comprehensive documentation of these effects. In addition to a complete reduction of immune response, we also observed negative enrichment of multiple GO terms associated with antioxidant responses following an immune challenge. This is particularly relevant as antioxidant production is a demonstrated component of both the coral immune response (Mydlarz *et al.* 2010;Palmer *et al.* 2011;Palmer *et al.* 2009;Pinzon *et al.* 2014b), and host response to thermal stress and breakdown of symbiosis resulting in bleaching (Barshis *et al.* 2013;Jin *et al.* 2016). Previous studies in *Exaptasia pallida* have indicated that enhancement of TGFβ signaling results in both decreases in bleaching susceptibility and production of nitric oxide following heat stress (Detournay *et al.* 2012). Therefore it is possible that the addition of exogenous TGFβ increases host stress tolerance, therefore

increasing thresholds for activation of responses such as antioxidant production, and resulting in the observed patterns.

In contrast, addition of anti-TGFβ to inhibit downstream signaling not only preserved innate immune response, but appeared to strengthen the response of corals to immune challenge as evidenced by a larger number of immune-related GO terms which were positively enriched. These GO terms were also related to more specific types of immune response such as interleukin and toll-like receptor signaling, both of which are key components of innate immune response (Mydlarz *et al.* 2016;Mydlarz *et al.* 2008;Palmer *et al.* 2008;Williams *et al.* 2018). Furthermore, comparison of a subset of immune-annotated contigs involved in these GO terms indicates contrasting patterns of expression between corals pretreated with anti-TGFβ compared to those pretreated with TGFβ. Contigs involved in inflammation and TLR signaling generally demonstrated strengthened immune responses in anti-TGFβ pretreated coral samples following immune challenge, whereas these contigs were either downregulated or weakly upregulated in corals treated with TGFβ. Inflammation and TLR signaling are two immune processes which are intimately linked with TGFβ signaling (Clark *et al.* 2011;Lee *et al.* 2011;Yoshimura&Muto 2011), therefore it is unsurprising to observe effects of manipulating TGFβ on expression of components of these pathways. Additionally it is interesting to note the upregulation of anti-inflammatory NLRC3 in samples pre-treated with anti-TGFβ, compared to downregulation of this same contig in samples treated with TGFβ. Related to its roles preventing excessive immune response, the TGFβ pathway often regulates inflammation (Yoshimura&Muto 2011;Yoshimura *et al.* 2010). Therefore the observed patterns of NLRC3 expression are indicative of a secondary

immuno-protective mechanism that host corals may employ to prevent excessive inflammatory responses to stimulation independent of TGFβ signaling.

Variation in TGFβ signaling has significant ecological implications under changing ocean conditions

Here we report contrasting effects of TGFβ signaling on host gene expression dependent on host context (constitutive vs. immune stimulation conditions) that may have significant ecological implications. A growing number of studies have indicated a role of the TGFβ pathway in the establishment and maintenance of symbiotic relationships in cnidarians (Berthelier *et al.* 2017;Detournay *et al.* 2012). Furthermore, there is indication that symbionts may directly manipulate and increase host TGFβ signaling (Berthelier *et al.* 2017;Detournay *et al.* 2012). It is reasonable to assume that perhaps observed variation in symbiotic relationships may result in variation in constitutive TGFβ signaling within and between coral species. Our findings here suggest important ecological context for the consequences of this variation in a changing environment.

While we observed limited effects of manipulation of the TGFβ pathway on corals under non-stressful conditions, this relationship changes considerably following immune challenge. Manipulating, and thereby creating variation in TGFβ signaling, directly impacts the ability of a coral to respond to an immune challenge. In particular the elimination of an immune response following increases in TGFβ signaling suggests a potential ecological trade-off between symbiosis and immune response. If indeed increased TGFβ signaling results in reduced capacity to respond to an immune challenge, and symbiont density is positively correlated to TGFβ signaling as would be expected from previous findings (Berthelier *et al.* 2017;Detournay *et al.* 2012), symbiosis and its benefits may come at the direct cost of

immune capacity. The idea that increased symbiont density is actually a determent to the host is not a foreign concept in existing literature; numerous studies have suggested that excessive amounts of symbionts may increase host susceptibility to bleaching (Cunning&Baker 2013, 2014). Here our results indicate that a similar phenomenon may be true in immune-contexts.

Additionally, the lack of effect of variation in this pathway on corals under constitutive contexts presents an interesting evolutionary situation. Disease has dramatically increased in severity and prevalence on reefs in recent decades (Daszak *et al.* 2001;Harvell *et al.* 1999;Sutherland *et al.* 2004) and likely was not a significant selective force prior to the rise of anthropogenic effects on the environment. Here we demonstrate that artificial manipulation, specifically enhancement, of TGFβ signaling (to mimic the effects of increased symbiont density) has a negative impact on corals only under these evolutionarily "new" ecological contexts. This suggests that this potential trade-off between symbiosis and immunity is a relatively new process and therefore we may be at the beginning of a significant selective event that will affect future coral-symbiont relationships. It is therefore important to further explore the relationship between symbiosis, TGFβ signaling, and immunity in cnidarians so as to not only better understand the factors contributing to host coral disease susceptibility, but also to understand potential future scenarios and selective pressures that will shape reef communities under rapidly changing conditions.

CONCLUSIONS

In conclusion, here we document significant effects of manipulating host coral TGFβ signaling on subsequent induced immune response. The use of pharmaceuticals to manipulate TGFβ signaling and mimic potential effects of variation in symbiont density has revealed significant potential ecological implications of this pathway. While corals respond minimally to

changes in this pathway under control conditions, their capacity to respond to a subsequent immune challenge is significantly reduced. Our findings not only solidify the function of TGFβ signaling in immune regulation in cnidarians, but also highlight significant ecological considerations regarding cost:benefit trade-offs between symbiosis and host immunity and suggest potential new selective forces shaping reefs in the face of rapidly changing environments. It is therefore essential to continue to explore the role of this pathway in both symbiotic relationships and immunity in cnidarians so as to better predict reef community trajectories in the coming years.

ACKNOWLEDGEMENTS

The authors would like to acknowledge the Center for Marine and Environmental Studies, University of the Virgin Islands for providing logistical support and laboratory space. Additionally, the authors would like to thank members of the Brandt and Mydlarz labs for support in the field and the staff of the Genetics Core Facility (UTA) for assistance with RNA extraction and initial quality control. The analyses were run on a server provided by the UTA Office of Information Technology.

FIGURES AND TABLES

Table 1: List of relevant contrasts examined to determine the effects of manipulation of the TGFβpathway, immune stimulation, and the combination of both treatments. Included are the specific effects examined in each contrast as well as the comparisons which were made between groups of differentially expressed contigs/significantly enriched GO terms affected by each contigs.

	Group 1 Treatments		Group 2 Treatments			
Abbreviation	**TGFβ**	**Immune**	**TGFβ**	**Immune**	**Effect Examined**	**Compared To**
SCvRC	Seawater	Control	Rabbit Antibody	Control	Effects of rabbit antibody	NA
SCvTC	Seawater	Control	TGFβ	Control	Effects of TGFβ pathway enhancement	NA
RCvAC	Rabbit Antibody	Control	Anti-TGFβ	Control	Effects of TGFβ pathway inhibition	SCvRC
SCvSL	Seawater	Control	Seawater	LPS	Baseline immune response	RCvRL, TCvTL, ACvAL
RCvRL	Rabbit Antibody	Control	Rabbit Antibody	LPS	Effects of rabbit antibody immune response	SCvSL, ACvAL
TCvTL	TGFβ	Control	TGFβ	LPS	Effects of TGFβ enhancement on immune response	SCvSL
ACvAL	Anti-TGFβ	Control	Anti-TGFβ	LPS	Effects of TGFβ inhibition on immune response	SCvSL, RCvRL, TCvTL

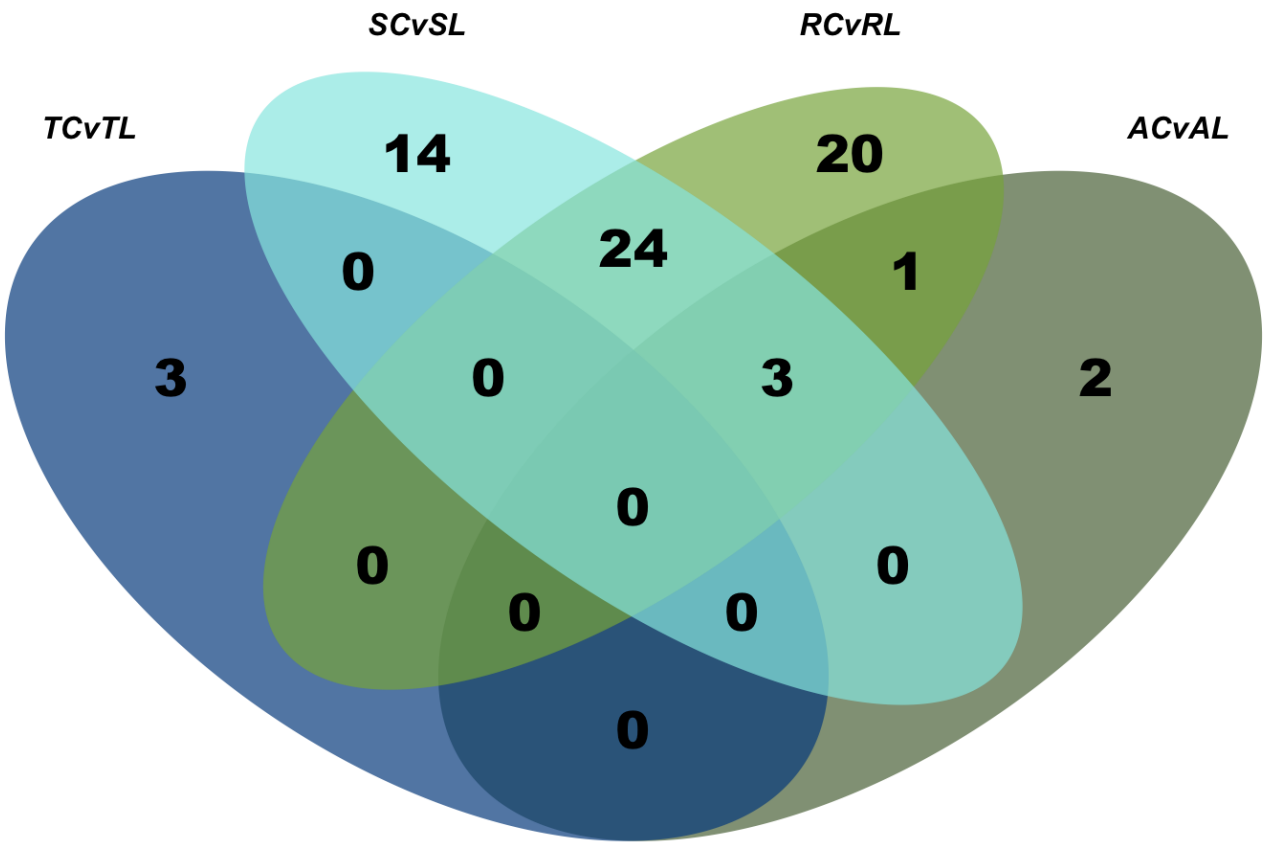

Figure 1: Summary of overlap of differentially expressed contigs as a result of immune challenge within each of the four TGFβ pretreatment groups. Numbers represent amount of contigs differentially expressed as a result of each contrast, or groups of contrasts.

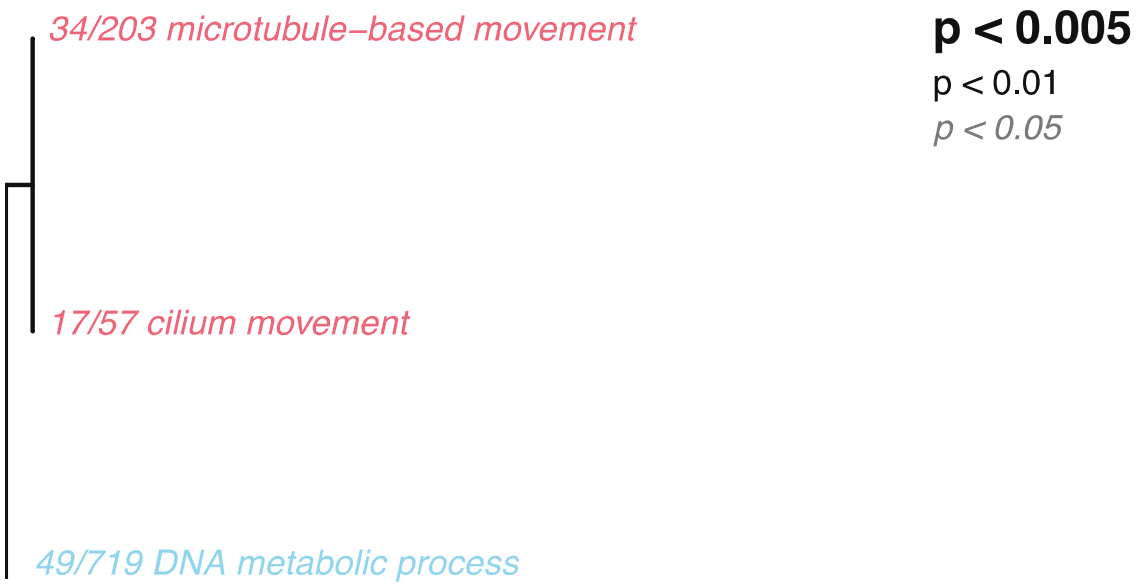

Figure 2: Hierarchical clustering of differentially expressed biological process gene ontology terms that were significantly enriched as a result of the addition of exogenous TGFβ to samples. Terms in red where positively enriched, terms in blue were negatively enriched. Ratios on each branch indicate the ratio of statistically significant contigs within a term compared to the total number of contigs included in that term.

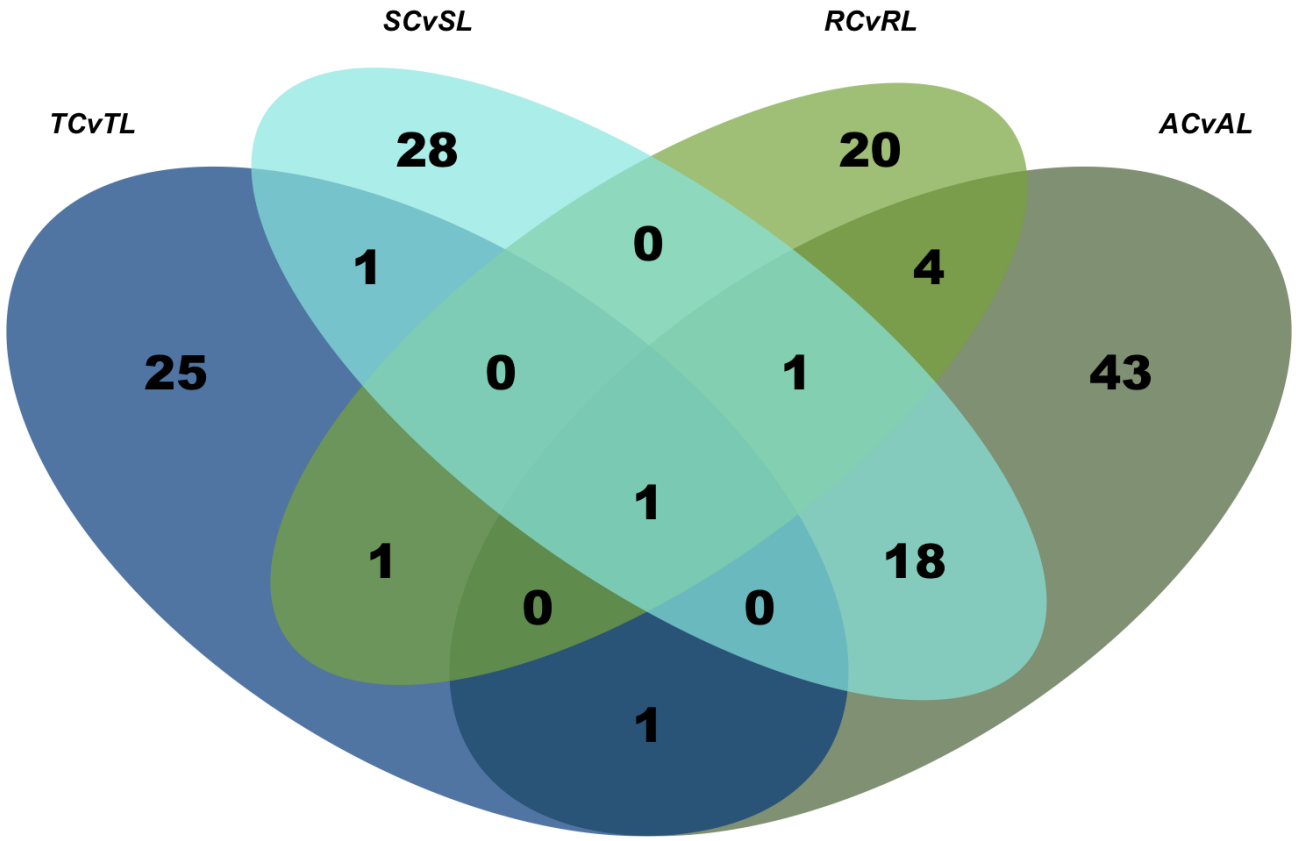

Figure 3: Summary of overlap of significantly enriched biological process GO terms as a result of immune challenge within each of the four TGFβ pretreatment groups. Numbers represent amount of enriched GO terms as a result of each contrast, or groups of contrasts.

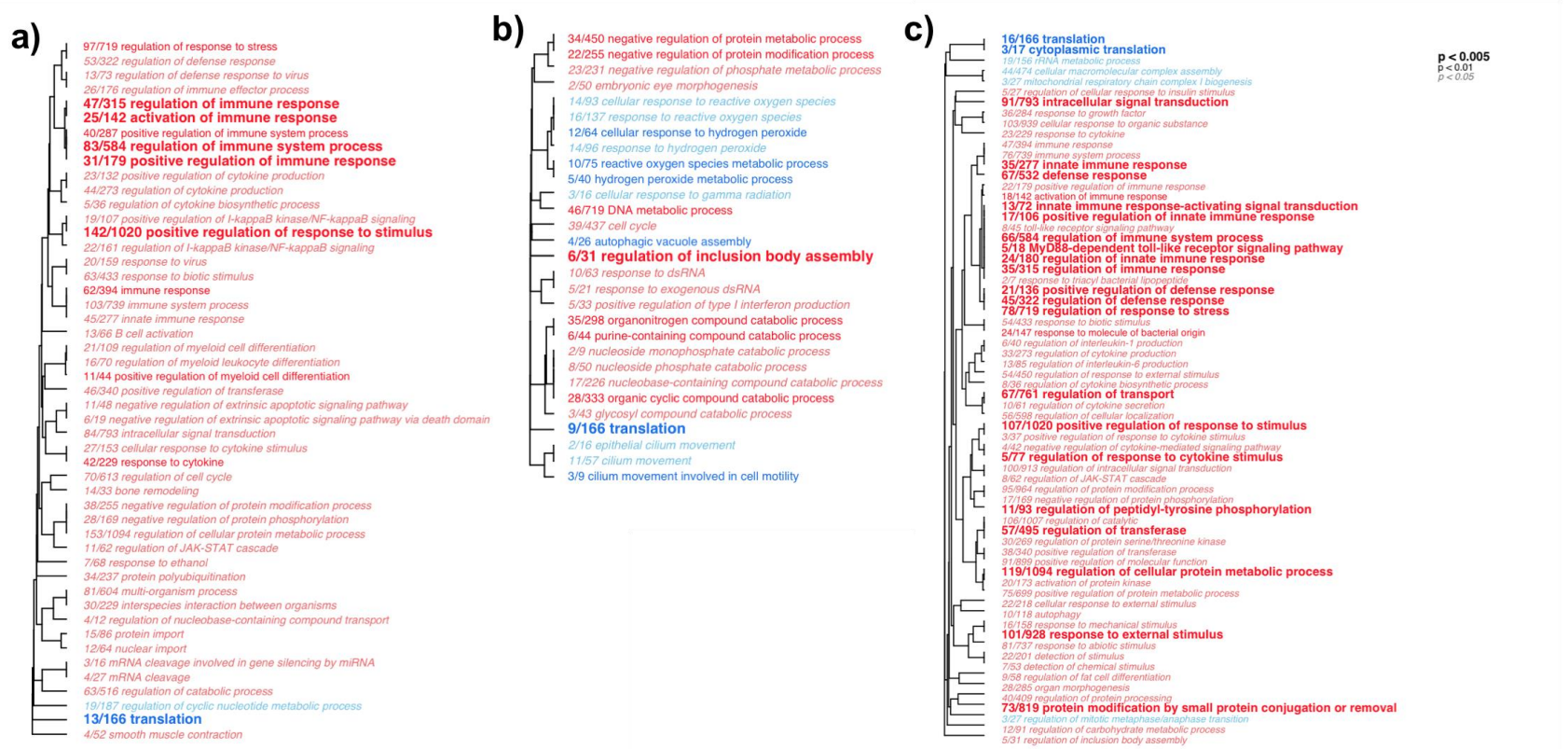

Figure 4: Hierarchical clustering of differentially expressed biological process gene ontology terms that were significantly enriched as a result of immune challenge in samples that were pretreated with **a)** seawater control **b)** exogenous TGFβ and **c)** anti-TGFβ. Terms in red where positively enriched, terms in blue were negatively enriched. Ratios on each branch indicate the ratio of statistically significant contigs within a term compared to the total number of contigs included in that term.

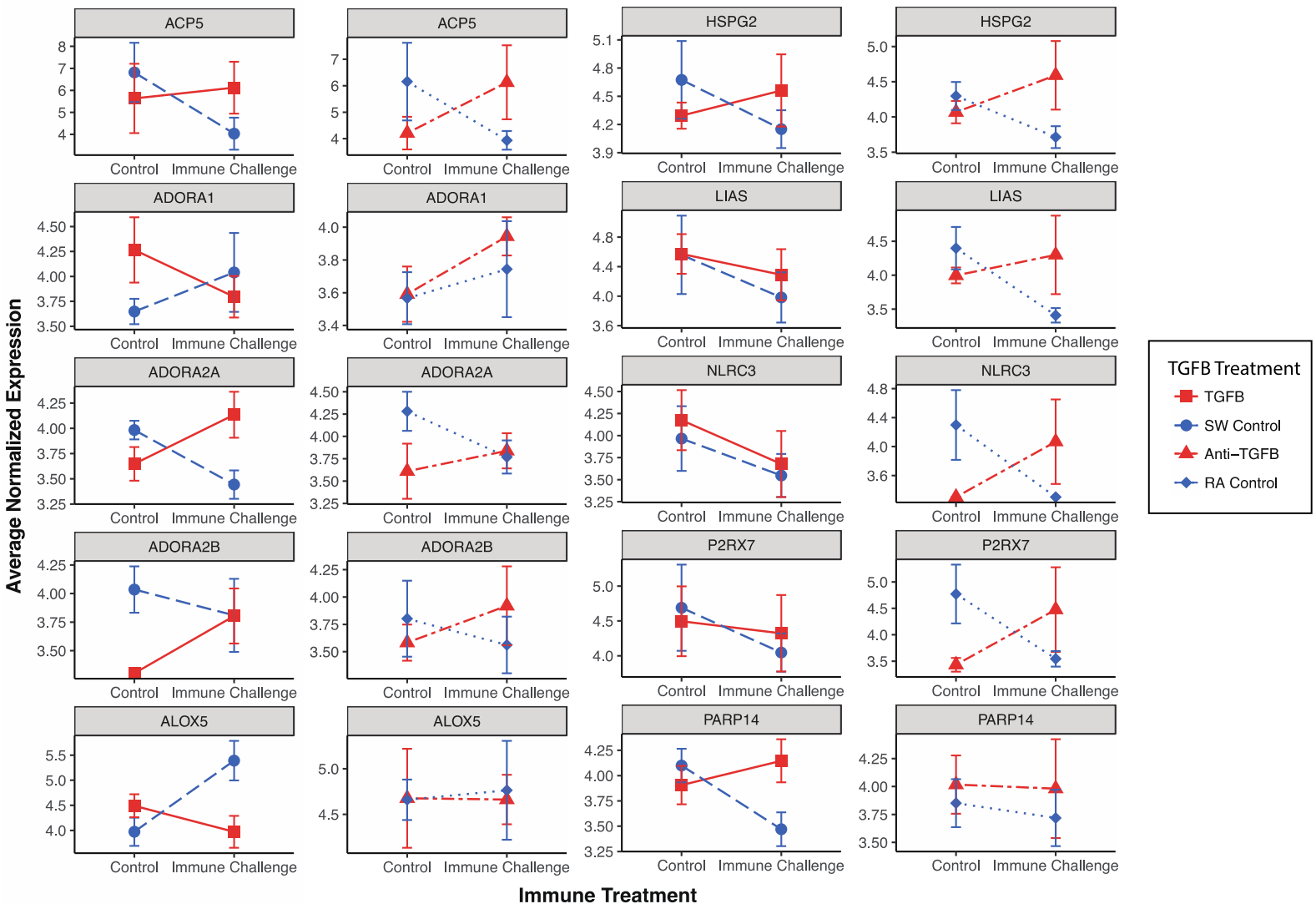

Figure 5: Paired interaction plots showing the effects of both immune challenge and manipulation of the TGFβ pathway on expression of genes involved inflammatory processes. Filtering parameters were used to select the displayed contigs. Those shown are contigs which were involved in a significantly enriched immune GO term, were expressed in all five colonies, underwent similar changes in expression as a result of both seawater and rabbit antibody control (direction of change was the same), and had the highest standard deviation in $\log_2$fold change as a result of immune challenge between samples pretreated with exogenous TGFβ and anti-TGFβ.

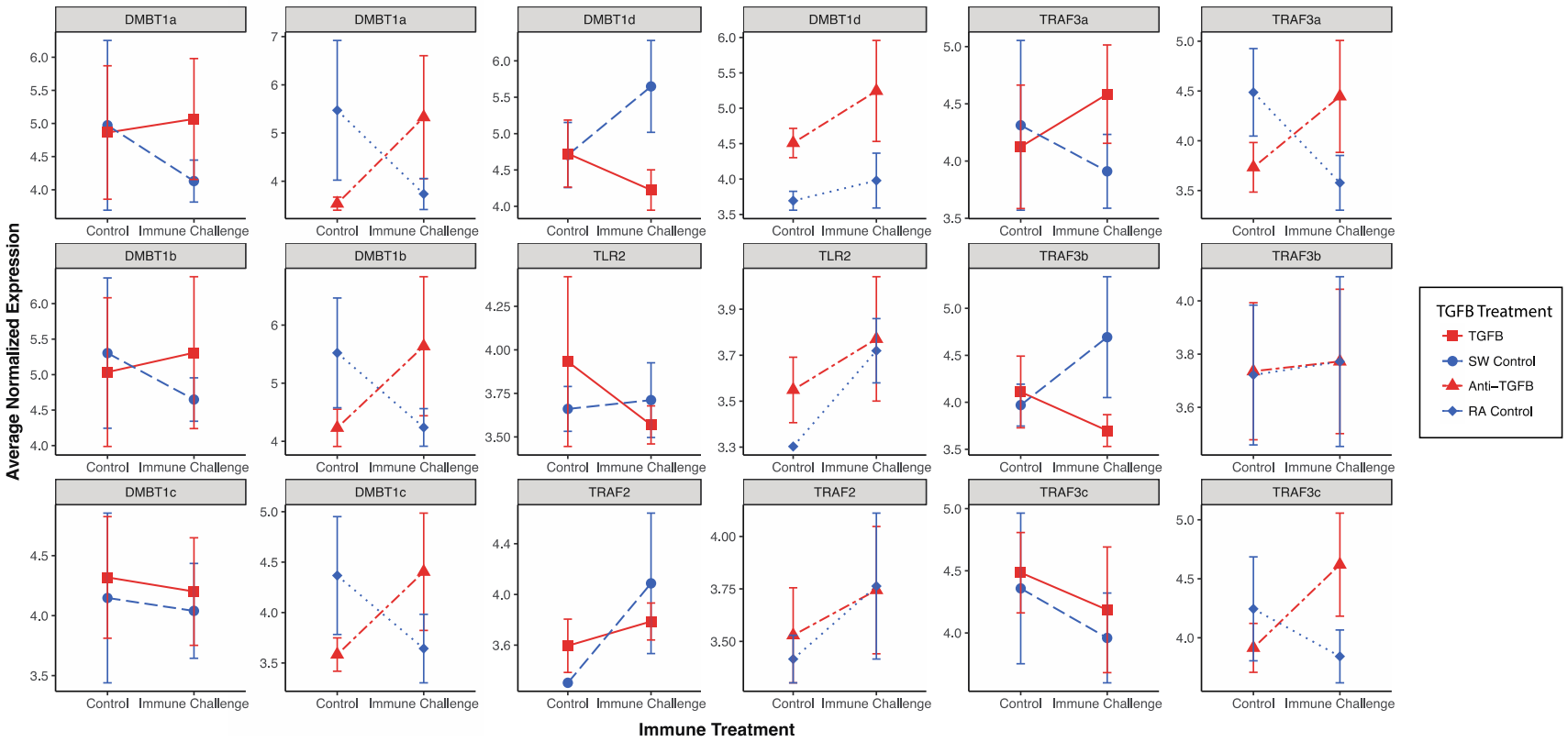

Figure 6: Paired interaction plots showing the effects of both immune challenge and manipulation of the TGFβ pathway on expression of genes involved in toll like receptor activity and downstream signaling. Filtering parameters were used to select the displayed contigs. Those shown are contigs which were involved in a significantly enriched immune GO term, were expressed in all five colonies, underwent similar changes in expression as a result of both seawater and rabbit antibody control (direction of change was the same), and had the highest standard deviation in $\log_2$fold change as a result of immune challenge between samples pretreated with exogenous TGFβ and anti-TGFβ.

SUPPLEMENTARY FIGURES AND TABLES

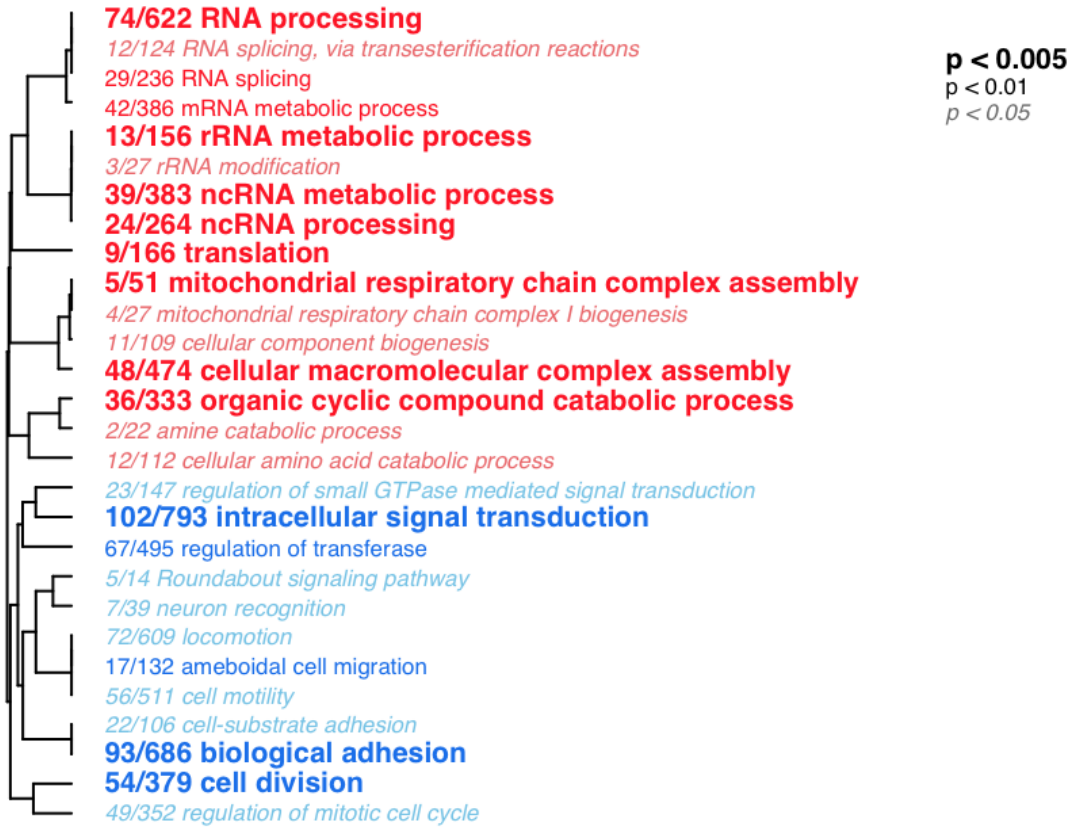

Supplementary Figure 1: Hierarchical clustering of differentially expressed biological process gene ontology terms that were significantly enriched as a result of immune challenge in samples pre-treated with rabbit antibody (RCvRL). Terms in red where positively enriched, terms in blue were negatively enriched. Ratios on each branch indicate the ratio of statistically significant contigs within a term compared to the total number of contigs included in that term.

Supplementary Table 1: List of all putative TGFβ that were expressed in one or more samples. Shown are annotations and log_2fold change values for all relevant contrasts

Locus	spID	Protein Name	Contrasts						
			SCvRC	SCvTC	RCvAC	SCvSL	RCvRL	TCvTL	ACvAL
XLOC_018127	Q90ZK6	Activin receptor type-1	0.0449	-0.0500	-0.4227	0.3925	-0.5497	0.1577	0.5425
XLOC_020640	P22004	Bone morphogenetic protein 6	0.7399	-0.7324	0.4004	-0.7513	0.5861	-0.0110	-0.0905
XLOC_029344	P18075	Bone morphogenetic protein 7	-0.3939	0.1022	-0.5914	0.1035	-0.8172	0.1161	0.6189
XLOC_029345	P18075	Bone morphogenetic protein 7	-0.3926	0.3394	0.0326	0.1624	-0.2154	0.2808	-0.1197
XLOC_046657	Q78EA7	Bone morphogenetic protein receptor type-1A	0.1311	0.1058	0.0047	-0.1760	0.0179	-0.1432	0.0491
XLOC_039044	Q91713	Chordin	0.3941	-0.0539	-0.3052	0.1785	-0.8767	0.1001	0.3055
XLOC_045590	Q92793	CREB-binding protein	0.5310	-0.1724	-0.5005	-0.1962	-0.7644	0.3500	0.9356
XLOC_045592	Q6JHU9	CREB-binding protein	0.8521	-0.5339	-1.7168	0.1692	-2.3200	0.4553	2.6867
XLOC_000170	Q5R4G6	Cullin-1	-0.1247	0.0472	-0.0866	0.0432	0.0026	-0.0590	0.1359
XLOC_010209	P85857	Growth/differentiation factor 6-A	0.1375	0.1334	0.1701	-0.5408	0.3188	-0.0953	-0.1350
XLOC_050698	Q9GZN2	Homeobox protein TGIF2	0.1941	-0.2055	0.3288	-0.2408	0.3199	0.0707	-0.2671
XLOC_014119	Q9IBG7	Kielin/chordin-like protein	-0.5437	-0.1260	-0.4841	-0.0845	-0.7524	0.7769	0.0986
XLOC_002738	P26696	Mitogen-activated protein kinase 1	0.0015	0.0032	-0.0667	-0.1579	0.0736	-0.1045	0.0839
XLOC_003479	Q1JQA2	Mothers against decapentaplegic homolog 1	0.2258	0.4913	0.2924	0.4937	-0.1830	-0.1411	-0.4356
XLOC_042307	P84023	Mothers against decapentaplegic homolog 3	-0.1039	0.0304	-0.1687	-0.0388	-0.1880	-0.0766	0.0005
XLOC_044689	O70437	Mothers against decapentaplegic homolog 4	-0.8354	0.9461	0.0128	1.4091	0.6790	-0.2921	0.5520
XLOC_044687	O70437	Mothers against decapentaplegic homolog 4	-0.3668	0.1715	-0.0877	0.2329	0.1434	-0.0692	-0.1407
XLOC_033053	P97471	Mothers against decapentaplegic homolog 4	-0.3548	-4.0643	-4.2210	-0.8280	-4.3921	0.2732	-0.3270
XLOC_043473	P97454	Mothers against decapentaplegic homolog 5	-0.3406	0.3534	-0.4937	0.8528	-0.4651	0.2506	0.5503

XLOC_043472	P97454	Mothers against decapentaplegic homolog 5	0.1661	-0.4372	-0.0075	-0.4425	0.0063	0.3213	-0.2058
XLOC_003478	Q9W7E7	Mothers against decapentaplegic homolog 5	0.1518	-0.0389	0.1506	1.0344	-1.0495	0.4588	0.0395
XLOC_013981	O43541	Mothers against decapentaplegic homolog 6	0.1109	-0.1582	0.3343	-0.3023	-0.0104	-0.0519	-0.2085
XLOC_026401	P18444	N-myc proto-oncogene protein	-0.4043	-0.1058	0.1106	0.2476	-0.1350	-0.0252	-0.5231
XLOC_005172	Q61477	Neuroblastoma suppressor of tumorigenicity 1	0.9515	-0.1133	0.8812	-0.3458	0.5090	-1.4606	-1.1037
XLOC_006684	Q9W741	Noggin-1	-0.1360	-0.1578	-0.4426	-0.2820	-0.5876	0.2146	0.1727
XLOC_024850	Q9W740	Noggin-2	0.7360	-0.6305	-0.4040	-3.9567	-0.9310	-0.9850	0.1836
XLOC_024851	Q9W740	Noggin-2	1.4124	-0.7351	1.3860	-1.1801	0.8366	-0.5267	-0.8955
XLOC_021087	P28749	Retinoblastoma-like protein 1	0.0651	0.0817	0.0107	0.2031	0.0636	0.2213	0.0426
XLOC_042943	P67999	Ribosomal protein S6 kinase beta-1	-0.5537	0.8527	-0.2681	0.1613	0.1437	-0.7202	0.3034
XLOC_042942	P67998	Ribosomal protein S6 kinase beta-1	-0.0696	0.4774	-0.7040	0.1394	-0.6250	-0.3677	0.8973
XLOC_050678	Q8QG64	RING-box protein 1	-0.0391	0.0277	-0.0120	-0.3051	0.1322	-0.1364	-0.2582
XLOC_049697	Q0P594	Serine/threonine-protein phosphatase 2A catalytic subunit beta isoform	0.0160	-0.0176	0.1514	0.2642	0.1082	-0.0631	-0.2413
XLOC_049698	Q0P594	Serine/threonine-protein phosphatase 2A catalytic subunit beta isoform	0.0739	0.2186	0.1730	0.1817	-0.0087	-0.1171	0.0571
XLOC_024678	P35441	Thrombospondin-1	-0.4140	-0.3868	-3.6426	-0.3258	-3.0923	1.4199	-0.3269
XLOC_051826	P35441	Thrombospondin-1	0.7195	4.0332	-1.8795	0.0095	-2.0505	-5.4177	2.1208
XLOC_033459	Q17QZ4	Transcription factor Dp-1	-0.0646	-0.1314	-0.0101	-0.1247	0.1914	0.1933	-0.1684
XLOC_004778	Q6DE14	Transcription factor E2F4	0.2123	-0.2412	-0.6443	-0.2043	-1.1498	0.3889	0.9263
XLOC_047933	O95405	Zinc finger FYVE domain-containing protein 9	-2.4153	1.7817	-1.0926	5.2000	1.3891	1.1814	3.5908
XLOC_047934	O95405	Zinc finger FYVE domain-containing protein 9	-1.6764	1.1260	1.0786	2.4644	-1.7920	0.0388	-0.7500
XLOC_039964	O95405	Zinc finger FYVE domain-containing protein 9	-0.0017	-0.0486	-0.4326	0.5005	-0.8947	0.3161	0.1524

CHAPTER SIX

CONCLUSIONS

Knowledge of cnidarian innate immunity has increased considerably over the past decades (Mydlarz *et al.* 2016;Palmer&Traylor-Knowles 2012). However despite this increase in mechanistic knowledge of coral immunity, many knowledge gaps still exist in our understanding of the disease ecology and ecoimmunology of reef systems (Harvell *et al.* 2004). This includes a lack of information on the causes and consequences of variation in immune response between coral species (Pinzon *et al.* 2014a), the fitness effects of mounting an immune response (Weil *et al.* 2009b), and the implications of symbiotic relationships on cnidarian immunity (Detournay *et al.* 2012). This dissertation employed a combination of laboratory and field-based studies in an effort to address several key ecoimmunological questions essential to predicting reef community trajectories under increasing disease susceptibility. In **Chapters 2** and **3**, I describe patterns of gene expression that may contribute to disease susceptibility within a vulnerable coral species, including those patterns that may underlie variation in disease susceptibility across a range of species. Together these chapters provide initial insight into the cellular level mechanisms that contribute to described variation among coral species in susceptibility to disease. This information is not only an excellent starting point for future investigation into similar questions, but also provides information that can assist in modeling reef futures under various scenarios.

The second half of my dissertation considers potential trade-offs related to immune response in cnidarians. In **Chapter 4** I use a natural disease outbreak of an octocoral species to highlight potential consequences of immune response. Here I show that immunity comes at the cost of reduced growth and potentially organismal reproduction. These findings suggest that the consequences of disease outbreaks on reef communities may extend beyond direct mortality,

necessitating shift in the way in which ecologists consider outcomes of disease. Finally, in **Chapter 5**, I examine how manipulation of an immune-regulatory pathway, which may be a key component of the establishment and maintenance of symbiotic relationships, significantly affects subsequence coral immune response. In this last chapter I note the evolutionary implications of this trade-off as preliminary results suggest that it is only of consequence under immune-challenge conditions. Importantly I conclude that potential trade-offs between symbiosis and immunity are likely to exert new selective pressure on reef corals under increasing disease pressure which will like result in future shifts in symbiotic relationships.

Together the four research chapters of my dissertation provide novel insight into ecological implications of coral disease on reef ecology as a whole. My dissertation research extends beyond mechanistic studies of coral immunity to provide insight that will assist researchers in understanding the futures of reef communities in a rapidly changing environment. This research therefore provides a strong foundation for future ecoimmunological work in this system and will no doubt be invaluable to coral physiologists and ecologists alike.

REFERENCES

Adamo S. A., Jensen M., Younger M. (2001) Changes in lifetime immunocompetence in male and female *Gryllus texensis* (formerly *G. integer*)*: trade-offs between immunity and reproduction. Animal Behavior 62, 417-425.

Aderem A., Ulevitch R. J. (2000) Toll-like receptors in the induction of the innate immune response. Nature 406, 782-787.

Adger W. N., Hughes T. P., Folke C., Carpenter S. R., Rockstrom J. (2005) Social-ecological resilience to coastal disasters. Science 309, 1036-1039.

Ainsworth T. D., Kvennefors E. C., Blackall L. L., Fine M., Hoegh-Guldberg O. (2007) Disease and cell death in white syndrome of *Acroporid* corals on the Great Barrier Reef. Marine Biology 151, 19-29.

Akamatsu A., Shimamoto K., Kawano Y. (2016) Crosstalk of signaling mechanisms involved in host defense and symbiosis against microorganisms in rice. Current Genomics 17, 297-307.

Akira S., Takeda K. (2004) Toll-like receptor signalling. Nature Reviews Immunology 4, 499-511.

Akira S., Uematsu S., Takeuchi O. (2006) Pathogen recognition and innate immunity. Cell 124, 783-801.

Al-Sofyani A. A., Floos Y. A. M. (2013) Effect of temperature on two reef-building corals *Pocillopora damicornis* and *P. verrucosa* in the Red Sea. Oceanologia 55, 917-935.

Alers S., Loffler A. S., Wesselborg S., Stork B. (2012) Role of AMPK-mTOR-Ulk1/2 in the regulation of autophagy: cross talk, shortcuts, and feedbacks. Molecular and Cellular Biology 32, 2-11.

Allam B., Pales Espinosa E., Tanguy A., *et al.* (2014) Transcriptional changes in Manila clam (*Ruditapes philippinarum*) in response to Brown Ring Disease. Fish & Shellfish Immunology 41, 2-11.

Anbutsu H., Fukatsu T. (2010) Evasion, suppression and tolerance of *Drosophila* innate immunity by a male-killing *Spiroplasma endosymbiont*. Insect Molecular Biology 19, 481-488.

Anders S., Pyl P. T., Huber W. (2015) HTSeq-a Python framework to work with high-throughput sequencing data. Bioinformatics 31, 166-169.

Anderson A. C., Anderson D. E., Bregoli L., *et al.* (2007) Promotion of tissue inflammation by the immune receptor Tim-3 expressed on innate immune cells. Science 318, 1141-1143.

Anderson D. A., Walz M. e., Weil E., Tonellato P., Smith M. C. (2016) RNA-Seq of the Caribbean reef-building coral *Orbicella faveolata* (Scleractinia-Merulinidae) under bleaching and disease stress expands models of coral innate immunity. PeerJ, 4:e1616.

Aronson R. B., Precht W. F. (2001) White-band disease and the changing face of Caribbean coral reefs. Hydrobiologia 460, 25-38.

Arthur J. S., Ley S. C. (2013) Mitogen-activated protein kinases in innate immunity. Nature Reviews Immunology 13, 679-692.

Aruoma O. I. (1998) Free radicals, oxidative stress, and antioxidants in human health and disease. Journal of the American Oil Chemists Society 75, 199-212.

Asea A., Rehli M., Kabingu E., *et al.* (2002) Novel signal transduction pathway utilized by extracellular *HSP70*: role of toll-like receptor (TLR) 2 and TLR4. Journal of Biological Chemistry 277, 15028-15034.

Assefa Z., Van Laethem A., Garmyn M., Agostinis P. (2005) Ultraviolet radiation-induced apoptosis in keratinocytes: On the role of cytosolic factors. Biochimica et Biophysica Acta 1755, 90-106.
Baehrecke E. H. (2005) Autophagy: dual roles in life and death? Nature Reviews: Molecular Cell Biology 6, 505-510.
Baker A. C., Glynn P. W., Riegl B. (2008) Climate change and coral reef bleaching: An ecological assessment of long-term impacts, recovery trends and future outlook. Estuarine, Coastal and Shelf Science 80, 435-471.
Barshis D. J., Ladner J. T., Oliver T. A., Palumbi S. R. (2014) Lineage-specific transcriptional profiles of *Symbiodinium spp.* unaltered by heat stress in a coral host. Molecular Biology and Evolution 31, 1343-1352.
Barshis D. J., Ladner J. T., Oliver T. A., *et al.* (2013) Genomic basis for coral resilience to climate change. Proceedings of the National Academy of Sciences of the United States of America 110, 1387-1392.
Bascunan-Garcia A. P., Lara C., Cordoba-Aguilar A. (2010) Immune investment impairs growth, female reproduction and survival in the house cricket, *Acheta domesticus*. Journal of Insect Physiology 56, 204-211.
Batut J., Howell M., Hill C. S. (2007) Kinesin-mediated transport of Smad2 is required for signaling in response to TGF-beta ligands. Developmental Cell 12, 261-274.
Becker K., Tilley L., Vennerstrom J. L., *et al.* (2004) Oxidative stress in malaria parasite-infected erythrocytes: host-parasite interactions. International Journal of Parasitology 34, 163-189.
Bell J. K., Mullen G. E., Leifer C. A., *et al.* (2003) Leucine-rich repeats and pathogen recognition in Toll-like receptors. Trends in Immunology 24, 528-533.
Bellard C., Bertelsmeier C., Leadley P., Thuiller W., Courchamp F. (2012) Impacts of climate change on the future of biodiversity. Ecology Letters 15, 365-377.
Bellwood D. R., Hughes T. P. (2001) Regional-scale assembly rules and biodiversity of coral reefs. Science 292, 1532-1535.
Bellwood D. R., Hughes T. P., Folke C., Nystrom M. (2004) Confronting the coral reef crisis. Nature 429, 827-833.
Bellwood D. R., Wainwright P. C., Fulton C. J., Hoey A. S. (2006) Functional versatility supports coral reef biodiversity. Proceedings, Biological Science 273, 101-107.
Berthelier J., Schnitzler C. E., Wood-Charlson E. M., *et al.* (2017) Implication of the host TGFb pathway in the onset of symbiosis between larvae of the coral *Fungia scutaria* and the dinoflagellate *Symbiodinium sp.* (clade C1f). Coral Reefs.
Bikker F. J., Ligtenberg A. J., Nazmi K., *et al.* (2002) Identification of the bacteria-binding peptide domain on salivary agglutinin (gp-340/DMBT1), a member of the scavenger receptor cysteine-rich superfamily. Journal of Biological Chemistry 277, 32109-32115.
Black N. A., Voellmy R., Szmant A. S. (1995) Heat shock protein induction in *Montastraea faveolata* and *Aiptasia pallida* exposed to elevated temperatures. Biological Bulletin 188, 234-240.
Bolger A. M., Lohse M., Usadel B. (2014) Trimmomatic: a flexible trimmer for Illumina sequence data. Bioinformatics 30, 2114-2120.
Bosch T. C., Augustin R., Anton-Erxleben F., *et al.* (2009) Uncovering the evolutionary history of innate immunity: the simple metazoan *Hydra* uses epithelial cells for host defence. Developmental & Comparative Immunology 33, 559-569.

Bowman J., Rodgers M. A., Shi M., *et al.* (2015) Posttranslational Modification of HOIP Blocks Toll-Like Receptor 4-Mediated Linear-Ubiquitin-Chain Formation. MBio 6, e01777-01715.
Bozec Y. M., Yakob L., Bejarano S., Mumby P. J. (2013) Reciprocal facilitation and non-linearity maintain habitat engineering on coral reefs. Oikos 122, 428-440.
Brinkhuis V., Lunz K. (2015) Investigation of a previously undescribed octocoral disease affecting the Florida reef tract. Florida State Wildlife Grant.
Brinkhuis V. I. P. (2009) Assessment of gorgonian transplantation techniques offshore Southeast Florida, Nova Southeastern University Oceanographic Center.
Brock P. M., Murdock C. C., Martin L. B. (2014) The history of ecoimmunology and its integration with disease ecology. Integrative and Comparative Biology 54, 353-362.
Brown T., Bourne D., Rodriguez-Lanetty M. (2013) Transcriptional activation of c3 and hsp70 as part of the immune response of *Acropora millepora* to bacterial challenges. PLoS One 8, e67246.
Bruckner A. W., Hill R. L. (2009) Ten years of change to coral communities off Mona and Desecheo Islands, Puerto Rico, from disease and bleaching. Diseases of Aquatic Organisms 87, 19-31.
Brundrett M. C. (2009) Mycorrhizal associations and other means of nutrition of vascular plants: understnding global diversity of host plants by resolving conflicting information and developing reliable means of diagnosis. Plant and Soil 320, 37-77.
Bruno J. F., Ellner S. P., Vu I., Kim K., Harvell C. D. (2011) Impacts of aspergillosis on sea fan coral demography: modeling a moving target. Ecological Monographs 81, 123-139.
Bruno J. F., Petes L. E., Harvell C. D., Hettinger A. (2003) Nutrient enrichment can increase the severity of coral diseases. Ecology Letters 6, 1056-1061.
Bruno J. F., Selig E. R., Casey K. S., *et al.* (2007) Thermal stress and coral cover as drivers of coral disease outbreaks. PLoS Biology 5, 1220-1227.
Buchanan S. G., Gay N. J. (1996) Structural and functional diversity in the leucine-rich repeat family of proteins. Progress in Biophysics and Molecular Biology 65, 1-44.
Burge C. A., Douglas N. L., Conti-Jerpe I., *et al.* (2012) Friend or foe: the association of *Labyrinthulomycetes* with the Caribbean sea fan *Gorgonia ventalina*. Diseases of Aquatic Organisms 101, 1-12.
Burge C. A., Mark Eakin C., Friedman C. S., *et al.* (2014) Climate change influences on marine infectious diseases: implications for management and society. Annual Review of Marine Science 6, 249-277.
Burge C. A., Mouchka M. E., Harvell C. D., Roberts S. (2013) Immune response of the Caribbean sea fan, *Gorgonia ventalina*, exposed to an *Aplanochytrium* parasite as revealed by transcriptome sequencing. Frontiers in Physiology 4, 180.
Campagna D., Gasparini F., Franchi N., *et al.* (2016) Transcriptome dynamics in the asexual cycle of the chordate *Botryllus schlosseri*. BMC Genomics 17, 275.
Carlton E. D., Cooper C. L., Demas G. E. (2014) Metabolic stressors and signals differentially affect energy allocation between reproduction and immune function. General and Comparative Endocrinology 208, 21-29.
Caron E., Hall A. (1998) Identification of two distinct mechanisms of phagocytosis controlled by different Rho GTPases. Science 282, 1717-1721.
Cary L. R. (1914) Observation on the growth rate and oecology of gorgonians. Carnegie Institution of Washington Publication 43, 79-90.

Cerenius L., Kawabata S. I., Lee B. L., Nonaka M., Soderhall K. (2010) Proteolytic cascades and their involvement in invertebrate immunity. Trends in Biochemical Sciences 35, 575-583.
Cerenius L., Lee B. L., Soderhall K. (2008) The proPO-system: pros and cons for its role in invertebrate immunity. Trends in Immunology 29, 263-271.
Cerenius L., Soderhall K. (2004) The prophenoloxidase-activating system in invertebrates. Immunological Reviews 198, 116-126.
Cervino J. M., Hayes R. L., Polson S. W., *et al.* (2004) Relationship of *Vibrio* species infection and elevated temperature to yellow blotch/band disease in Caribbean corals. Applied Environmental Microbiology 70, 6855-6864.
Cervino J. M., Thompson F. L., Gomez-Gil B., *et al.* (2008) The Vibrio core group induces yellow band disease in Caribbean and Indo-Pacific reef-building corals. Journal of Applied Microbiology 105, 1658-1671.
Cheng T. C., Rodrick G. E., Foley D. A., Koehler S. A. (1975) Release of lysozyme from hemolymph cells of Mercenaria mercenaria during phagocytosis. Journal of Invertebrate Pathology 25, 261-265.
Chevin L. M., Lande R., Mace G. M. (2010) Adaptation, plasticity, and extinction in a changing environment: towards a predictive theory. PLoS Biology 8, e1000357.
Chiarelli R., Martino C., Agnello M., Bosco L., Roccheri M. C. (2016) Autophagy as a defense strategy against stress: focus on *Paracentrotus lividus* sea urchin embryos exposed to cadmium. Cell Stress & Chaperones 21, 19-27.
Chow J. C., Young D. W., Golenbock D. T., Christ W. J., Gusovsky F. (1999) Toll-like receptor-4 mediates lipopolysaccharide-induced signal transduction. Journal of Biological Chemistry 274, 10689-10692.
Christensen S. T., Morthorst S. K., Mogensen J. B., Pedersen L. B. (2017) Primary cilia and coordination of receptor tyrosine kinase (RTK) and transforming growth factor beta (TGF-beta) signaling. Cold Spring Harb Perspect Biol 9.
Chu H., Mazmanian S. K. (2013) Innate immune recognition of the microbiota promotes host-microbial symbiosis. Nature Immunology 14, 668-675.
Clark R. I., Woodcock K. J., Geissmann F., Trouillet C., Dionne M. S. (2011) Multiple TGF-beta superfamily signals modulate the adult *Drosophila* immune response. Current Biology 21, 1672-1677.
Cooney R., Baker J., Brain O., *et al.* (2010) NOD2 stimulation induces autophagy in dendritic cells influencing bacterial handling and antigen presentation. Nature Medicine 16, 90-97.
Correa A. M. S., Brandt M. E., Smith T. B., Thornhill D. J., Baker A. C. (2009) *Symbiodinium* associations with diseased and healthy scleractinian corals. Coral Reefs 28, 437-448.
Couch C. S., Mydlarz L. D., Harvell C. D., Douglas N. L. (2008) Variation in measures of immunocompetence of sea fan coral, *Gorgonia ventalina*, in the Florida Keys. Marine Biology 155, 281-292.
Croquer A., Weil E. (2009) Changes in Caribbean coral disease prevalence after the 2005 bleaching event. Dis Aquat Organ 87, 33-43.
Császár N. B. M., Seneca F. O., van Oppen M. J. H. (2009) Variation in antioxidant gene expression in the scleractinian coral *Acropora millepora* under laboratory thermal stress. Marine Ecology Progress Series 392, 93-102.
Cunning R., Baker A. C. (2013) Excess algal symbionts increase the susceptibility of reef corals to bleaching. Nature Climate Change 3, 259-262.

Cunning R., Baker A. C. (2014) Not just who, but how many: the importance of partner abundance in reef coral symbioses. Frontiers in Microbiology 5, 400.
Cunning R., Silverstein R. N., Baker A. C. (2015a) Investigating the causes and consequences of symbiont shuffling in a multi-partner reef coral symbiosis under environmental change. Proceedings Biological Sciences 282, 20141725.
Cunning R., Vaughan N., Gillette P., *et al.* (2015b) Dynamic regulation of partner abundance mediates response of reef coral symbioses to environmental change. Ecology 96, 1411-1420.
Cunning R., Yost D. M., Guarinello M. L., Putnam H. M., Gates R. D. (2015c) Variability of *Symbiodinium* communities in waters, sediments, and corals of thermally distinct reef pools in American Samoa. PLoS One 10, e0145099.
Danielsen F., Sorensen M. K., Olwig M. F., *et al.* (2005) The Asian tsunami: a protective role for coastal vegetation. Science 310, 643.
Dash B., Metz R., Huebner H. J., Porter W., Phillips T. D. (2007) Molecular characterization of two superoxide dismutases from *Hydra vulgaris*. Gene 387, 93-108.
Dash B., Phillips T. D. (2012) Molecular characterization of a catalase from *Hydra vulgaris*. Gene 501, 144-152.
Daszak P., Cunningham A. A., Hyatt A. D. (2001) Anthropogenic environmental change and the emergence of infectious diseases in wildlife. Acta Tropica 78, 103-116.
de Roij J., MacColl A. D. C. (2012) Consistent differences in macroparasite community composition among populations of three-spined sticklebacks, *Gasterosteus aculeatus* L. Parasitology 139, 1478-1491.
De'ath G., Fabircius K. (2010) Water quality as a regional driver of coral biodiversity and macroalgae on the Great Barrier Reef. Ecological Applications 20, 840-850.
De'ath G., Fabricius K. E., Sweatman H., Puotinen M. (2012) The 27-year decline of coral cover on the Great Barrier Reef and its causes. Proceedings of the National Academy of Sciences of the United States of America 109, 17995-17999.
Delgado M. A., Elmaoued R. A., Davis A. S., Kyei G., Deretic V. (2008) Toll-like receptors control autophagy. EMBO J 27, 1110-1121.
Deretic V., Levine B. (2009) Autophagy, immunity, and microbial adaptations. Cell Host & Microbe 5, 527-549.
DeSalvo M. K., Voolstra C. R., Sunagawa S., *et al.* (2008) Differential gene expression during thermal stress and bleaching in the Caribbean coral *Montastraea faveolata*. Molecular Ecology Notes 17, 3952-3971.
Detournay O., Schnitzler C. E., Poole A., Weis V. M. (2012) Regulation of cnidarian-dinoflagellate mutualisms: Evidence that activation of a host TGFbeta innate immune pathway promotes tolerance of the symbiont. Developmental & Comparative Immunology 38, 525-537.
Detournay O., Weis V. M. (2011) Role of the sphingosine rheostat in the regulation of cnidarian-dinoflagellate symbioses. The Biological Bulletin 221, 261-269.
Dheilly N. M., Raftos D. A., Haynes P. A., Smith L. C., Nair S. V. (2013) Shotgun proteomics of coelomic fluid from the purple sea urchin, *Strongylocentrotus purpuratus*. Developmental & Comparative Immunology 40, 35-50.
Domisch S., JÄHnig S. C., Haase P. (2011) Climate-change winners and losers: stream macroinvertebrates of a submontane region in Central Europe. Freshwater Biology 56, 2009-2020.

Dong C. M., Li Z. R., Alvarez R., Feng X. H., Goldschmidt-Clermont P. J. (2000) Microtubule binding to Smads may regulate TGF beta activity. Molecular Cell 5, 27-34.
Dove S., Ortiz J. C., Enríquez S., *et al.* (2006) Response of holosymbiont pigments from the scleractinian coral *Montipora monasteriata* to short-term heat stress. Limnology and Oceanography 51, 1149-1158.
Edinger E. N., Jompa J., Limmon G. v., Widjatmoko W., Risk M. J. (1998) Reef degradation and coral biodiversity in Indonesia: effects of land-based pollution, destructive fishing practices and changes over time. Marine Pollution Bulletin 36, 617-630.
Eisenberg-Lerner A., Bialik S., Simon H. U., Kimchi A. (2009) Life and death partners: apoptosis, autophagy and the cross-talk between them. Cell Death and Differentiation 16, 966-975.
Evans R., Patzak I., Svensson L., *et al.* (2009) Integrins in immunity. Journal of Cell Science 122, 215-225.
Feder M. E., Hofmann G. E. (1999) Heat-shock proteins, molecular chaperones, and the stress response: evolutionary and ecological physiology. Annual Review of Physiology 61, 243-282.
Foden W. B., Butchart S. H., Stuart S. N., *et al.* (2013) Identifying the world's most climate change vulnerable species: a systematic trait-based assessment of all birds, amphibians and corals. PLoS One 8, e65427.
Forman H. J., Torres M. (2002) Reactive oxygen species and cell signaling: respiratory burst in macrophage signaling. American Journal of Respiratory and Critical Care Medicine 166, S4-8.
Franzenburg S., Fraune S., Kunzel S., *et al.* (2012) MyD88-deficient *Hydra* reveal an ancient function of TLR signaling in sensing bacterial colonizers. Proceedings of the National Academy of Sciences of the United States of America 109, 19374-19379.
French S. S., Moore M. C., Demas G. E. (2009) Ecological immunology: The organism in context. Integrative and Comparative Biology 49, 246-253.
Fuess L. E., Eisenlord M. E., Closek C. J., *et al.* (2015) Up in arms: Immune and nervous system response to sea star wasting disease. PLoS One 10, e0133053.
Fuess L. E., Pinzon C. J., Weil E., Grinshpon R. D., Mydlarz L. D. (2017) Life or death: disease-tolerant coral species activate autophagy following immune challenge. Proceedings Biological Sciences 284.
Fuess L. E., Pinzon C. J., Weil E., Mydlarz L. D. (2016) Associations between transcriptional changes and protein phenotypes provide insights into immune regulation in corals. Developmental & Comparative Immunology 62, 17-28.
Fulda S., Gorman A. M., Hori O., Samali A. (2010) Cellular stress responses: cell survival and cell death. International Journal of Cell Biology 2010, 214074.
Ghosh J., Man Lun C., Majeske A. J., *et al.* (2011) Invertebrate immune diversity. Developmental & Comparative Immunology 35, 959-974.
Glynn P. W. (1993) Coral-reef bleaching - ecological perspectives. Coral Reefs 12, 1-17.
Gomes L. C., Dikic I. (2014) Autophagy in antimicrobial immunity. Molecular Cell 54, 224-233.
Grabherr M. G., Haas B. J., Yassour M., *et al.* (2011) Full-length transcriptome assembly from RNA-Seq data without a reference genome. Nature Biotechnology 29, 644-U130.
Graham A. L., Shuker D. M., Pollitt L. C., *et al.* (2011) Fitness consequences of immune responses: strengthening the empirical framework for ecoimmunology. Functional Ecology 25, 5-17.

Graham N. A. J., Nash K. L. (2013) The importance of structural complexity in coral reef ecosystems. Coral Reefs 32, 315-326.
Greijer A. E., van der Wall E. (2004) The role of hypoxia inducible factor 1 (HIF-1) in hypoxia induced apoptosis. Journal of Clinical Pathology 57, 1009-1014.
Grottoli A. G., Warner M. E., Levas S. J., *et al.* (2014) The cumulative impact of annual coral bleaching can turn some coral species winners into losers. Global Change Biol 20, 3823-3833.
Gwynn D., Callaghan A., Gorham J., Walters K. F. A., Fellowes M. D. E. (2005) Resistance is costly: trade-offs between immunity, fecundity, and survival in the pea aphid. Proceedings: Biological Sciences 272, 1803–1808.
Haas B. J., Papanicolaou A., Yassour M., *et al.* (2013) De novo transcript sequence reconstruction from RNA-seq using the Trinity platform for reference generation and analysis. Nature Protocols 8, 1494-1512.
Halpern B. S., Selkoe K. A., Micheli F., Kappel C. V. (2007) Evaluating and ranking the vulnerability of global marine ecosystems to anthropogenic threats. Conservation Biology 21, 1301-1315.
Halpern B. S., Walbridge S., Selkoe K. A., *et al.* (2008) A global map of human impact on marine ecosystems. Science 319, 948-952.
Harvell C. D., Kim K., Burkholder J. M., *et al.* (1999) Emerging marine diseases--climate links and anthropogenic factors. Science 285, 1505-1510.
Harvell C. D., Mitchell C. E., Ward J. R., *et al.* (2002) Climate warming and disease risks for terrestrial and marine biota. Science 296, 2158-2162.
Harvell D., Aronson R., Baron N., *et al.* (2004) The rising tide of ocean diseases: unsolved problems and research priorities. Frontiers in Ecology and the Environment 2, 375-382.
Hawley D. M., Altizer S. M. (2011) Disease ecology meets ecological immunology: understanding the links between organismal immunity and infection dynamics in natural populations. Functional Ecology 25, 48-60.
Hayes M. L., Eytan R. I., Hellberg M. E. (2010) High amino acid diversity and positive selection at a putative coral immunity gene (tachylectin-2). BMC Evolutionary Biology 10, 150.
Heath-Heckman E. A., Gillette A. A., Augustin R., *et al.* (2014) Shaping the microenvironment: evidence for the influence of a host galaxin on symbiont acquisition and maintenance in the squid-vibrio symbiosis. Environmental Microbiology 16, 3669-3682.
Hentschel U., Steinert M., Hacker J. (2000) Common molecular mechanisms of symbiosis and pathogenesis. Trends in Microbiology 8, 226-231.
Hodge M. R., Ranger A. M., Charles de la Brousse F., *et al.* (1996) Hyperproliferation and dysregulation of IL-4 expression in NF-ATp-deficient mice. Immunity 4, 397-405.
Hoegh-Guldberg O., Bruno J. F. (2010) The impact of climate change on the world's marine ecosystems. Science 328, 1523-1528.
Hoegh-Guldberg O., Mumby P. J., Hooten A. J., *et al.* (2007) Coral reefs under rapid climate change and ocean acidification. Science 318, 1737-1742.
Hoffmann A. A., Sgro C. M. (2011) Climate change and evolutionary adaptation. Nature 470, 479-485.
Holmlund C. M., Hammer M. (1999) Ecosystem services generated by fish populations. Ecological Economics 29, 253–268.
Hughes T. P. (1994) Catastrophes, phase shifts, and large-scale degradation of a Caribbean coral reef. Science 265, 1547-1551.

Hughes T. P., Baird A. H., Bellwood D. R., *et al.* (2003) Climate change, human impacts, and the resilience of coral reefs. Science 301, 929-933.
Hughes T. P., Rodrigues M. J., Bellwood D. R., *et al.* (2007) Phase shifts, herbivory, and the resilience of coral reefs to climate change. Current Biology 17, 360-365.
Inohara N., Chamaillard M., McDonald C., Nunez G. (2005) NOD-LRR proteins: role in host-microbial interactions and inflammatory disease. Annual Review of Biochemistry 74, 355-383.
Iwanaga S., Lee B. L. (2005) Recent advances in the innate immunity of invertebrate animals. Journal of Biochemistry and Molecular Biology 38, 128-150.
Jackson J. B., Kirby M. X., Berger W. H., *et al.* (2001) Historical overfishing and the recent collapse of coastal ecosystems. Science 293, 629-637.
Janeway C. A., Jr., Medzhitov R. (2002) Innate immune recognition. Annual Review of Immunology 20, 197-216.
Jensen P. R., Harvell C. D., Wirtz K., Fenical W. (1996) Antimicrobial activity of extracts of Caribbean gorgonian corals. Marine Biology 125, 411-419.
Jiggins F. M., Kim K. W. (2006) Contrasting evolutionary patterns in *Drosophila* immune receptors. Journal of Molecular Evolution 63, 769-780.
Jiggins F. M., Kim K. W. (2007) A screen for immunity genes evolving under positive selection in *Drosophila*. Journal of Evolutionary Biology 20, 965-970.
Jin Y. K., Lundgren P., Lutz A., *et al.* (2016) Genetic markers for antioxidant capacity in a reef-building coral. Scientific Advances 2, e1500842.
Johnson N. C., Graham J. H., Smith F. A. (1997) Functioning of mycorrhizal associations along the mutualism-parasitism continuum. The New Phytologist 135, 575-586.
Kapela W., Lasker H. R. (1999) Size-dependent reproduction in the Caribbean gorgonian *Pseudoplexaura porosa*. Marine Biology 135, 107-114.
Kaufman S. H. E. (1990) Heat shock proteins and the immune response. Immunology Today 11, 129-136.
Kawabata S., Iwanaga S. (1999) Role of lectins in the innate immunity of horseshoe crab. Deveolopmental & Comparative Immunology 23, 391-400.
Kawai T., Akira S. (2011) Toll-like receptors and their crosstalk with other innate receptors in infection and immunity. Immunity 34, 637-650.
Kawai T., Sato S., Ishii K. J., *et al.* (2004) Interferon-alpha induction through Toll-like receptors involves a direct interaction of IRF7 with MyD88 and TRAF6. Nature Immunology 5, 1061-1068.
Kenkel C. D., Meyer E., Matz M. V. (2013) Gene expression under chronic heat stress in populations of the mustard hill coral (*Porites astreoides*) from different thermal environments. Molecular Ecology 22, 4322-4334.
Kent W. J. (2002) BLATL: the BLAST-like alignment tool. Genome Research 12, 656-664.
Kilpatrick A. M., Briggs C. J., Daszak P. (2010) The ecology and impact of chytridiomycosis: an emerging disease of amphibians. Trends in Ecology and Evolution 25, 109-118.
Kim J., Kundu M., Viollet B., Guan K. L. (2011) AMPK and mTOR regulate autophagy through direct phosphorylation of Ulk1. Nature Cell Biology 13, 132-141.
Kobasa D., Jones S. M., Shinya K., *et al.* (2007) Aberrant innate immune response in lethal infection of macaques with the 1918 influenza virus. Nature 445, 319-323.
Koprivnikar J., Macrogliese D. J., Rohr J. R., Orlofske S. A., Raffel T. R. (2012) Macroparasite infections of amphibians: What can they tell us? EcoHealth 9, 342-360.

Kroemer G., Levine B. (2008) Autophagic cell death: the story of a misnomer. Nature Reviews Molecular Cell Biology 9, 1004-1010.
Kroemer G., Marino G., Levine B. (2010) Autophagy and the integrated stress response. Molecular Cell 40, 280-293.
Kuchroo V. K., Umetsu D. T., DeKruyff R. H., Freeman G. J. (2003) The TIM gene family: emerging roles in immunity and disease. Nature Reviews Immunology 3, 454-462.
Kulkarni A. B., Huh C. G., Becker D., *et al.* (1993) Transforming growth factor beta 1 null mutation in mice causes excessive inflammatory response and early death. Proceedings of the National Academy of Sciences of the United States of America 90, 770-774.
Kumar H., Kawai T., Akira S. (2011) Pathogen Recognition by the Innate Immune System. International Reviews of Immunology 30, 16-34.
Kvennefors E. C., Leggat W., Kerr C. C., *et al.* (2010) Analysis of evolutionarily conserved innate immune components in coral links immunity and symbiosis. Developmental & Comparative Immunology 34, 1219-1229.
Labour M. N., Riffault M., Christensen S. T., Hoey D. A. (2016) TGF beta 1-induced recruitment of human bone mesenchymal stem cells is mediated by the primary cilium in a SMAD3-dependent manner. Scientific Reports 6.
LaJeunesse T. C., Smith R., Walther M., *et al.* (2010) Host-symbiont recombination versus natural selection in the response of coral-dinoflagellate symbioses to environmental disturbance. Proceedings: Biological Sciences 277, 2925-2934.
Langfelder P., Horvath S. (2008) WGCNA: an R package for weighted correlation network analysis. BMC Bioinformatics 9, 559.
Lasker H. R., Sanchez J. A. (2002) Allometry and astogeny of modular organisms. In: Reproductive Biology of Invertebrates (ed. Hughes R. N.), pp. 207-253. Wiley, New York.
Lavine M. D., Strand M. R. (2002) Insect hemocytes and their role in immunity. Insect Biochemistry and Molecular Biology 32, 1295-1309.
Lazzaro B. P., Sackton T. B., Clark A. G. (2006) Genetic variation in *Drosophila melanogaster* resistance to infection: a comparison across bacteria. Genetics 174, 1539-1554.
Lazzaro B. P., Sceurman B. K., Clark A. G. (2004) Genetic basis of natural variation in *D. melanogaster* antibacterial immunity. Science 303, 1873-1876.
Lee K. A. (2006) Linking immune defenses and life history at the levels of the individual and the species. Integrative and Comparative Biology 46, 1000-1015.
Lee Y. S., Park J. S., Kim J. H., *et al.* (2011) Smad6-specific recruitment of Smurf E3 ligases mediates TGF-beta1-induced degradation of MyD88 in TLR4 signalling. Nature Communications 2, 460.
Letterio J. J., Roberts A. B. (1998) Regulation of immune responses by TGF-beta. Annual Review of Immunology 16, 137-161.
Levine B., Mizushima N., Virgin H. W. (2011) Autophagy in immunity and inflammation. Nature 469, 323-335.
Levine B., Yuan J. (2005) Autophagy in cell death: an innocent convict? The Journal of Clinical Investigation 115, 2679-2688.
Libro S., Kaluziak S. T., Vollmer S. V. (2013) RNA-seq profiles of immune related genes in the staghorn coral *Acropora cervicornis* infected with white band disease. PLoS One 8, e81821.
Libro S., Vollmer S. V. (2016) Genetic signature of resistance to white band disease in the Caribbean staghorn coral *Acropora cervicornis*. PLoS One 11, e0146636.

Linares C., Coma R., Garrabou J., Diaz D., Zabala M. (2008) Size distribution, density and disturbance in two Mediterranean gorgonians: *Paramuricea clavata* and *Eunicella singularis*. Journal of Applied Ecology 45, 688-699.
Liu H., Jiravanichpaisal P., Cerenius L., *et al.* (2007) Phenoloxidase is an important component of the defense against *Aeromonas hydrophila* infection in a crustacean, *Pacifastacus leniusculus*. Journal of Biological Chemistry 282.
Liu Y., Schiff M., Czymmek K., *et al.* (2005) Autophagy regulates programmed cell death during the plant innate immune response. Cell 121, 567-577.
Lotze H. K., Lenihan H. S., Bourque B. J., *et al.* (2006) Depletion, degradation, and recovery potential of estuaries and coastal seas. Science 312, 1806-1809.
Love M. I., Huber W., Anders S. (2014) Moderated estimation of fold change and dispersion for RNA-seq data with DESeq2. Genome Biology 15, 550.
Lu Y. C., Yeh W. C., Ohashi P. S. (2008) LPS/TLR4 signal transduction pathway. Cytokine 42, 145-151.
Magnadóttir B. (2006) Innate immunity of fish (overview). Fish and Shellfish Immunology 20, 137-151.
Maiuri M. C., Zalckvar E., Kimchi A., Kroemer G. (2007) Self-eating and self-killing: crosstalk between autophagy and apoptosis. Nature Reviews, Molecular and Cell Biology 8, 741-752.
Man S. M., Kanneganti T. D. (2016) Converging roles of caspases in inflammasome activation, cell death and innate immunity. Nature Reviews Immunology 16, 7-21.
Mann R., Harding J. M., Southworth M. J. (2009) Reconstructing pre-colonial oyster demographics in the Chesapeake Bay, USA. Estuarine Coastal and Shelf Science 85, 217-222.
Mann W. T., Beach-Letendre J., Mydlarz L. D. (2014) Interplay between proteases and protease inhibitors in the sea fan—*Aspergillus pathosystem*. Marine Biology 161, 2213-2220.
Marino G., Niso-Santano M., Baehrecke E. H., Kroemer G. (2014) Self-consumption: the interplay of autophagy and apoptosis. Nature Reviews Molecular Cell Biology 15, 81-94.
Martin L. B., Hawley D. M., Ardia D. R. (2011) An introduction to ecological immunology. Functional Ecology 25, 1-4.
Martinon F., Tschopp J. (2005) NLRs join TLRs as innate sensors of pathogens. Trends in Immunology 26, 447-454.
Massague J. (1998) TGF-beta signal transduction. Annual Review of Biochemistry 67, 753-791.
Mayor A., Martinon F., De Smedt T., Petrilli V., Tschopp J. (2007) A crucial function of SGT1 and HSP90 in inflammasome activity links mammalian and plant innate immune responses. Nature Immunology 8, 497-503.
Medzhitov R. (2007) Recognition of microorganisms and activation of the immune response. Nature 449, 819-826.
Medzhitov R., Preston-Hurlburt P., Kopp E., *et al.* (1998) MyD88 Is an Adaptor Protein in the hToll/IL-1 Receptor Family Signaling Pathways. Molecular Cell 2, 253–258.
Merle P. L., Sabourault C., Richier S., Allemand D., Furla P. (2007) Catalase characterization and implication in bleaching of a symbiotic sea anemone. Free Radical Biology & Medicine 42, 236-246.
Mihaylova M. M., Shaw R. J. (2011) The AMPK signalling pathway coordinates cell growth, autophagy and metabolism. Nature Cell Biology 13, 1016-1023.

Miller D. J., Ball E. E., Forêt S., Satoh N. (2011) Coral genomics and transcriptomics — Ushering in a new era in coral biology. Journal of Experimental Marine Biology and Ecology 408, 114-119.
Miller D. J., Hemmrich G., Ball E. E., *et al.* (2007) The innate immune repertoire in Cnidaria--ancestral complexity and stochastic gene loss. Genome Biology 8, R59.
Mizushima N., Komatsu M. (2011) Autophagy: renovation of cells and tissues. Cell 147, 728-741.
Molina-Cruz A., Garver L. S., Alabaster A., *et al.* (2013) The human malaria parasite Pfs47 gene mediates evasion of the mosquito immune system. Science 340, 984-987.
Moy R. H., Cherry S. (2013) Antimicrobial autophagy: a conserved innate immune response in *Drosophila*. Journal of Innate Immunity 5, 444-455.
Multerer K. A., Smith L. C. (2004) Two cDNAs from the purple sea urchin, *Strongylocentrotus purpuratus*, encoding mosaic proteins with domains found in factor H, factor I, and complement components C6 and C7. Immunogenetics 56, 89-106.
Murphy G. E., Romanuk T. N. (2014) A meta-analysis of declines in local species richness from human disturbances. Ecol Evol 4, 91-103.
Muscatine L. (1984) Fate of photosynthetically fixed carbon in light and shade-adapted colonies of the symbiotic coral, *Stylophora pistillata*. Proceedings of the Royal Society of London, Series B: Biological Sciences 222, 181-202.
Muscatine L. (1990) The role of symbiotic algae in carbon and energy flux in reef corals. Elsevier Science Publishing Company, Inc., Amsterdam, The Netherlands.
Muscatine L., Porter J. W. (1977) Reef corals - mutualistic symbioses adapted to nutrient-poor environments. Bioscience 27, 454-460.
Mydlarz L. D., Couch C. S., Weil E., Smith G., Harvell C. D. (2009) Immune defenses of healthy, bleached and diseased *Montastraea faveolata* during a natural bleaching event. Diseases of Aquatic Organisms 87, 67-78.
Mydlarz L. D., Fuess L., Mann W., Pinzón J. H., Gochfeld D. J. (2016) Cnidarian Immunity: From Genomes to Phenomes. In: The Cnidaria, Past, Present and Future (eds. Goffredo S.,Dubinsky Z.), pp. 441-466. Springer, Netherlands.
Mydlarz L. D., Harvell C. D. (2007) Peroxidase activity and inducibility in the sea fan coral exposed to a fungal pathogen. Comparative Biochemistry and Physiology, Part A Molecular & Integrative Physiology 146, 54-62.
Mydlarz L. D., Holthouse S. F., Peters E. C., Harvell C. D. (2008) Cellular responses in sea fan corals: granular amoebocytes react to pathogen and climate stressors. PLoS One 3, e1811.
Mydlarz L. D., Jones L. E., Harvell C. D. (2006) Innate immunity environmental drivers and disease ecology of marine and freshwater invertebrates. Annual Review of Ecology Evolution and Systematics 37, 251-288.
Mydlarz L. D., McGinty E. S., Harvell C. D. (2010) What are the physiological and immunological responses of coral to climate warming and disease? Journal of Experimental Biology 213, 934-945.
Mydlarz L. D., Palmer C. V. (2011) The presence of multiple phenoloxidases in Caribbean reef-building corals. Comparative Biochemistry and Physiology A Molecular & Integrative Physiology 159, 372-378.
Nakagawa I., Amano A., Mizushima N., *et al.* (2004) Autophagy defends cells against invading group A *Streptococcus*. Science 306, 1037-1040.

Nakamoto M., Moy R. H., Xu J., *et al.* (2012) Virus recognition by Toll-7 activates antiviral autophagy in *Drosophila*. Immunity 36, 658-667.
Nappi A. J., Christensen B. M. (2005) Melanogenesis and associated cytotoxic reactions: Applications to insect innate immunity. Insect Biochemistry and Molecular Biology 35, 443-459.
Nauseef W. M. (2007) How human neutrophils kill and degrade microbes: an integrated view. Immunological Reviews 219, 88-102.
Ndungu F. M., Urban B. C., Marsh K., Langhorne J. (2005) Regulation of immune response by *Plasmodium*-infected red blood cells. Parasite Immunology 27, 373-384.
Nelson R. E., Fessler L. I., Takagi Y., *et al.* (1994) Peroxidasin: a novel enzyme-matrix protein of *Drosophila* development. EMBO J 13, 3438-3447.
Newton K., Dixit V. M. (2012) Signaling in innate immunity and inflammation. Cold Spring Harb Perspect Biol 4.
Nishikawa A., Katoh M., Sakai K. (2003) Larval settlement rates and gene flow of broadcast-spawning (*Acropora tenuis*) and planula-brooding (*Stylophora pistillata*) corals. Marine Ecology Progress Series 256, 87-97.
Nugues M. M. (2002) Impact of a coral disease outbreak on coral communities in St. Lucia: What and how much has been lost? Marine Ecology Progress Series 229, 69-71.
O'Shea J. J., Plenge R. (2012) JAK and STAT signaling molecules in immunoregulation and immune-mediated disease. Immunity 36, 542-550.
Ocampo I. D., Zarate-Potes A., Pizarro V., *et al.* (2015) The immunotranscriptome of the Caribbean reef-building coral *Pseudodiploria strigosa*. Immunogenetics 67, 515-530.
Odum H. T., Odum E. P. (1955) Trophic structure and productivity of a windward coral reef community on Eniwetok Atoll. Ecological Monographs 25, 291-320.
Ogata M., Hino S., Saito A., *et al.* (2006) Autophagy is activated for cell survival after endoplasmic reticulum stress. Molecular Cell Biology 26, 9220-9231.
Palmer C. V., Bythell J. C., Willis B. L. (2010) Levels of immunity parameters underpin bleaching and disease susceptibility of reef corals. FASEB Journal 24, 1935-1946.
Palmer C. V., McGinty E. S., Cummings D. J., *et al.* (2011) Patterns of coral ecological immunology: variation in the responses of Caribbean corals to elevated temperature and a pathogen elicitor. Journal of Experimental Biology 214, 4240-4249.
Palmer C. V., Modi C. K., Mydlarz L. D. (2009) Coral fluorescent proteins as antioxidants. PLoS One 4, 7298-7298.
Palmer C. V., Mydlarz L. D., Willis B. L. (2008) Evidence of an inflammatory-like response in non-normally pigmented tissues of two scleractinian corals. Proceedings: Biological Sciences 275, 2687-2693.
Palmer C. V., Traylor-Knowles N. (2012) Towards an integrated network of coral immune mechanisms. Proceedings: Biological Sciences 279, 4106-4114.
Palmer T. M., Brody A. K. (2013) Enough is enough: the effects of symbiotic ant abundance on herbivory, growth, and reproduction in an African acacia. Ecology 94, 683-691.
Palumbi S. R., Barshis D. J., Traylor-Knowles N., Bay R. A. (2014) Mechanisms of reef coral resistance to future climate change. Science 344, 895-898.
Pandolfi J. M., Bradbury R. H., Sala E., *et al.* (2003) Global trajectories of the long-term decline of coral reef ecosystems. Science 301, 955-958.

Park S. Y., Bae D. J., Kim M. J., Piao M. L., Kim I. S. (2012) Extracellular low pH modulates phosphatidylserine-dependent phagocytosis in macrophages by increasing stabilin-1 expression. Journal of Biological Chemistry 287, 11261-11271.
Pauly D., Watson R., Alder J. (2005) Global trends in world fisheries: impacts on marine ecosystems and food security. Philosophical transactions of the Royal Society of London. Series B, Biological sciences 360, 5-12.
Perez-Ortega S., Rios Ade L., Crespo A., Sancho L. G. (2010) Symbiotic lifestyle and phylogenetic relationships of the bionts of *Mastodia tessellata* (Ascomycota, *incertae sedis*). American Journal of Botany 97, 738-752.
Pimm S. L., Jenkins C. N., Abell R., *et al.* (2014) The biodiversity of species and their rates of extinction, distribution, and protection. Science 344.
Pinzon C. J., Beach-Letendre J., Weil E., Mydlarz L. D. (2014a) Relationship between phylogeny and immunity suggests older Caribbean coral lineages are more resistant to disease. PLoS One 9, e104787.
Pinzon C. J., Dornberger L., Beach-Letendre J., Weil E., Mydlarz L. D. (2014b) The link between immunity and life history traits in scleractinian corals. PeerJ 2, e628.
Pinzon J. H., Kamel B., Burge C. A., *et al.* (2015) Whole transcriptome analysis reveals changes in expression of immune-related genes during and after bleaching in a reef-building coral. Royal Society Open Science 2, 140214-140214.
Poellinger L., Lendahl U. (2008) Modulating Notch signaling by pathway-intrinsic and pathway-extrinsic mechanisms. Current Opinion in Genetics & Development 18, 449-454.
Poole A. Z., Weis V. M. (2014) TIR-domain-containing protein repertoire of nine anthozoan species reveals coral-specific expansions and uncharacterized proteins. Developmental & Comparative Immunoloy 46, 480-488.
Pratchett M. S., McCowan D., Maynard J. A., Heron S. F. (2013) Changes in bleaching susceptibility among corals subject to ocean warming and recurrent bleaching in Moorea, French Polynesia. PLoS One 8, e70443.
Putnam N. H., Srivastava M., Hellsten U., *et al.* (2007) Sea anemone genome reveals ancestral eumetazoan gene repertoire and genomic organization. Science 317, 86-94.
Raymundo L. J., Rosell K. B., Reboton C. T., Kaczmarsky L. (2005) Coral diseases on Philippine reefs: genus *Porites* is a dominant host. Diseases of Aquatic Organisms 64, 181-191.
Renema W., Bellwood D. R., Braga J. C., *et al.* (2008) Hopping hotspots: global shifts in marine biodiversity. Science 321, 654-657.
Richier S., Merle P. L., Furla P., *et al.* (2003) Characterization of superoxide dismutases in anoxia- and hyperoxia-tolerant symbiotic cnidarians. Biochimica et Biophysica Acta 1621, 84-91.
Rijiravanich A., Browdy C. L., Withyachumnarnkul B. (2008) Knocking down caspase-3 by RNAi reduces mortality in Pacific white shrimp *Penaeus* (Litopenaeus) *vannamei* challenged with a low dose of white-spot syndrome virus. Fish & Shellfish Immunology 24, 308-313.
Roberts C. M. (1995) Effects of fishing on the ecosystem structure of coral-reefs. Conservation Biology 9, 988-995.
Roff G., Mumby P. J. (2012) Global disparity in the resilience of coral reefs. Trends in Ecology and Evolution 27, 404-413.
Rolff J., Siva-Jothy M. T. (2003) Invertebrate ecological immunology. Science 301, 472-475.

Rosenstiel P., Sina C., End C., *et al.* (2007) Regulation of DMBT1 via NOD2 and TLR4 in Intestinal Epithelial Cells Modulates Bacterial Recognition and Invasion. The Journal of Immunology 178, 8203-8211.
Roth M. S., Deheyn D. D. (2013) Effects of cold stress and heat stress on coral fluorescence in reef-building corals. Scientific Reports 3, 1421.
Ruckelshaus M., Doney S. C., Galindo H. M., *et al.* (2013) Securing marine ecosystem services in the face of climate change. Marine Policy 40, 154–159.
Sadd B. M., Schmid-Hempel P. (2009) Principles of ecological immunology. Evolutionary Applications 2, 113-121.
Sanchez J. A., Lasker H. R. (2003) Patterns of morphological integration in marine modular organisms: supra-module organization in branching octocoral colonies. Proceedings Biological Science 270, 2039-2044.
Schrader M., Reuber B. E., Morrell J. C., *et al.* (1998) Expression of PEX11beta mediates peroxisome proliferation in the absence of extracellular stimuli. Journal of Biological Chemistry 273, 29607-29614.
Schutte V. G. W., Selig E. R., Bruno J. F. (2010) Regional spatio-temporal trends in Caribbean coral reef benthic communities. Marine Ecology Progress Series 402, 115-122.
Schwarz R. S., Hodes-Villamar L., Fitzpatrick K. A., *et al.* (2007) A gene family of putative immune recognition molecules in the hydroid *Hydractinia*. Immunogenetics 59, 233-246.
Sebens K. P. (1994) Biodiversity of coral-reefs - what are we losing and why. American Zoologist 34, 115-133.
Seppala O. (2015) Natural selection on quantitative immune defence traits: a comparison between theory and data. Journal of Evolutionary Biology 28, 1-9.
Shelly S., Lukinova N., Bambina S., Berman A., Cherry S. (2009) Autophagy is an essential component of *Drosophila* immunity against vesicular stomatitis virus. Immunity 30, 588-598.
Shen H. M., Codogno P. (2011) Autophagic cell death: Loch Ness monster or endangered species? Autophagy 7, 457-465.
Shi C. S., Kehrl J. H. (2008) MyD88 and Trif target Beclin 1 to trigger autophagy in macrophages. Journal of Biological Chemistry 283, 33175-33182.
Shimada T., Park B. G., Wolf A. J., *et al.* (2010) *Staphylococcus aureus* evades lysozyme-based peptidoglycan digestion that links phagocytosis, inflammasome activation, and IL-1beta secretion. Cell Host Microbe 7, 38-49.
Shinzato C., Shoguchi E., Kawashima T., *et al.* (2011) Using the *Acropora digitifera* genome to understand coral responses to environmental change. Nature 476, 320-U382.
Silverstein R. N., Correa A. M. S., Baker A. C. (2012) Specificity is rarely absolute in coral-algal symbiosis: implications for coral response to climate change. Proceedings of the Royal Society B-Biological Sciences 279, 2609-2618.
Simmons K. J., Nde P. N., Kleshchenko Y. Y., Lima M. F., Villalta F. (2006) Stable RNA interference of host thrombospondin-1 blocks *Trypanosoma cruzi* infection. FEBS Letters 580, 2365-2370.
Smith K. F., Sax D. F., Lafferty K. D. (2006) Evidence for the role of infectious disease in species extinction and endangerment. Conservation Biology 20, 1349-1357.
Smith-Keune C., Dove S. (2008) Gene expression of a green fluorescent protein homolog as a host-specific biomarker of heat stress within a reef-building coral. Marine Biotechnology (NY) 10, 166-180.

Somero G. N. (2010) The physiology of climate change: how potentials for acclimatization and genetic adaptation will determine 'winners' and 'losers'. Journal of Experimental Biology 213, 912-920.
Spurgeon J. P. G. (1992) The economic valuation of coral reefs. Marine Pollution Bulletin 24, 529-536.
Stat M., Bird C. E., Pochon X., *et al.* (2011) Variation in *Symbiodinium* ITS2 sequence assemblages among coral colonies. PLoS One 6, e15854.
Sutherland K. P., Porter J. W., Torres C. (2004) Disease and immunity in Caribbean and Indo-Pacific zooxanthellate corals. Marine Ecology Progress Series 266, 273-302.
Syvitski J. P., Vorosmarty C. J., Kettner A. J., Green P. (2005) Impact of humans on the flux of terrestrial sediment to the global coastal ocean. Science 308, 376-380.
Takeuchi O., Akira S. (2010) Pattern recognition receptors and inflammation. Cell 140, 805-820.
Tang D., Kang R., Coyne C. B., Zeh H. J., Lotze M. T. (2012) PAMPs and DAMPs: signal 0s that spur autophagy and immunity. Immunological Reviews 249, 158-175.
Tchernov D., Kvitt H., Haramaty L., *et al.* (2011) Apoptosis and the selective survival of host animals following thermal bleaching in zooxanthellate corals. Proceedings of the National Academy of Sciences of the United States of America 108, 9905-9909.
Thomas P. D., Campbell M. J., Kejariwal A., *et al.* (2003) PANTHER: a library of protein families and subfamilies indexed by function. Genome Research 13, 2129-2141.
Toth K., Stacey G. (2015) Does plant immunity play a critical role during initiation of the legume-rhizobium symbiosis? Frontiers in Plant Science.
Trapnell C., Hendrickson D. G., Sauvageau M., *et al.* (2013) Differential analysis of gene regulation at transcript resolution with RNA-seq. Nature Biotechnology 31, 46-53.
Trapnell C., Pachter L., Salzberg S. L. (2009) TopHat: discovering splice junctions with RNA-Seq. Bioinformatics 25, 1105-1111.
Trapnell C., Williams B. A., Pertea G., *et al.* (2010) Transcript assembly and quantification by RNA-Seq reveals unannotated transcripts and isoform switching during cell differentiation. Nature Biotechnology 28, 511-515.
Travis M. A., Sheppard D. (2014) TGF-beta activation and function in immunity. Annual Review of Immunology 32, 51-82.
Tsirogianni A. K., Moutsopoulos N. M., Moutsopoulos H. M. (2006) Wound healing: immunological aspects. Injury 37 Suppl 1, S5-12.
Underhill D. M., Ozinsky A. (2002) Phagocytosis of microbes: complexity in action. Annual Review of Immunology 20, 825-852.
van de Water J., Chaib De Mares M., Dixon G. B., *et al.* (2018) Antimicrobial and stress responses to increased temperature and bacterial pathogen challenge in the holobiont of a reef-building coral. Mol Ecol.
van der Laan L. J., Dopp E. A., Haworth R., *et al.* (1999) Regulation and functional involvement of macrophage scavenger receptor MARCO in clearance of bacteria in vivo. Journal of Immunology 162, 939-947.
van Woesik R., Sakai K., Ganase A., Loya Y. (2011) Revisiting the winners and the losers a decade after coral bleaching. Marine Ecology Progress Series 434, 67-76.
Vega Thurber R. L., Burkepile D. E., Fuchs C., *et al.* (2014) Chronic nutrient enrichment increases prevalence and severity of coral disease and bleaching. Global Change Biology 20, 544-554.

Verheij M., Bose R., Lin X. H., *et al.* (1996) Requirement for ceramide-initiated SAPK/JNK signalling in stress-induced apoptosis. Nature 380, 75-79.
Vicencio J. M., Galluzzi L., Tajeddine N., *et al.* (2008) Senescence, apoptosis or autophagy? When a damaged cell must decide its path--a mini-review. Gerontology 54, 92-99.
Vidal-Dupiol J., Dheilly N. M., Rondon R., *et al.* (2014) Thermal stress triggers broad *Pocillopora damicornis* transcriptomic remodeling, while *Vibrio coralliilyticus* infection induces a more targeted immuno-suppression response. PLoS One 9, e107672.
Vidal-Dupiol J., Ladriere O., Destoumieux-Garzon D., *et al.* (2011a) Innate immune responses of a scleractinian coral to vibriosis. Journal of Biological Chemistry 286, 22688-22698.
Vidal-Dupiol J., Ladriere O., Meistertzheim A. L., *et al.* (2011b) Physiological responses of the scleractinian coral *Pocillopora damicornis* to bacterial stress from *Vibrio coralliilyticus*. Journal of Experimental Biology 214, 1533-1545.
Waghabi M. C., Keramidas M., Feige J. J., Araujo-Jorge T. C., Bailly S. (2005) Activation of transforming growth factor beta by *Trypanosoma cruzi*. Cell Microbiology 7, 511-517.
Walter P., Ron D. (2011) The unfolded protein response: from stress pathway to homeostatic regulation. Science 334, 1081-1086.
Wang B., Qiu Y. L. (2006) Phylogenetic distribution and evolution of mycorrhizas in land plants. Mycorrhiza 16, 299-363.
Ward J. R., Lafferty K. D. (2004) The elusive baseline of marine disease: are diseases in ocean ecosystems increasing? PLoS Biology 2, E120.
Ward J. R., Rypien K. L., Bruno J. F., *et al.* (2006) Coral diversity and disease in Mexico. Disease of Aquatic Organisms 69, 23-31.
Watanabe T., Fukuda I., China K., Isa Y. (2003) Molecular analyses of protein components of the organic matrix in the exoskeleton of two scleractinian coral species. Comparative Biochemistry and Physiology, Part B, Biochemistry & Molecular Biology 136, 767-774.
Watson R. O., Manzanillo P. S., Cox J. S. (2012) Extracellular *M. tuberculosis* DNA targets bacteria for autophagy by activating the host DNA-sensing pathway. Cell 150, 803-815.
Weil E. (2004) Coral reef diseases in the wider Caribbean. In: Coral Health and Disease (eds. Rosenberg E.,Loya Y.), pp. 35-67. Springer, Berlin.
Weil E., Croquer A., Urreiztieta I. (2009a) Temporal variability and impact of coral diseases and bleaching in La Parguera, Puerto Rico from 2003-2007. Caribbean Journal of Science 34, 221-246.
Weil E., Croquer A., Urreiztieta I. (2009b) Yellow band disease compromises the reproductive output of the Caribbean reef-building coral *Montastraea faveolata* (Anthozoa, Scleractinia). Diseases of Aquatic Organisms 87, 45-55.
Weil E., Rogers C. (2011) Coral reef diseases in the Atlantic-Caribbean. In: Coral Reefs: An Ecosystem in Transition (eds. Dubinsky Z.,Stambler N.), pp. 465-491. Springer, Dordrecht.
Weiss Y., Foret S., Hayward D. C., *et al.* (2013) The acute transcriptional response of the coral *Acropora millepora* to immune challenge: expression of GiMAP/IAN genes links the innate immune responses of corals with those of mammals and plants. BMC Genomics 14, 400.
Welker N. C., Habig J. W., Bass B. L. (2007) Genes misregulated in *C. elegans* deficient in Dicer, RDE-4, or RDE-1 are enriched for innate immunity genes. RNA 13, 1090-1102.
Whitten M. M. A., Tew I. F., Lee B. L., Ratcliffe N. A. (2004) A novel role for an insect apolipoprotein (Apolipophorin III) in -1,3-glucan pattern recognition and cellular encapsulation reactions. The Journal of Immunology 172, 2177-2185.

Williams L. M., Fuess L. E., Brennan J. J., *et al.* (2018) A conserved Toll-like receptor-to-NF-kappaB signaling pathway in the endangered coral *Orbicella faveolata*. Developmental & Comparative Immunology 79, 128-136.
Wolenski F. S., Garbati M. R., Lubinski T. J., *et al.* (2011) Characterization of the core elements of the NF-κB signaling pathway of the sea anemone *Nematostella vectensis*. Molecular and cellular biology 31, 1076-1087.
Wood-Charlson E. M., Weis V. M. (2009) The diversity of C-type lectins in the genome of a basal metazoan, *Nematostella vectensis*. Developmental & Comparative Immunology 33, 881-889.
Wright R. M., Aglyamova G. V., Meyer E., Matz M. V. (2015) Gene expression associated with white syndromes in a reef building coral, *Acropora hyacinthus*. BMC Genomics 16, 371.
Wright R. M., Kenkel C. D., Dunn C. E., *et al.* (2017) Intraspecific differences in molecular stress responses and coral pathobiome contribute to mortality under bacterial challenge in *Acropora millepora*. Scientific Reports 7, 2609.
Xu C., Bailly-Maitre B., Reed J. C. (2005) Endoplasmic reticulum stress: cell life and death decisions. Journal of Clinical Investigation 115, 2656-2664.
Xu Y., Fattah E. A., Liu X.-D., Jagannath C., Eissa N. T. (2013) Harnessing of TLR-mediated autophagy to combat mycobacteria in macrophages. Tuberculosis 93, S33-S37.
Xu Y., Jagannath C., Liu X. D., *et al.* (2007) Toll-like receptor 4 is a sensor for autophagy associated with innate immunity. Immunity 27, 135-144.
Yang R. B., Mark M. R., Gray A., *et al.* (1998) Toll-like receptor-2 mediates lipopolysaccharide-induced cellular signalling. Nature 395, 284-288.
Yano T., Mita S., Ohmori H., *et al.* (2008) Autophagic control of listeria through intracellular innate immune recognition in *Drosophila*. Nautre Immunology 9, 908-916.
Yasuda M., Miwa H., Masuda S., *et al.* (2016) Effector-triggered immunity determines host genotype-specific incompatibility in legume-rhizobium symbiosis. Plant and Cell Physiology 57, 1791-1800.
Yoshida H., Jono H., Kai H., Li J. (2005) The tumor suppressor cylindromatosis (CYLD) acts as a negative regulator for toll-like receptor 2 signaling via negative cross-talk with TRAF6 AND TRAF7. J Biol Chem 280, 41111-41121.
Yoshimura A., Muto G. (2011) TGF-beta function in immune suppression. Current Topics in Microbiology and Immunology 350, 127-147.
Yoshimura A., Wakabayashi Y., Mori T. (2010) Cellular and molecular basis for the regulation of inflammation by TGF-beta. Journal of Biochemistry 147, 781-792.
Yoshioka P. M. (1994) Size-specific life history pattern of a shallow-water gorgonian. Journal of Experimental Marine Biology and Ecology 184, 111-122.
Yu V. W., Gauthier C., St-Arnaud R. (2006) Inhibition of ATF4 transcriptional activity by FIAT/gamma-taxilin modulates bone mass accrual. Annals of the New York Academy of Science 1068, 131-142.
Yvan-Charvet L., Wang N., Tall A. R. (2010) Role of HDL, ABCA1, and ABCG1 transporters in cholesterol efflux and immune responses. Arterioscler Thromb Vasc Biol 30, 139-143.
Zdybicka-Barabas A., Cytryńska M. (2013) Apolipophorins and insects immune response. Invertebrate Survival Journal 10, 58-68.
Zeigler D. (2014) Chapter 12 - Symbiosis. In: Evolution: Components and Mechanisms, pp. 101-110. Academic Press.

Zhang Y., Ma C. J., Wang J. M., *et al.* (2012) Tim-3 regulates pro- and anti-inflammatory cytokine expression in human CD14(+) monocytes. Journal of Leukocyte Biology 91, 189-196.